eCAM Evidence-Based Complementary and Alternative Medicine

Complementary and Alternative Medicine in Cancer Prevention and Therapy

Guest Editors: Peng Cao, Senthamil R. Selvan, Esra Küpeli Akkol, Ning Wang, Hongjun Yang, and Xiaolan Cheng

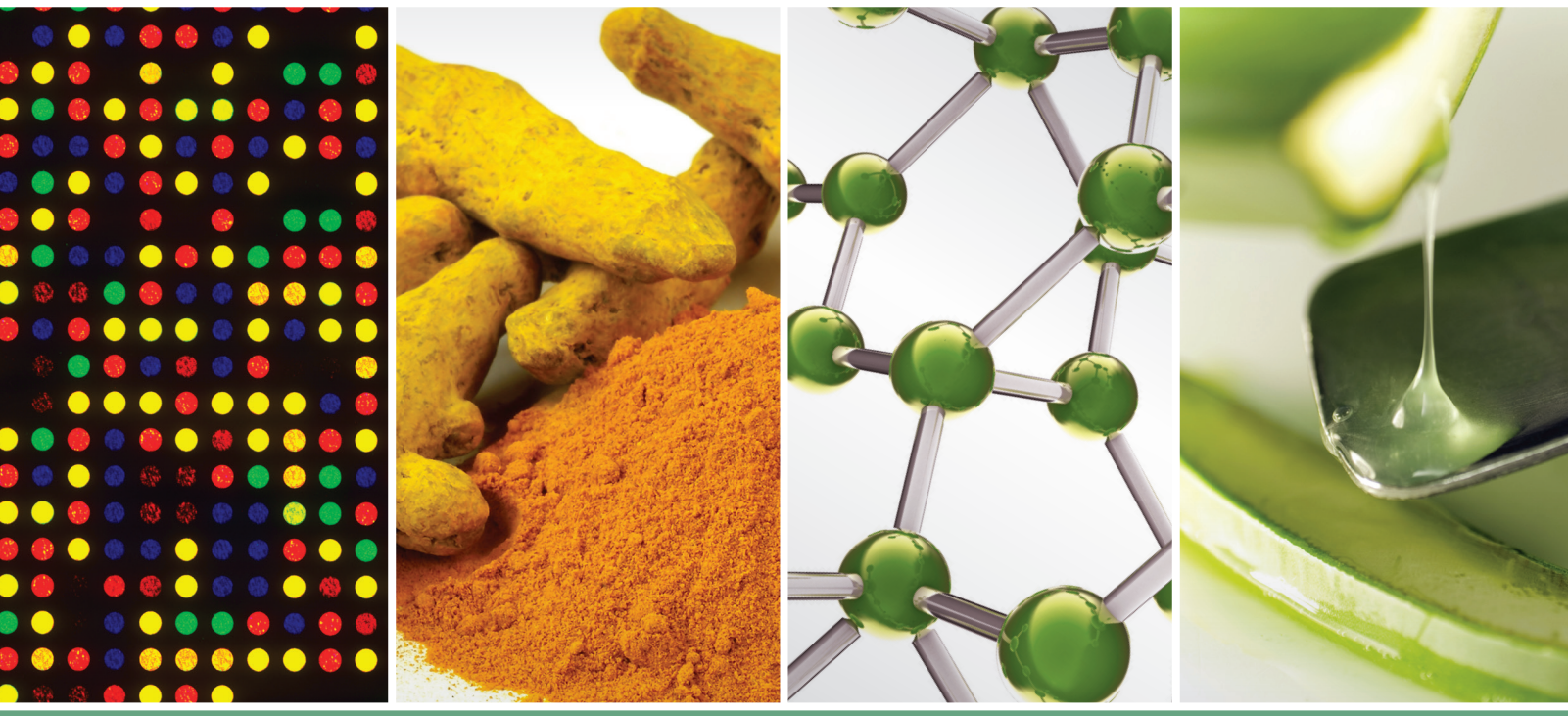

Complementary and Alternative Medicine in Cancer Prevention and Therapy

Evidence-Based Complementary and Alternative Medicine

Complementary and Alternative Medicine in Cancer Prevention and Therapy

Guest Editors: Peng Cao, Senthamil R. Selvan, Esra Küpeli Akkol, Ning Wang, Hongjun Yang, and Xiaolan Cheng

Editorial Board

Contents

Hindawi Publishing Corporation
Evidence-Based Complementary and Alternative Medicine
Volume 2015, Article ID 639372, 2 pages
http://dx.doi.org/10.1155/2015/639372

Editorial

Complementary and Alternative Medicine in Cancer Prevention and Therapy

Peng Cao,[1] Senthamil R. Selvan,[2] Esra Küpeli Akkol,[3] Ning Wang,[4] Hongjun Yang,[5] and Xiaolan Cheng[1]

[1]*Laboratory of Cellular and Molecular Biology, Jiangsu Province Institute of Traditional Chinese Medicine, Nanjing 210028, China*
[2]*Department of Medical Oncology, Thomas Jefferson University, Philadelphia, PA 19107, USA*
[3]*Department of Pharmacognosy, Faculty of Pharmacy, Gazi University, Etiler, 06330 Ankara, Turkey*
[4]*Department of Oncology, Luxembourg Institute of Health, 84 Val Fleuri, 1526 Luxembourg, Luxembourg*
[5]*Institute of Chinese Materia Medica, China Academy of Chinese Medical Sciences, China*

Correspondence should be addressed to Peng Cao; pcao79@yahoo.com

Received 12 January 2015; Accepted 12 January 2015

Although there have been great achievements in the battle against cancer over the past decades, cancer is still the leading cause of death in developing countries like China. Complementary and alternative medicine (CAM), especially traditional Chinese medicine (TCM), usually having good clinical tolerability, is applied as an adjuvant therapy to treat cancer in China based on TCM or modern pharmacological theories. In the west, CAM has increasingly become popular in cancer patients. It is estimated that the United States National Cancer Institute (NCI) spends around $120 million each year on complementary and alternative medicine related research projects. However, a fact is that although a lot of CAMs are widely used clinically, most evidence supporting their use came from poorly reported published clinical studies or studies with questionable methodology. Call for high quality evidence is a mission of this special issue. This issue on CAM for treatment or prevention of cancer compiles 13 exciting manuscripts, most of which reporting the efficacy and possible mechanisms of action of CAM or active constituents on cancer prevention and/or therapy in clinical and experimental levels.

S. S. M. Fong et al. contributed high quality evidence about Tai Chi Qigong Training for balance performance in irradiated survivors of nasopharyngeal cancer by a well-designed, well-conducted, and well-reported randomized controlled trial. Totally 120 senior adults participated in the study voluntarily. In this cross-sectional exploratory study, they have done very well on the ethics issues including protocol approval by ethical committee, properly informed consent, and high quality methodological issues, including the randomization method and allocation procedure, the recruitment of patients, the data management, the analysis method of results. All of the procedures were conducted according to the Declaration of Helsinki. This transparency makes readers confident to trust the result of the study. This is the first study to show that participating survivors of NPC had inferior OLS balance performances in all of the visual and supporting surface conditions compared with age-matched healthy counterparts. TC Qigong might be a potential rehabilitation exercise to improve the somatosensory function and single-leg standing balance performance of survivors of NPC. The shortcoming of this study is that it uses a convenience sample which may have introduced a self-selection bias that may threaten the internal validity of the study. In addition, homogenous subject group, small sample size, and OLS clinical test for balance performance assessment may limit the generalizability of results. However, we still believe that this study and its report could be a good evidence for efficacy of CAMs.

This edition also includes a review that discusses the possibility of TCM as maintenance therapy for advanced nonsmall cell lung cancer. The review concludes that TCM

as maintenance therapy can improve the QOL and prolong the PFS of advanced NSCLC patients. Besides, TCM can be applied for NSCLC patients not limited in population selection. However, there are only small sample clinical trials about TCM as maintenance therapy for advanced NSCLC. More large-scale trials of TCM as maintenance therapy for advanced NSCLC are expected.

For experimental study, A. Movahedi et al. investigated the capability of the decoction of *Teucrium polium* L. from Lamiaceae family to protect liver cells against hepatocellular carcinoma in carcinogenesis-induced animal model. After 28 weeks of treatment, they found that serum biochemical markers (ALT, AST, AFP, GGT, ALP, HCY, TNF-α, α2MG, and CBG), total antioxidant status, liver lesion, and glucocorticoid activity were all regulated auspiciously by *Teucrium polium* L. Y. Lin et al. studied that elemene, a compound found in an herb used in traditional Chinese medicine, has the effect of protecting cancer cells from death either in apatinib induced nutrient deficient environment or in serum-free induced starvation. Further data on the mechanism study revealed that elemene induced protective autophagy and prevented human hematoma cancer cells from undergoing apoptosis.

In addition to the mentioned papers above, other studies included in this issue provide sufficient scientific evidence from CAM research to clarify their mechanism of action and demonstrate their efficacy and safety. Through the rigorous researches, the benefits of CAM therapies will be highlighted, and this will support the clinical use of CAMs and help integrating CAM into the mainstream medicine. We hope that this special issue informs us about the rationale use of CAM in cancer prevention and therapy. We also hope that the papers included in this issue play a role in reflecting the recent advancement in the field of CAM.

Peng Cao
Senthamil R. Selvan
Esra Küpeli Akkol
Ning Wang
Hongjun Yang
Xiaolan Cheng

Hindawi Publishing Corporation
Evidence-Based Complementary and Alternative Medicine
Volume 2015, Article ID 276946, 11 pages
http://dx.doi.org/10.1155/2015/276946

Research Article

1,2,3,4,6-Penta-*O*-galloylglucose within Galla Chinensis Inhibits Human LDH-A and Attenuates Cell Proliferation in MDA-MB-231 Breast Cancer Cells

Shihab Deiab, Elizabeth Mazzio, Suresh Eyunni, Oshlii McTier, Nelly Mateeva, Faisel Elshami, and Karam F. A. Soliman

College of Pharmacy and Pharmaceutical Sciences, Florida A&M University, Tallahassee, FL 32307, USA

Correspondence should be addressed to Karam F. A. Soliman; karam.soliman@famu.edu

Received 14 August 2014; Revised 20 November 2014; Accepted 20 November 2014

Academic Editor: Esra Küpeli Akkol

A characteristic feature of aggressive malignancy is the overexpression of lactic acid dehydrogenase- (LDH-) A, concomitant to pericellular accumulation of lactate. In a recent high-throughput screening, we identified *Rhus chinensis* (Mill.) gallnut (RCG) (also known as Galla Chinensis) extract as a potent (IC_{50} < 1 μg/mL) inhibitor of human LDH-A (*h*LDH-A). In this study, through bioactivity guided fractionation of the crude extract, the data demonstrate that penta-1,2,3,4,6-*O*-galloyl-β-D-glucose (PGG) was a primary constituent responsible for *h*LDH-A inhibition, present at ~9.95 ± 0.34% dry weight. Theoretical molecular docking studies of *h*LDH-A indicate that PGG acts through competitive binding at the NADH cofactor site, effects confirmed by functional enzyme studies where the IC_{50} = 27.32 nM was reversed with increasing concentration of NADH. Moreover, we confirm protein expression of *h*LDH-A in MDA-231 human breast carcinoma cells and show that PGG was toxic (LC_{50} = 94.18 μM), parallel to attenuated lactic acid production (IC_{50} = 97.81 μM). In a 72-hour cell proliferation assay, PGG was found to be a potent cytostatic agent with ability to halt cell division (IC_{50} = 1.2 μM) relative to paclitaxel (IC_{50} < 100 nM). In summary, these findings demonstrate that PGG is a potent *h*LDH-A inhibitor with significant capacity to halt proliferation of human breast cancer cells.

1. Introduction

Cancer is the second leading cause of death worldwide. While major advances have been made in design of chemotherapy agents, radiation, and surgical procedures, mortality rates remain high. Terminal cancer requires innovative therapeutic approaches, which are currently limited. Traditional use of herbs to treat diverse human illnesses dates back to thousands of years, but in today's society the use of natural product remedies is defined amongst others under the classification of "complementary and alternative medicines" (CAMs) [1–3]. The field of CAM is of global interest, in particular to augment traditional chemotherapies, prevent cancer remission, or serve as basic chemopreventive strategies [4–7].

Rhus chinensis (Mill.) belongs to the genus *Rhus* and the family *Anacardiaceae*. *Rhus chinensis* gall (RCG) is the abnormal growth of *Rhus chinensis* leaves caused by Chinese aphid *Schlechtendalia chinensis* [8, 9], also used for decades by indigenous people in the treatment of diarrhea, hemorrhage, and inflammation [10–17]. In a recent study conducted in our laboratory, a high-throughput screening of natural products revealed the extract of RGC to halt the proliferation of human breast cancer cells [7] and inhibit *h*LDH-A [18], an enzyme which plays a significant role in driving aggressive malignancies [2, 19–21], chemo- and radiotherapy resistance [22, 23], tumorigenic potential [24–26], and metastatic processes [22]. It is believed that the abundance of lactic acid produced and released by tumor cells assists in invasion and motility [27] where a low pH weakens the extracellular stroma which helps tumor cells to dislodge and burrow in the blood and lymphatic systems [28].

Given the potential value in the identification of novel *h*LDH-A inhibitors to augment targeted cancer therapies [16, 29], we further investigate the constituent properties of *Rhus chinensis* gallnut so as to isolate the chemical responsible for *h*LDH-A inhibition. This was achieved through bioactivity

guided fractionation, theoretical molecular docking, and functional enzyme studies, followed by *in vitro* evaluation in a human breast cancer cell line with dominant protein expression of *h*LDH-A.

2. Materials and Methods

Materials used were Hanks Balanced Salt Solution, 4-(2-hydroxyethyl)-1-piperazineethanesulfonic acid (HEPES), ethanol, 96-well plates, general reagents and supplies, and *h*LDH-A from Abcam (Cambridge, MA, USA). *Rhus chinensis* gallnut was purchased from Kalyx Natural Marketplace (Camden, NY), cell lines were purchased from ATCC (Manassas, VA, USA), and penta-1,2,3,4,6-*O*-galloyl-β-D-glucose, chemical reagents, and HPLC supplies and columns were purchased from Sigma Aldrich (St. Louis, MO, USA) and VWR International (Suwanee, GA, USA).

2.1. Herbal Extract. Dry RCG (500 g) was ground, homogenized, and then extracted in 90% ethanol three times for 24 h and the solutions were then combined and evaporated to obtain the crude extract. Extract was then dissolved in water and successively fractionated by liquid-liquid partitioning between petroleum ether (three times, 200 mL), ethyl acetate (six times, 300 mL each), and n-butanol (three times, 200 mL each) to yield a petroleum ether soluble portion 3.5 g, ethyl acetate soluble portion 86 g, n-butanol soluble portion 7 g, and water-soluble portion 12 g. The different fractions were tested against *h*LDH-A (0.02 units/mL) activity at concentrations ranging from 0.7 to 0.0007 mg/mL (all serial dilutions were made using diluents consisting of HBSS with 10-mM HEPES adjusted to a pH 7.4). The dried ethyl acetate fraction showed *h*LDH-A inhibitory activity at a concentration of 0.0007 mg/mL.

2.2. Bioactivity-Guided Isolation and Identification. The ethyl acetate fraction (20 g) was flash chromatographed over silica gel (200–400 mesh) and eluted at 10 mL/min with chloroform: methanol gradient (100 : 0, 10 : 90) solvent system. A total of 500 (15 mL) fractions were collected. Fractions were pooled according to their R_f value on TLC and then combined to give 5 distinct fractions which were then evaporated to yield 0.5 g (1–166), 11.5 g (167–215), 4.2 g (216–267), 2.1 g (268–350), and 1.2 g (351–500). The resulting fractions were tested for activity at 0.7–0.0007 mg/mL. Fractions (167–215) showed significant *h*LDH-A inhibitory activity relative to other fractions. 1.5 g of the active fraction, 167–215, was further analyzed and separated into four major fractions by RP-HPLC with UV detection at 214 nm on PRP-15 um 15 × 2.1 mm column and eluted with a gradient system of acetonitrile: water consisting of 0.2% TFA.

Fraction 1 (0.8 g) showed significant activity compared to the other three fractions and was further separated over RP-column chromatography on a C18–125 Å 55–105 um column and eluted with 30% acetonitrile to yield three fractions. Fractions 2 (0.2 g) and 3 (0.15 g) showed similar activity and then were identified by 1H-NMR and 13C-NMR to be the same and then later combined. The substance extracted was identified as PGG (1,2,3,4,6-pentagalloylglucose) a solid, off-white powder. The melting point was determined on a Mel-Temp II apparatus (Laboratory Devices) and found to be 337°C. MW was 940.67 $C_{41}H_{32}O_{26}$. 1H NMR spectra were 7.146, 7.085, 7.061, 7.012, 6.985, 6.933, 6.279, 6.258, 5.939, 5.652, 5.622, 4.878, 4.796, 4.665, 4.524, and 4.235. 13C NMR spectra were 167.02, 166.38, 166.38, 166.10, 166.00, 165.30, 145.60, 145.51, 145.34, 139.84, 139.42, 139.20, 139.08, 120.08, 119.38, 119.25, 118.75, 109.66, 94.92, 74.72, 74.13, 68.96, and 63.92.

2.3. Quantification of PGG. PGG concentration in whole crude ethanol RCG extract was quantified using a Shimadzu HPLC system equipped with an SPD-20A UV detector set at 280 nm, a workstation containing EZSTART version 7.4 software and an SS420X instrument interface docked to a Waters Autosampler Model 717 Plus (Shimadzu Scientific Instruments, Columbia, MD, USA; Waters, Milford, MA, USA). Mobile phase consisted of 2.5% acetic acid in 82% acetonitrile; flow rate was isocratic at 1.4 mls/minute; the column used was a 5 um 300A 4.6 × 100 mM C-18 Venusil ABS (VWR, Radnor, PA, USA). PGG external standards were prepared in mobile phase, Chinese gallnut ethanol extract was diluted in mobile phase, and injection volume was set at 25 uL.

2.4. Cell Culture. MDA-MB-231 (ATCC HTB-26) human breast cancer cells were obtained from ATCC (Manassas, VA). MDA-MB-231 cells were brought up in ATCC-formulated Leibovitz's L-15 medium [Catalog number 30-2008], supplemented with 10% FBS and penicillin/streptomycin (100 U/0.1 mg/mL). After confluence, the cells were subcultured and grown in DMEM containing phenol red, 10% FBS, 4 mM L-glutamine, 20 μM sodium pyruvate, and penicillin/streptomycin (100 U/0.1 mg/mL). Culture conditions were maintained [37°C-5% CO_2/atmosphere] and every 2–5 days, the media were replaced and cells subcultured. For experiments, plating media consisted of DMEM, 1% FBS (24-hour toxicity studies), or 5% FBS (72-hour proliferation studies) + penicillin/streptomycin (100 U/0.1 mg/mL), 25 mM glucose, 2 mM sodium pyruvate, and 3 mM L-glutamine.

2.5. Cell Count. Viable cell count was quantified using resazurin (Alamar Blue) indicator dye [30]. A working solution of resazurin was prepared in sterile PBS, phenol red (0.5 mg/mL), and added (15% v/v) to each sample. Samples were returned to the incubator for 6–8 hr, and reduction of the dye by viable cells (to resorufin, a fluorescent compound) was quantitatively analyzed using a microplate fluorometer, Model 7620, version 5.02 (Cambridge Technologies Inc., Watertown, MA) with settings at [550/580], [excitation/emission].

2.6. Human LDH-A Activity. A continuous *h*LDH-A assay using recombinant full length human LDHA (amino acids 1–332) with N terminal His tag, 352 amino acids with tag, and MW 38.8 kDa, enzyme commission (EC) number 1.1.1.27 (BRENDA | IUBMB) (Abcam, Cambridge, MA), was used, where we previously confirmed the identity of the enzyme

using matrix assisted laser desorption ionisation (MALDI) mass spectrometry and analysis by Mascot ID [18]. Briefly, the enzyme assay buffer consisted of HBSS + calcium and Mg, pH adjusted to 7.0. PGG was added at various concentrations to *h*LDH-A enzyme (final concentration .02 units/mL) and β-nicotinamide adenine dinucleotide, reduced form solution (β-NADH) (final working concentration of 500 μM), and a prereading at 340 nm was established to eliminate background. The reaction was started with a solution containing the substrate pyruvate (final concentration = 3 mM) and a reading was taken intermittently over 60 minutes at 340 nm using a 96-well microplate reader (Bio-Tek Instruments, Inc., Winooski, VT, USA).

2.7. Western Blot: hLDH-A Protein Expression. The presence of *h*LDH-A in MDA-MB-231 cells was determined using recombinant *h*LDH-A as the standard. Cells were washed and centrifuged and the supernatant was discarded using ice-cold sterile PBS at 4°C. The pellet was resuspended and homogenized/sonicated in RIPA lysis buffer containing protease inhibitors. Samples were placed on ice for 30 min and centrifuged at 10,000 ×g for 10 minutes at 4°C. The supernatant was added at 1 : 1 of Laemmli sample buffer (Biorad number 161-0737) + fresh β-ME and boiled for 5 minutes. Approximately 50 μg of protein was loaded/lane and separated using 5%–15% SDS-PAGE gels, running buffer, 25 mM Tris, 192 mM glycine, and pH 8.3 (Biorad #161-0734) and applying 200 constant V constant ~35 min. The proteins were transferred to polyvinylidene fluoride membranes (100 V for 30–60 minutes) in ice-cold transfer buffer containing 25 mM Tris, 192 mM glycine, and 20% methanol. The membranes were placed in a blocking buffer consisting of 5% bovine serum albumin fraction V (BSA) w/v in TBS + 0.05% Tween-20, pH 7.4. The membranes were washed and placed in 1° rabbit anti-human LDH-A antibody (1 : 500) containing 1% BSA in TTBS at RT for 2 Hr. The membranes were washed in TTBS and incubated in 2° goat anti-rabbit IgG (Fc specific) peroxidase conjugate (1 : 4000) in 2% nonfat dried milk in PBS for 1.5 Hr at RT. After a final wash, peroxidase was detected with Sigma FAST DAB (3,3′-diaminobenzidine tetrahydrochloride) with a metal enhancer cobalt chloride. Images were scanned using an Epson Stylus CX-8400. Intensity analysis was performed using ImageJ software provided from the National Institutes of Health [31].

2.8. Lactic Acid Determination. Cellular production of lactic acid was determined in 96-well plates using a colorimetric enzymatic assay (procedure number 735, Sigma Diagnostics, St. Louis, MO). Briefly, lactate was quantified by conversion to pyruvate and H_2O_2 using a base lactate reagent containing lactate oxidase (400 U/L) and horseradish peroxidase 2400 U/L (Trinity Biotech Jamestown, NY, USA). The reagent was added to a chromogen and samples were incubated for 10 minutes at 37°C. Lactate was quantified at 490 nm on a UV microplate spectrophotometer (BioTek Instruments, Inc., Winooski, VT, USA).

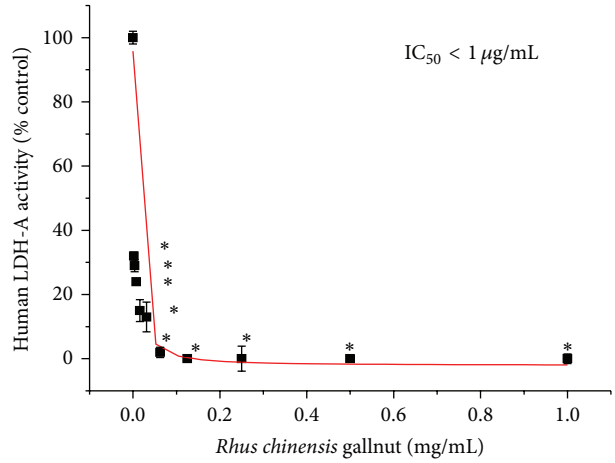

Figure 1: Potent *h*LDH-A enzyme inhibition by RCG extract. The data represent *h*LDH-A activity as % control (NADH oxidation) at 60 minutes and are expressed as the mean ± SEM, $n = 4$, with significance from controls using a one-way ANOVA followed by a Bonferroni's multiple comparison test; $^{*}P < 0.05$, $IC_{50} < 1\,\mu$g/mL.

2.9. Molecular Docking. The X-ray crystal structure of human LDH (M form), predominantly found in human muscle, was downloaded from the RCSB protein data bank (PDB: 1I10). Chain A was extracted and selected for the docking studies. The chain A of the protein was then refined using the structure preparation tool of the biopolymer module offered by Sybyl-X 1.3 suite [26]. In this process, mislabeled atom types from the pdb file were corrected, backbone and side chains repaired, side-chain bumps fixed, side chain amides checked to maximize potential hydrogen bonding, and all hydrogen atoms added to the protein. The protein was then subjected to energy minimization following the gradient termination of the Powell method for 10,000 iterations using MMFF94s force field incorporating MMFF94 charges with nonbonding cut-off set at 8.0 and dielectric constant set at 1.0. The resulting refined protein was used for docking purposes.

The 3D conformer of the compound in present study, PGG structure, was download from the PubChem database and subjected to minimization following the gradient termination of the conjugate gradient method for 5000 iterations using Tripos force field incorporating Gasteiger-Huckel charges with the nonbonding cut-off set at 8.0 and dielectric constant set at 1.0. Thus optimized compound PGG was docked in the catalytic active site of the chain A of the LDH protein complex (PDB: 1I10) using high precision Surlex-Dock GeomX program as implemented in Sybyl software by incremental construction approach of building the structure in the active site so as to favor the binding affinity. In this process, initially, protomol was generated using the bound ligand 1,4-dihydronicotinamide adenine dinucleotide (NAI), allowing us to map the active site for docking the test ligand PGG. During the entire docking process, ring flexibility of the ligand was considered. Predock and postdock minimizations were performed and a self-scoring term was included for optimum results.

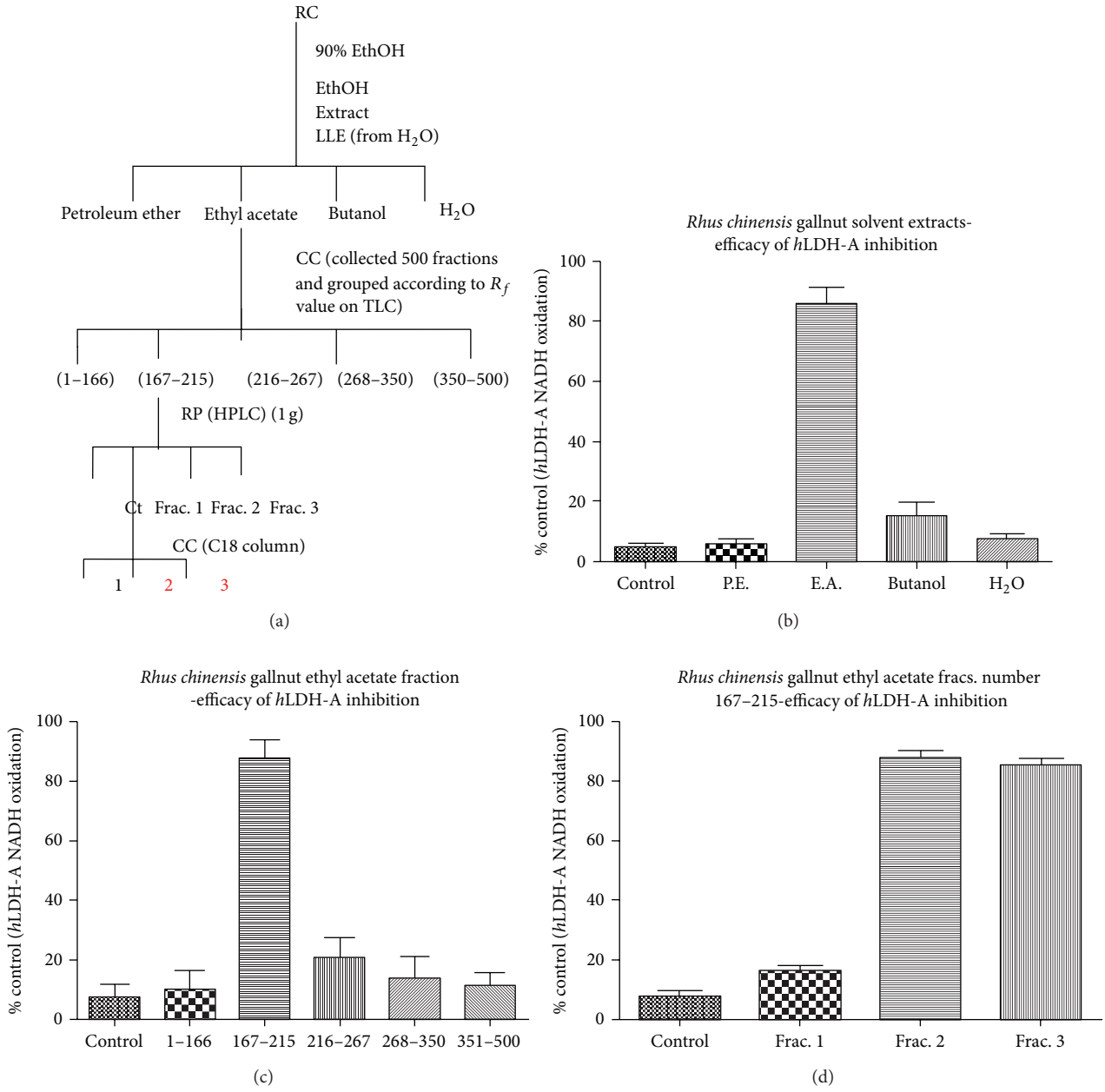

Figure 2: (a) Process of separation and isolation of *h*LDH-A inhibitor fractions from RCG. (b) *h*LDH-A inhibition by solvent extracts (PE: petroleum ether, EA: ethyl acetate). The data represent *h*LDH-A activity as % control and are expressed as the mean ± SEM, $n = 4$. (c) *h*LDH-A enzyme inhibition by further fractionation of the ethyl acetate fraction. The data represent *h*LDH-A activity as % control and are expressed as the mean ± SEM, $n = 4$. (d) *h*LDH-A enzyme inhibition by further fractionation of the ethyl acetate 167–215 fractions. The data represent *h*LDH-A activity as % control and are expressed as the mean ± SEM, $n = 4$.

2.10. Statistics. Statistical analysis was performed using Graph Pad Prism (version 3.0; Graph Pad Software Inc., San Diego, CA, USA) with IC_{50}s determined by regression analysis using Origin Software (OriginLab, Northampton, MA). Significance of difference between multiple groups was assessed using a one-way ANOVA, followed by Bonferroni's multiple comparison test or Student's *t*-test.

3. Results

High-throughput screening has identified *Rhus chinensis* gallnut ethanol extract with inhibitory activity on human recombinant *h*LDH-A. As previously reported, this was one of the most potent natural products elucidated with an $IC_{50} < 1\,\mu g/mL$ [18]. In order to elucidate the active constituents

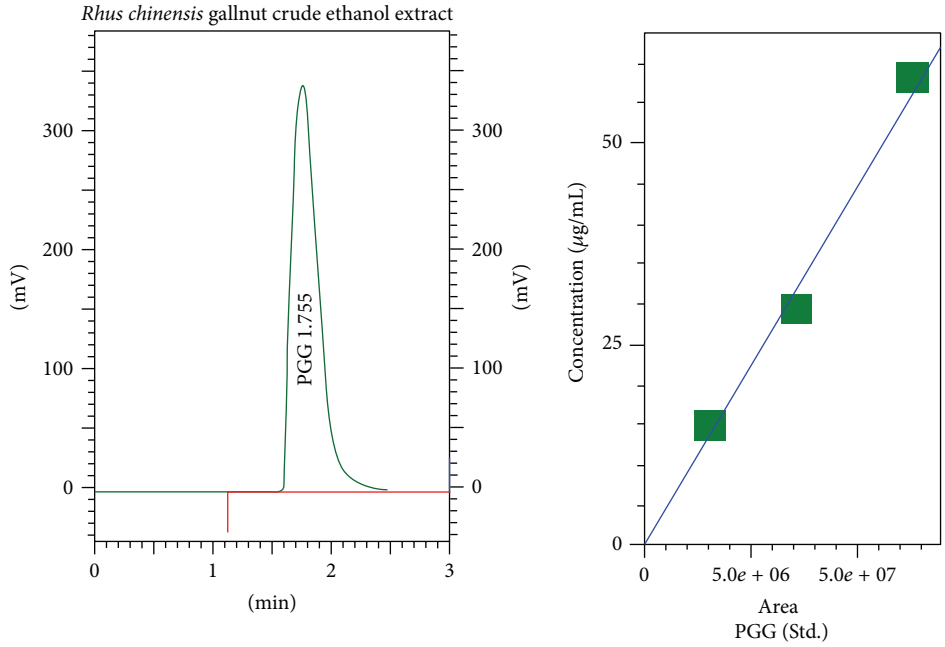

(a) UV/VIS trace (b) PGG-ESTD-UV/VIS

Figure 3: PGG concentration of RGC crude ethanol extract (a) determined by HPLC at 280 nm using external PGG standard (b). Crude extract concentration of PGG was approximately 9.95 ± .34% of weight (Chinese gallnut extract (250 μg/mL) = 24.88 ± 0.85 μg/mL), $n = 4$.

within the RCG extract responsible for *h*LDH-A inhibition, bioactivity guided fractionation (Figure 2(a)) was conducted to where *h*LDH-A activity was inhibited by the ethyl acetate fraction (167–215) (Figures 2(b), and 2(c)), which further yielded two active fractions within (Figure 2(d)).

Fractions 2 (0.2 g) and 3 (0.15 g) showed similar activity and then were identified by 1H-NMR and 13C-NMR to be the same and then later combined. The molecule is identified as PGG (1,2,3,4,6-pentagalloylglucose) which is a solid and an off-white substance. The melting point was determined on a Mel-Temp II apparatus (Laboratory Devices) and found to be 337°C. MW was 940.67 $C_{41}H_{32}O_{26}$. 1H NMR spectra were 7.146, 7.085, 7.061, 7.012, 6.985, 6.933, 6.279, 6.258, 5.939, 5.652, 5.622, 4.878, 4.796, 4.665, 4.524, and 4.235. 13C NMR spectra were 167.02, 166.38, 166.38, 166.10, 166.00, 165.30, 145.60, 145.51, 145.34, 139.84, 139.42, 139.20, 139.08, 120.08, 119.38, 119.25, 118.75, 109.66, 94.92, 74.72, 74.13, 68.96, and 63.92. Quantification and further validation of PGG in RCG extract were accomplished with HPLC (Figure 3) where an external standard (b) versus extract (a) indicating PGG was present at 24.8 ± .85 μg/mL, which is equivalent to 9.95 ± .34 of crude extract.

To assess if PGG could theoretically inhibit *h*LDH-A, molecular docking studies were conducted and the data show predicted competitive binding of PGG (Figure 4(a)) within the NADH binding cofactor site of the *h*LDH-A enzyme (Figures 4(b) and 4(c)). Docking studies showed H bond interactions between the docked ligand PGG and the protein in the cofactor site (Figures 5(a) and 5(b)). HO···HO (TYR_82) = 1.70 Å; HO···HN (ALA_29) = 1.77 Å; OH···O=C (THR_94) = 1.87 Å; HO···HN (VAL_30) = 2.05 Å; HO···HN (GLY_96) = 2.27 Å; HO···HN (ALA_29) = 2.57 (Figures 1 and 2). When compound PGG was docked alongside the bound ligand 1,4-dihydronicotinamide adenine dinucleotide (NAI), the total scores which are expressed as—$\log(K_d)$ obtained were 5.86 and 12.61, respectively, for PGG and the bound ligand NIA, respectively. These effects were also confirmed by functional studies (Figure 5(a)), where PGG was found to be an extremely potent *h*LDH-A inhibitor within the therapeutic range IC_{50} = 27.17 nM compared to a known *h*LDH-A inhibitor oxalic acid (Figure 5(b)) demonstrating a relative weak potency reflected by an IC_{50} > 6 mM. Competitive binding of PGG versus NADH clearly shows that the site has greater affinity for PGG than NADH (Figure 6).

In order to determine the effects of PGG *in vitro*, a human breast cancer cell line (MDA-MB-231) lysate was evaluated for the baseline expression of *h*LDH-A by Western blot (Figure 7). These findings validate the identity of the recombinant protein used in this study, as well as demonstrating dominant expression level in MDA-MB-231 cells, further subject to *in vitro* effects incurred by PGG.

In vitro analyses on the lethality of PGG versus reduction in lactic acid accumulated in the supernatant were near identical (Figures 8(a) and 8(b)). However, given that all toxic compounds regardless of mechanism of action will reduce lactic acid as a process of cell death in tumor cells, there is no conclusion drawn from this data. If loss of lactate significantly preceded cell death, one could say there was a correlation, but further analysis will be required. The antiproliferative effects of PGG relative to paclitaxel were evaluated over a three-day growth period (Figure 9). In this study, we provide data to

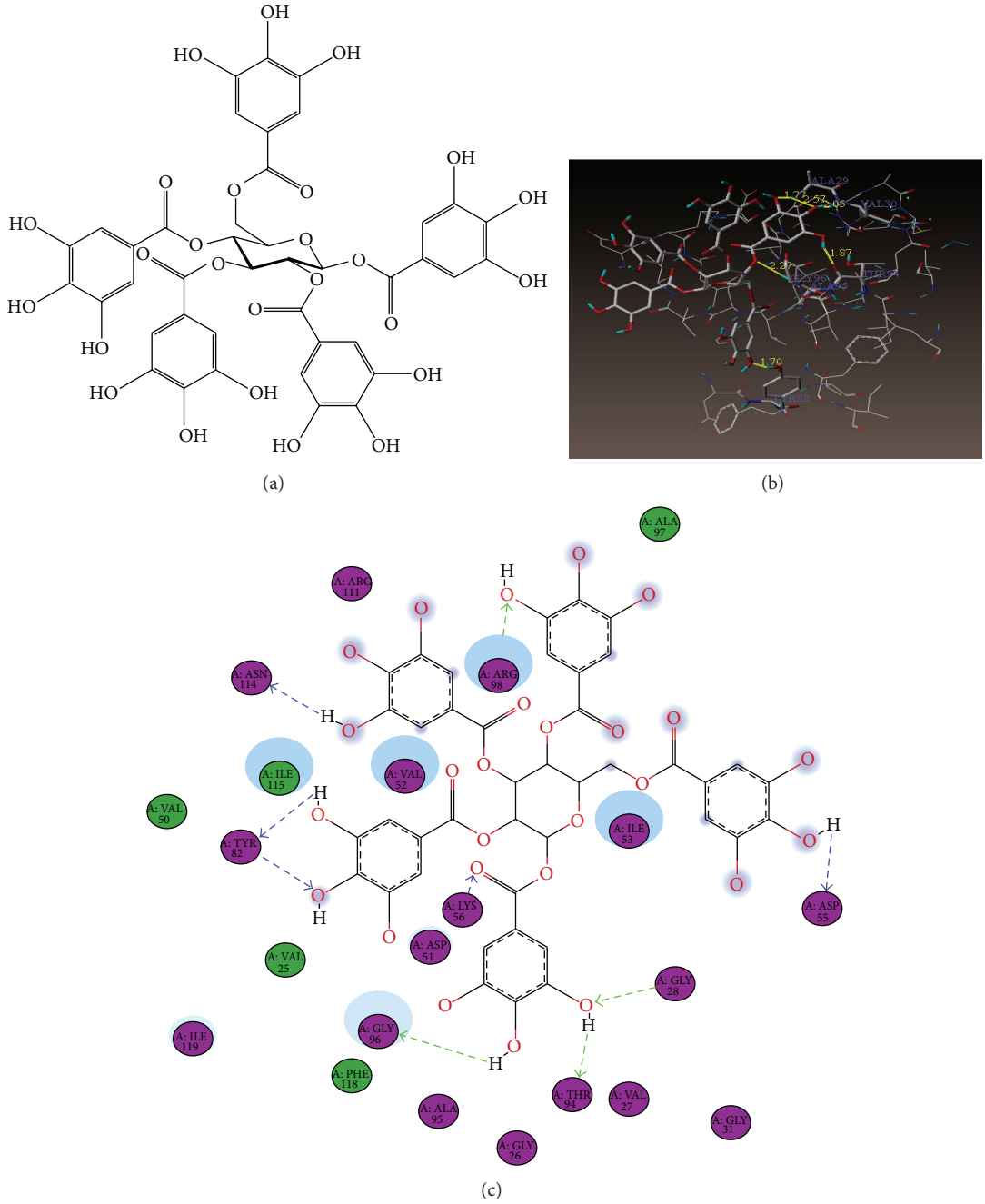

Figure 4: Molecular docking studies (PGG inhibition of human LDH-A). (a) Structure of 1,2,3,4,6-*O*-galloyl-*β*-D-glucose, pentagalloylglucose. (b) Binding mode of compound CID65238, PGG, in the coenzyme active site of *h*LDH-A (PDB: 1|10). (c) Simplified binding mode of compound CID65238, PGG, in the coenzyme binding site of *h*LDH-A (PDB: 1|10).

support that PGG, a component of RGC extract, can inhibit human LDH-A and halt proliferation of a human tumor cell line MDA-MB-231, which highly expresses the human LDH-A protein.

4. Discussion

The data in this study confirm penta-1,2,3,4,6-*O*-galloyl-*β*-D-glucose (PGG)—a component in RCG—as a newly identified *h*LDH-A inhibitor with potential application as a CAM for use in cancer treatment. Our work supports/builds on the findings of others in describing therapeutic value of this molecule as an anticancer agent, now having been established in the suppression of prostate cancer metastasis [32], angiogenesis, with capacity to initiate apoptosis [33–36], and halt cell cycle at the G1 phase [37, 38] at the DNA replication S-phase [39], corresponding to the primary basis of proposed therapeutic use in treatment of cancers [40].

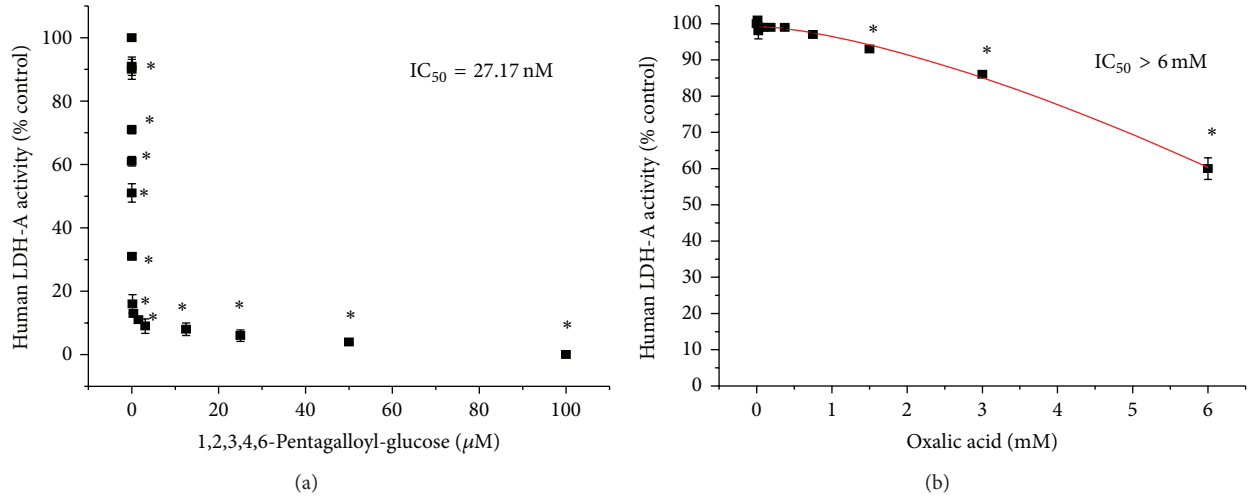

Figure 5: (a) *h*LDH-A (0.02 units/mL) enzyme inhibition by PGG. The data represent *h*LDH-A activity as % control (NADH oxidation) at 60 minutes and are expressed as the mean ± SEM, with significance from controls determined with a one-way ANOVA followed by Bonferroni's multiple comparison test; $^{*}P < 0.05$, $n = 4$. $IC_{50} = 27.17$ nM. (b) *h*LDH-A enzyme inhibition by reference known inhibitor (oxalic acid). The data represent *h*LDH-A activity as % control (NADH oxidation) at 60 minutes and are expressed as the mean ± SEM, with significance from controls determined using a one-way ANOVA followed by Bonferroni's multiple comparison test; $^{*}P < 0.05$, $n = 4$, $IC_{50} > 6$ mM.

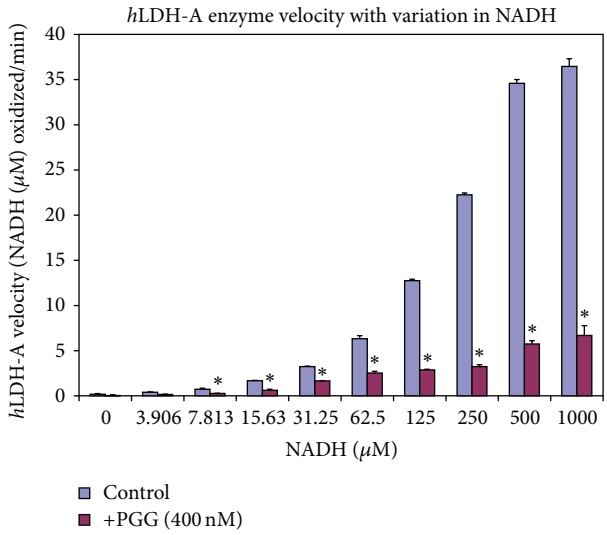

Figure 6: *h*LDH-A enzyme velocity ± 400 nM PGG. The data are presented as the average rate of reaction: NADH oxidized over 60 minutes at RT and displayed as the mean ± SEM, $n = 4$. Significance of difference between NADH controls and PGG treated samples was analyzed by a Student's *t*-test; $^{*}P < 0.05$.

At the same time, the RGC extract as a whole is equally capable of inhibiting angiogenesis, inducing apoptosis in cancer cells [34] and as a cytostatic agent [7]. Moreover, its medicinal value has been described in the scientific literature for its multidimensional therapeutic value, also effective against harmful intestinal and periodontal bacteria [9, 41], hepatitis carcinoma virus [15], severe acute respiratory syndrome corona [42] and as an anti-inflammatory [11, 43–45].

The data in this study also confirm the ability of PGG to inhibit *h*LDH-A which is a therapeutic target in particular given its role in tumor initiation, progression, and metastasis [46, 47] and in aggressive malignancies such as pheochromocytomas, paragangliomas [48], or breast cancer [49]. Interestingly, while LDH is a specific therapeutic target in tumor cells, its exact mechanism of action to exert anticancer effects remains unknown.

It is believe that elevated *h*LDH-A protein expression in tumor cells, and subsequent over production of lactic acid contributes to development of radiation and chemotherapy resistance [27, 28]. Tumor cell overproduction of lactic acid (in the absence or presence of O_2) was described almost a century ago by Otto Warburg, having been termed "the Warburg effect." While many scientists theorize that this aberration is a function of altered metabolism, studies in our laboratory exploring this phenomenon using current technologies such as whole-genomic, proteomic MALDI-TOF-MS and metabolite analysis show that the Warburg effect has a functional role not in metabolism, but in regulating acidic pericellular pH (pHe). For some unknown reason, cancer cells inherently thrive in slightly acidic pH, are extremely vulnerable to necrosis as the pH shifts toward alkaline, and will sustain a steady state pH through metabolic inversion or fluctuating dominance between glycolytic-rate substrate level phosphorylation (SLP) and mitochondrial (mt) oxidative phosphorylation to control lactic acid production [50]. If this is the case, then *h*LDH-A would comprise a vehicle to maintain acidic pH where tumor cells thrive, but the question after much work still remains as to why tumor cells require ample concentrations of acid.

Acidity alone, can trigger aggressive forms of malignancy, augment metastases, and initiate chemoresistance all of which correlate to low survival rates [51, 52]. Data collected from our lab and by others seems to indicate that acid can

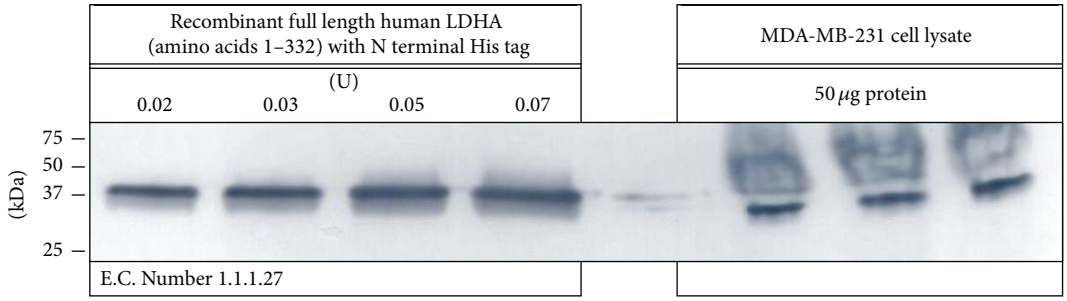

Figure 7: Western blot confirmation of human *h*LDH-A in MDA-MB-231 breast tumor cells (*in vitro* studies) and pure recombinant *h*LDH-A used (enzyme kinetic studies).

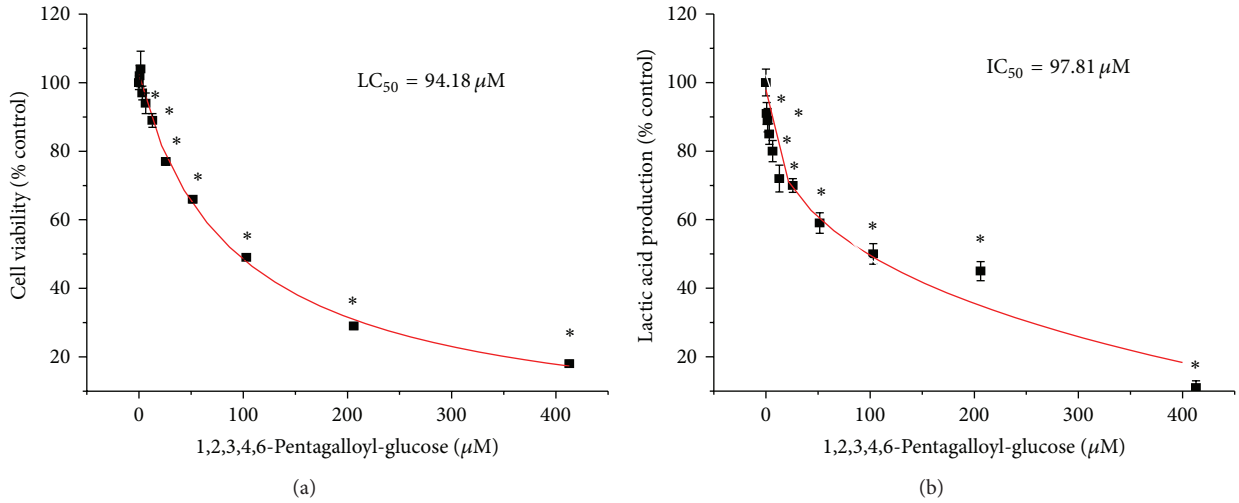

Figure 8: The effect of PGG on viability/metabolism and lactic acid produced by MDA-MB-231 human breast cancer cells (5.0×10^6 cells per well) low serum [2%] phenol-free media supplemented with amino acids at 24 hours. The data represent cell viability (% control) (a) and lactic acid (% control) (b) and are expressed as the mean ± SEM with significance from controls determined using a one-way ANOVA followed by Bonferroni's multiple comparison test; $^* = P < 0.05$, $n = 4$.

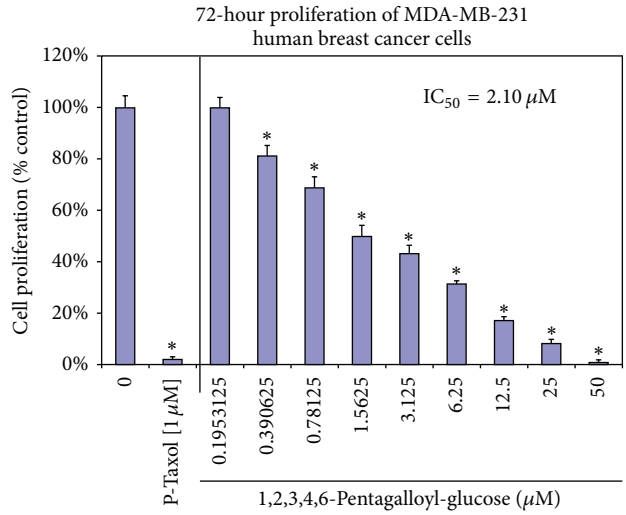

Figure 9: Inhibitory growth properties of PGG on MDA-MB-231 human breast carcinoma cells relative to 1 μM paclitaxel. The data represent growth from an initial plating density of 4,000 cells/well in 96-well plates over a 72-hour period as proliferation (% untreated controls) established with resazurin (Alamar Blue) fluorometric analysis. The data represents cell proliferation as % control and is presented as the mean ± SEM, $n = 4$, with significance from controls determined using a one-way ANOVA followed by Bonferroni's multiple comparison test; $^* = P < 0.05$.

turn on anabolic processes in tumor cells, due to energy efficiency with elevated protein expression for nutrient sensor GβL (G protein, beta protein subunit-like), a component of *m*TOR (mammalian target of rapamycin), PI3K/Akt signaling, and its downstream eIF4E tumor promoting target [53]. These changes are indicative that feedback sensors (such as acid) could switch the metabolic state of tumor cells from anabolic to catabolic [54].

While the exact role of *h*LDH-A remains elusive, it is known that *h*LDH-A knockdown, or lowering the functional capacity of *h*LDH-A, can lead to suppressed tumor growth and metastasis indicating this enzyme as a novel targeted cancer therapy strategy. In this study, we provide data to support therapeutic efficacy of PGG, a component of RGC extract, to inhibit human LDH-A and halt proliferation of a human tumor cell line MDA-MB-231, which highly expresses the *h*LDH-A protein.

5. Conclusion

Pentagalloylglucose, PGG, a component of RGC, shows a remarkable competitive inhibitory activity against *h*LDH-A at the NADH cofactor docking site. Its effect in tumor cells baring high expression of *h*LDH-A resulted in blocking proliferation. Future research will be required to determine in detail cause-effect relationship between *h*LDH-A inhibition and biochemical metabolic or process related effects in tumor cells.

Conflict of Interests

The authors declare that there is no conflict of interests regarding the publication of this paper.

Acknowledgments

This research was supported by a Grant from NIH NCRR RCMI Program (G12RR 03020) and the National Institute on Minority Health and Health Disparities, NIH (8G12MD007582-28 and 1P20 MD006738-01).

References

[1] O. Akerele, "Nature's medicinal bounty: don't throw it away," *World Health Forum*, vol. 14, no. 4, pp. 390–395, 1993.

[2] H. Xie, V. A. Valera, M. J. Merino et al., "LDH-A inhibition, a therapeutic strategy for treatment of hereditary leiomyomatosis and renal cell cancer," *Molecular Cancer Therapeutics*, vol. 8, no. 3, pp. 626–635, 2009.

[3] J. D. Phillipson, "Phytochemistry and medicinal plants," *Phytochemistry*, vol. 56, no. 3, pp. 237–243, 2001.

[4] A. Sood, D. L. Barton, B. A. Bauer, and C. L. Loprinzi, "A critical review of complementary therapies for cancer-related fatigue," *Integrative Cancer Therapies*, vol. 6, no. 1, pp. 8–13, 2007.

[5] S. Wang, S. Penchala, S. Prabhu, J. Wang, and Y. Huang, "Molecular basis of traditional chinese medicine in cancer chemoprevention," *Current Drug Discovery Technologies*, vol. 7, no. 1, pp. 67–75, 2010.

[6] T. Schnoller, R. Kufer, T. Eismann, and L. Rinnab, "Complementary medicine in oncology," *Der Urologe*, vol. 48, no. 11, pp. 1302–1307, 2009.

[7] E. Mazzio, R. Badisa, N. Mack, S. Deiab, and K. F. Soliman, "High throughput screening of natural products for anti-mitotic effects in MDA-MB-231 human breast carcinoma cells," *Phytotherapy Research*, vol. 28, no. 6, pp. 856–867, 2014.

[8] Z. Ren, B. Zhu, D. Wang, E. Ma, D. Su, and Y. Zhong, "Comparative population structure of Chinese sumac aphid *Schlechtendalia chinensis* and its primary host-plant *Rhus chinensis*," *Genetica*, vol. 132, no. 1, pp. 103–112, 2008.

[9] Y.-J. Ahn, C.-O. Lee, J.-H. Kweon, J.-W. Ahn, and J.-H. Park, "Growth-inhibitory effects of Galla Rhois-derived tannins on intestinal bacteria," *Journal of Applied Microbiology*, vol. 84, no. 3, pp. 439–443, 1998.

[10] J.-C. Chen, T.-Y. Ho, Y.-S. Chang, S.-L. Wu, and C.-Y. Hsiang, "Anti-diarrheal effect of Galla Chinensis on the *Escherichia coli* heat-labile enterotoxin and ganglioside interaction," *Journal of Ethnopharmacology*, vol. 103, no. 3, pp. 385–391, 2006.

[11] R.-B. An, H. Oh, and Y.-C. Kim, "Phenolic constituents of Galla Rhois with hepatoprotective effects on tacrine- and nitrofurantoin-induced cytotoxicity in Hep G2 cells," *Biological & Pharmaceutical Bulletin*, vol. 28, no. 11, pp. 2155–2157, 2005.

[12] E.-A. Bae, M. J. Han, N.-J. Kim, and D.-H. Kim, "Anti-*Helicobacter pylori* activity of herbal medicines," *Biological and Pharmaceutical Bulletin*, vol. 21, no. 9, pp. 990–992, 1998.

[13] Y. Cai, Q. Luo, M. Sun, and H. Corke, "Antioxidant activity and phenolic compounds of 112 traditional Chinese medicinal plants associated with anticancer," *Life Sciences*, vol. 74, no. 17, pp. 2157–2184, 2004.

[14] X.-L. Huang, M.-D. Liu, J.-Y. Li, X.-D. Zhou, and J. M. Ten Cate, "Chemical composition of *Galla chinensis* extract and the effect of its main component(s) on the prevention of enamel demineralization *in vitro*," *International Journal of Oral Science*, vol. 4, no. 3, pp. 146–151, 2012.

[15] D. Duan, Z. Li, H. Luo, W. Zhang, L. Chen, and X. Xu, "Antiviral compounds from traditional Chinese medicines Galla Chinese as inhibitors of HCV NS3 protease," *Bioorganic & Medicinal Chemistry Letters*, vol. 14, no. 24, pp. 6041–6044, 2004.

[16] S.-H. Kim, H.-H. Park, S. Lee et al., "The anti-anaphylactic effect of the gall of *Rhus javanica* is mediated through inhibition of histamine release and inflammatory cytokine secretion," *International Immunopharmacology*, vol. 5, no. 13-14, pp. 1820–1829, 2005.

[17] S. Rayne and G. Mazza, "Biological activities of extracts from sumac (Rhus spp.): a review," *Plant Foods for Human Nutrition*, vol. 62, no. 4, pp. 165–175, 2007.

[18] S. Deiab, E. Mazzio, S. Messeha, N. Mack, and K. F. Soliman, "High-throughput screening to identify plant derived human LDH-A inhibitors," *European Journal of Medicinal Plants*, vol. 3, no. 4, pp. 603–615, 2013.

[19] Z.-Y. Wang, T. Y. Loo, J.-G. Shen et al., "LDH-A silencing suppresses breast cancer tumorigenicity through induction of oxidative stress mediated mitochondrial pathway apoptosis," *Breast Cancer Research and Treatment*, vol. 131, no. 3, pp. 791–800, 2012.

[20] M. I. Koukourakis, A. Giatromanolaki, and E. Sivridis, "Lactate dehydrogenase isoenzymes 1 and 5: differential expression by neoplastic and stromal cells in non-small cell lung cancer and other epithelial malignant tumors," *Tumor Biology*, vol. 24, no. 4, pp. 199–202, 2003.

[21] V. R. Fantin, J. St-Pierre, and P. Leder, "Attenuation of LDH-A expression uncovers a link between glycolysis, mitochondrial physiology, and tumor," *Cancer Cell*, vol. 9, no. 6, pp. 425–434, 2006.

[22] S. L. Sheng, J. J. Liu, Y. H. Dai, X. G. Sun, X. P. Xiong, and G. Huang, "Knockdown of lactate dehydrogenase A suppresses tumor growth and metastasis of human hepatocellular carcinoma," *FEBS Journal*, vol. 279, no. 20, pp. 3898–3910, 2012.

[23] L. M. Nilsson, T. Z. P. Forshell, S. Rimpi et al., "Mouse genetics suggests cell-context dependency for myc-regulated metabolic enzymes during tumorigenesis," *PLoS Genetics*, vol. 8, no. 3, Article ID e1002573, 2012.

[24] J. W. Jaroszewski, O. Kaplan, and J. S. Cohen, "Action of gossypol and rhodamine 123 on wild type and multidrug-resistant MCF-7 human breast cancer cells: 31P nuclear magnetic resonance and toxicity studies," *Cancer Research*, vol. 50, no. 21, pp. 6936–6943, 1990.

[25] T. Coyle, S. Levante, M. Shetler, and J. Winfield, "*In vitro* and *in vivo* cytotoxicity of gossypol against central nervous system tumor cell lines," *Journal of Neuro-Oncology*, vol. 19, no. 1, pp. 25–35, 1994.

[26] R. K. Koiri, S. K. Trigun, L. Mishra, K. Pandey, D. Dixit, and S. K. Dubey, "Regression of Dalton's lymphoma in vivo via decline in lactate dehydrogenase and induction of apoptosis by a ruthenium(II)-complex containing 4-carboxy *N*-ethylbenzamide as ligand," *Investigational New Drugs*, vol. 27, no. 6, pp. 503–516, 2009.

[27] A. W. Partin, J. L. Mohler, and D. S. Coffey, "Cell motility as an index of metastatic ability in prostate cancers: results with an animal model and with human cancer cells," in *Therapy for Genitourinary Cancer*, vol. 59 of *Cancer Treatment and Research*, pp. 121–130, 1992.

[28] N. K. Martin, E. A. Gaffney, R. A. Gatenby, and P. K. Maini, "Tumour-stromal interactions in acid-mediated invasion: a mathematical model," *Journal of Theoretical Biology*, vol. 267, no. 3, pp. 461–470, 2010.

[29] A. Le, C. R. Cooper, A. M. Gouw et al., "Inhibition of lactate dehydrogenase A induces oxidative stress and inhibits tumor progression," *Proceedings of the National Academy of Sciences of the United States of America*, vol. 107, no. 5, pp. 2037–2042, 2010.

[30] S. M. Evans, A. Casartelli, E. Herreros et al., "Development of a high throughput in vitro toxicity screen predictive of high acute in vivo toxic potential," *Toxicology In Vitro*, vol. 15, no. 4-5, pp. 579–584, 2001.

[31] V. Girish and A. Vijayalakshmi, "Affordable image analysis using NIH Image/ImageJ," *Indian Journal of Cancer*, vol. 41, no. 1, p. 47, 2004.

[32] P.-T. Kuo, T.-P. Lin, L.-C. Liu et al., "Penta-*O*-galloyl-β-D-glucose suppresses prostate cancer bone metastasis by transcriptionally repressing EGF-induced MMP-9 expression," *Journal of Agricultural and Food Chemistry*, vol. 57, no. 8, pp. 3331–3339, 2009.

[33] E. Jaszewska, A. Kosmider, A. K. Kiss, and M. Naruszewicz, "Oenothera paradoxa defatted seeds extract containing pentagalloylglucose and procyanidins potentiates the cytotoxicity of vincristine," *Journal of Physiology and Pharmacology*, vol. 61, no. 5, pp. 637–643, 2010.

[34] J.-E. Huh, E.-O. Lee, M.-S. Kim et al., "Penta-O-galloyl-beta-D-glucose suppresses tumor growth via inhibition of angiogenesis and stimulation of apoptosis: roles of cyclooxygenase-2 and mitogen-activated protein kinase pathways," *Carcinogenesis*, vol. 26, no. 8, pp. 1436–1445, 2005.

[35] Y. Cao, S. C. Evans, E. Soans, A. Malki, Y. Liu, and X. Chen, "Insulin receptor signaling activated by penta-*O*-galloyl-α-D-glucopyranose induces p53 and apoptosis in cancer cells," *Apoptosis*, vol. 16, no. 9, pp. 902–913, 2011.

[36] H. Hu, Y. Chai, L. Wang et al., "Pentagalloylglucose induces autophagy and caspase-independent programmed deaths in human PC-3 and mouse TRAMP-C2 prostate cancer cells," *Molecular Cancer Therapeutics*, vol. 8, no. 10, pp. 2833–2843, 2009.

[37] G.-S. Oh, H.-O. Pae, H. Oh et al., "In vitro anti-proliferative effect of 1,2,3,4,6-penta-O-galloyl-beta-D-glucose on human hepatocellular carcinoma cell line, SK-HEP-1 cells," *Cancer Letters*, vol. 174, no. 1, pp. 17–24, 2001.

[38] J. Zhang, L. Li, S.-H. Kim, A. E. Hagerman, and J. Lü, "Anti-cancer, anti-diabetic and other pharmacologic and biological activities of penta-galloyl-glucose," *Pharmaceutical Research*, vol. 26, no. 9, pp. 2066–2080, 2009.

[39] Y. Chai, H.-J. Lee, A. A. Shaik et al., "Penta-O-galloyl-β-D-glucose induces G_1 arrest and DNA replicative S-phase arrest independently of P21 cyclin-dependent kinase inhibitor 1A, P27 cyclin-dependent kinase inhibitor 1B and P53 in human breast cancer cells and is orally active against triple-negative xenograft growth," *Breast Cancer Research*, vol. 12, article R67, 2010.

[40] K. Alzoubi, S. Honisch, M. Abed, and F. Lang, "Triggering of suicidal erythrocyte death by penta-*O*-galloyl-β-D-glucose," *Toxins*, vol. 6, no. 1, pp. 54–65, 2013.

[41] C. D. Wu-Yuan, C. Y. Chen, and R. T. Wu, "Gallotannins inhibit growth, water-insoluble glucan synthesis, and aggregation of mutans streptococci," *Journal of Dental Research*, vol. 67, no. 1, pp. 51–55, 1988.

[42] L. Yi, Z. Li, K. Yuan et al., "Small molecules blocking the entry of severe acute respiratory syndrome coronavirus into host cells," *Journal of Virology*, vol. 78, no. 20, pp. 11334–11339, 2004.

[43] H. L. Seung, H.-H. Park, J.-E. Kim et al., "Allose gallates suppress expression of pro-inflammatory cytokines through attenuation of NF-κB in human mast cells," *Planta Medica*, vol. 73, no. 8, pp. 769–773, 2007.

[44] S. J. Lee, I. S. Lee, and W. Mar, "Inhibition of inducible nitric oxide synthase and cyclooxygenase-2 activity by 1,2,3,4,6-penta-O-galloyl-beta-D-glucose in murine macrophage cells," *Archives of Pharmacal Research*, vol. 26, no. 10, pp. 832–839, 2003.

[45] D. G. Kang, M. K. Moon, D. H. Choi, J. K. Lee, T. O. Kwon, and H. S. Lee, "Vasodilatory and anti-inflammatory effects of the 1,2,3,4,6-penta-*O*-galloyl-β-D-glucose (PGG) via a nitric oxide-cGMP pathway," *European Journal of Pharmacology*, vol. 524, no. 1–3, pp. 111–119, 2005.

[46] V. Estrella, T. Chen, M. Lloyd et al., "Acidity generated by the tumor microenvironment drives local invasion," *Cancer Research*, vol. 73, no. 5, pp. 1524–1535, 2013.

[47] I. Kareva and P. Hahnfeldt, "The emerging "hallmarks" of metabolic reprogramming and immune evasion: distinct or linked?" *Cancer Research*, vol. 73, no. 9, pp. 2737–2742, 2013.

[48] S. M. J. Fliedner, N. Kaludercic, X.-S. Jiang et al., "Warburg effect's manifestation in aggressive pheochromocytomas and paragangliomas: insights from a mouse cell model applied to human tumor tissue," *PLoS ONE*, vol. 7, no. 7, Article ID e40949, 2012.

[49] M. I. Koukourakis, E. Kontomanolis, A. Giatromanolaki, E. Sivridis, and V. Liberis, "Serum and tissue ldh levels in patients

with breast/gynaecological cancer and benign diseases," *Gynecologic and Obstetric Investigation*, vol. 67, no. 3, pp. 162–168, 2009.

[50] E. A. Mazzio, N. Boukli, N. Rivera, and K. F. A. Soliman, "Pericellular ph homeostasis is a primary function of the warburg effect: inversion of metabolic systems to control lactate steady state in tumor cells," *Cancer Science*, vol. 103, no. 3, pp. 422–432, 2012.

[51] H. Onozuka, K. Tsuchihara, and H. Esumi, "Hypoglycemic/hypoxic condition *in vitro* mimicking the tumor microenvironment markedly reduced the efficacy of anticancer drugs," *Cancer Science*, vol. 102, no. 5, pp. 975–982, 2011.

[52] F. Hirschhaeuser, U. G. A. Sattler, and W. Mueller-Klieser, "Lactate: a metabolic key player in cancer," *Cancer Research*, vol. 71, no. 22, pp. 6921–6925, 2011.

[53] K. M. A. Rouschop, L. Dubois, M. B. E. Schaaf et al., "Deregulation of cap-dependent mRNA translation increases tumour radiosensitivity through reduction of the hypoxic fraction," *Radiotherapy and Oncology*, vol. 99, no. 3, pp. 385–391, 2011.

[54] S. R. Kimball and L. S. Jefferson, "Signaling pathways and molecular mechanisms through which branched-chain amino acids mediate translational control of protein synthesis," *Journal of Nutrition*, vol. 136, no. 1, pp. 227S–231S, 2006.

Hindawi Publishing Corporation
Evidence-Based Complementary and Alternative Medicine
Volume 2015, Article ID 376029, 10 pages
http://dx.doi.org/10.1155/2015/376029

Research Article

Alterations in Salivary Proteome following Single Twenty-Minute Session of Yogic Breathing

Sundaravadivel Balasubramanian,[1] Michael G. Janech,[2] and Graham W. Warren[1,3]

[1]*Department of Radiation Oncology, Hollings Cancer Center, Medical University of South Carolina, Charleston, SC 29425, USA*
[2]*Division of Nephrology, Department of Medicine, Medical University of South Carolina, Charleston, SC 29425, USA*
[3]*Department of Cell and Molecular Pharmacology, Medical University of South Carolina, Charleston, SC 29425, USA*

Correspondence should be addressed to Sundaravadivel Balasubramanian; balasubr@musc.edu

Received 13 August 2014; Revised 5 December 2014; Accepted 22 December 2014

Academic Editor: Senthamil R. Selvan

Yogic breathing (YB) has been suggested to reduce stress and blood pressure and increase cognitive processes. However, alterations after YB at the molecular level are not well established. Twenty healthy volunteers were randomized into two groups ($N = 10$ per group): YB or attention controls (AC). The YB group performed two YB exercises, each for ten minutes, for a total of twenty minutes in a single session. AC group read a text of their choice for 20 minutes. Saliva was collected at baseline and at 5, 10, 15, and 20 minutes. Using Mass Spectrometry (MS), we initially found that 22 proteins were differentially expressed and then validated deleted in malignant brain tumor-1 (DMBT1) and Ig lambda-2 chain C region (IGLC2) using Western Blotting. DMBT1 was elevated in 7 of YB group by 10-fold and 11-fold at 10 and 15 minutes, respectively, whereas it was undetectable in the time-matched AC group ($P < 0.05$). There was a significant interaction between groups and time assessed by two-way ANOVA ($P < 0.001$). IGLC2 also showed a significant increase in YB group as measured by Western Blotting. These data are the first to demonstrate the feasibility of stimulating and detecting salivary protein biomarkers in response to an acute Yoga exercise. This trial is registered with ClincalTrials.gov NCT02108769.

1. Introduction

Cultural practices have long played an important role in human health. Incorporated into daily routines, food habits, ethics, sports, social activities, religious ceremonies, and festivities, these practices are considered to promote the overall well-being of individuals belonging to that cultural group [1]. Yoga is the collection of numerous mind-body techniques from the ancient Eastern cultural practices with the main theme of unification (the Tamil word "*okka*" or the Sanskrit word "*yok*" means to unite or equalize). Although practiced for its claimed benefits of healthy living and stress relief, the molecular mechanisms underlying how Yoga could improve health are only beginning to emerge. Yogic breathing (YB, also called *Pranayamam* or *Pranayama*) is one of the Yoga practices and is an active way of regulating breathing. Thirumoolar, a saint from ancient times, wrote Thirumanthiram, a Tamil literary work containing several Yogic and Tantric methods [2, 3]. There are 14 songs in Thirumanthiram specifically on Yogic breathing (verses 564–577). Although Yoga practitioners widely practice Pranayama techniques, the techniques of Thirumoolar have not yet been studied for their biological effects or molecular changes in biomarkers. Earlier physiological studies with other breathing regulation methods suggest that reducing the breathing frequency (around 15/min in normal adults [4]) could reduce blood pressure among heart failure patients [5]. As Pranayama leads to predominance in abdominal/diaphragmatic breathing [5–7], it increases vagal tone and parasympathetic dominance and decreases sympathetic discharges [8, 9].

Chanting Om is another type of YB, also called *Pranava Pranayama*. Chanting Om is an ancient cultural practice believed to improve physical and mental health. Early stage investigations on *Pranava Pranayama* suggest that it could (a) reduce heart rate and blood pressure in hypertensive patients [10], (b) promote physical and emotional well-being [11, 12],

(c) increase cutaneous peripheral vascular resistance [12], (e) induce vagal nerve stimulation (VNS) [13, 14], and (f) deactivate the limbic brain regions, amygdala, hippocampus, parahippocampal gyrus, insula, and orbitofrontal and anterior cingulate cortices and thalamus [12]. However, most if not all these studies are pilot in nature and therefore the results have to be validated for elucidating biological mechanism.

In this line recent studies have begun to unravel the molecular mechanisms of Yoga and other similar practices. For instance, in response to meditation, Black et al. reported the possible involvement of transcriptional regulation in peripheral blood lymphocytes indicative of overall reduction of stress response [15]. Similarly, Bhasin et al. have shown that Relaxation Response including Yoga, meditation, and repetitive prayer seems to improve mitochondrial resiliency by increasing the gene expression of ATPase and insulin function, while decreasing the gene expression of NF-κB associated stress response genes among practitioners [16]. Changes in gene expression following 2 hours of comprehensive Yoga practice involving postures, breathing, and meditation indicated significant change in gene expression in immune response genes in peripheral blood mononuclear cells [17]. Bower et al. have demonstrated a significant reduction in interferon-related transcription factors and NF-κB targets following 12-week Yoga intervention in breast cancer survivors [18]. These studies suggest that Yoga practices could potentially alter the expression of genes associated with inflammation and stress response. However, these studies have relied upon blood as the major source of biomarkers to study gene expression, and proteome level changes were not measured following Yoga practice. Moreover, the molecular mechanisms of Pranayama in isolation have not yet been studied in detail. Currently there are no established protein biomarkers to help measure the effects of YB on clinical outcomes or well-being. Identification of useful biomarkers would significantly increase the ability of differentiating objective from subjective responses reported by patients or participants in a study. Saliva is an easily accessed biological sample that contains numerous biomarkers including proteins, peptides, metabolites, mRNA, DNA, and miRNA of both human and oral microbial origin [19–22]. Due to the noninvasive nature and relative ease of sample collection, saliva has been increasingly recognized as a rich source of biomarkers useful in many diseases. For instance, salivary proteomic and mRNA profiling have identified significant differences between control and oral cancer subjects [23].

As salivation is one of the parasympathetic activation responses [24], we hypothesized that Pranayama might activate salivation and that the proteomic profile of saliva thus produced will be different from the basal saliva. Our initial mass spectrometry (MS) analysis revealed changes in the levels of 22 proteins following YB. To validate our MS data by Western Blotting, we chose the protein candidates deleted in malignant brain tumor 1 (DMBT1) and Ig lambda-2 chain C region (IGLC2) based on their abundance in saliva, spectral counts and level of statistical significance in MS data, and the roles of these proteins in immune regulation, epithelial differentiation, tumor suppression, and stress response [25, 26].

2. Methods

2.1. Human Subjects. A total of twenty healthy volunteers (male or female), aged 18 and above, were included in the study. The exclusion criteria were as follows: breathing problems (inability to breathe through nostrils, chronic bronchitis, emphysema, and asthma), speech problems that would prevent chanting, inability to listen and follow study exercise, sinus congestion, Sjogren's syndrome, chronic dry mouth due to medication or other conditions, and use of anticholinergic medications. Informed consent was obtained from each subject after initial interview. The study protocol was approved by the Institutional Review Board for Human Research, Medical University of South Carolina. Participants were enrolled after informed written consent. Recruitment of participants was carried out in Charleston Metro area from August 15, 2013, to October 31, 2013. The protocol requires the participant to attend only one 20-minute session with no follow-up. This study is registered at the ClinicalTrials.gov. This study was not registered prior to enrollment of participants owing to the small number of participants required for the protocol. The authors confirm that all ongoing and related trials for this drug/intervention are registered.

Enrolled participants were randomized to one of 2 conditions: Yogic breathing (YB) arm versus the Attention Control (AC) arm (see Figure 1 for CONSORT flowchart). Randomization was conducted in collaboration with a biostatistician to ensure equal gender distribution in the 2 experimental groups (YB versus AC). All the participants were tested one-on-one with a trained Yoga instructor. Prior to exercise and sample collection, the Yoga instructor taught each subject how to perform YB.

3. Treatment Conditions

3.1. Yogic Breathing. The YB exercise design is depicted in Figure 2. The study Yoga instructor taught the subjects how to perform the YB exercises, which consist of Om Chanting and Thirumoolar Pranayamam as detailed below.

3.1.1. Chanting Om. The subjects were seated in a chair with eyes closed while chanting. The subjects performed Chanting Om as follows: (a) long deep inhalation through both nostrils at the same time and (b) slow exhalation while chanting "Om." These two steps were repeated continuously for 10 min with a brief interruption at 5 minutes to collect saliva. Saliva was immediately placed on ice after collection.

3.1.2. Thirumoolar Pranayamam (TP). Following the chanting, the subjects performed TP as follows, as instructed by the Yoga instructor based on Thirumanthiram (verse 568) [2, 3]: During TP, the inhalation/holding/exhalation cycles each lasting in seconds were counted as follows using the combination of chanting and counting with fingers. Repeatedly chant a phrase within mind (e.g., "*I'm beautiful,*" "*I'm relaxed,*" "*Om Namasivaya,*" etc.) for two times (inhalation), eight times (holding), and four times (exhalation). (a) Close right nostril and inhale through left nostril for two chants

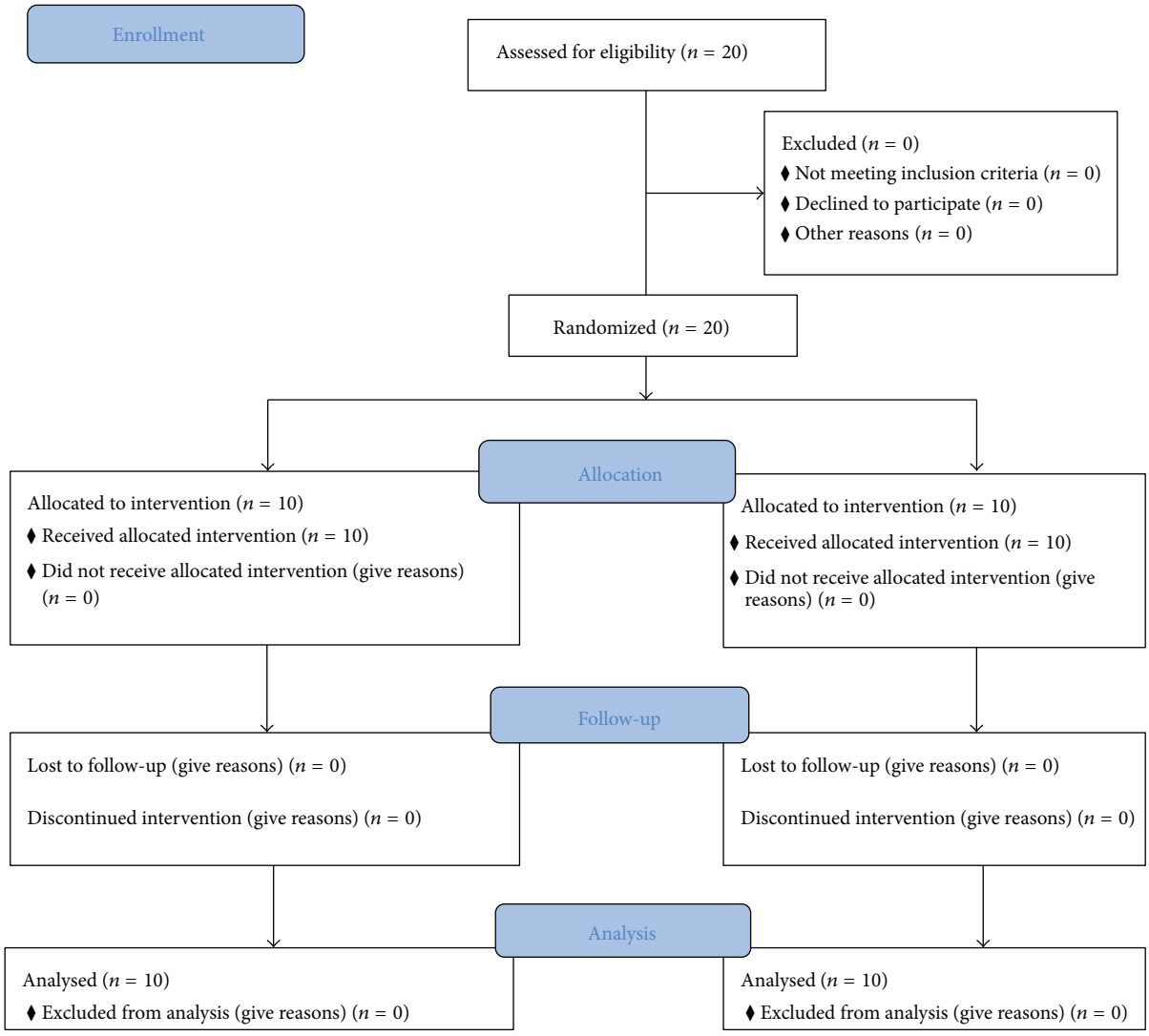

Figure 1: CONSORT flowchart. Details of the overall trial design.

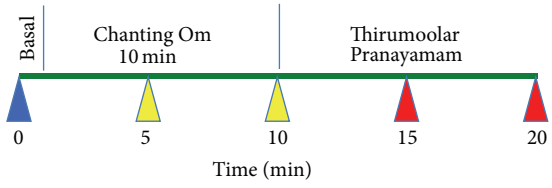

Figure 2: Yogic breathing intervention. Yogic breathing exercise contains two phases, namely, Chanting Om and Thirumoolar Pranayamam, each for 10 minutes. Saliva sample is collected starting from 0 min and every five minutes as shown.

and then close both nostrils so that no inhaled air escapes. (b) Hold breath in this position for eight chants mentally. (c) Open right nostril and exhale for four chants. Complete exhalation is required. (d) Go to step (a) and repeat. The subjects performed TP for 10 min. Salivary samples were collected at 5 and 10 minutes of TP (see below). Thus each individual provided the following five saliva samples: basal (0 min), Chanting Om (5, 10 min), and TP (15, 20 min).

3.2. Attention Control Group. Attention Control subjects performed quiet reading for 20 min in a seated position in the presence of the Yoga instructor. Saliva samples were collected at 0, 5, 10, 15, and 20 min similar to the YB group.

3.3. Collection of Saliva Samples. Salivary samples were collected once at the beginning of the protocol (Time 0) while the subjects are seated. Samples were subsequently collected at 5, 10, 15, and 20 min from both groups of participants. Saliva was naturally allowed to accumulate in the oral cavity and the participant discharged (1–4 mL) into the 15 mL polystyrene specimen tube with lid. Samples were immediately cooled on ice and stored at −80°C until analysis within 15 minutes of collection.

3.4. Liquid Chromatography-Tandem Mass Spectrometry (LC-MS-MS). For initial LC-MS-MS analysis we used saliva samples from a single individual, the Yoga instructor and the author of this paper. The saliva sample was collected before and after 20 minutes of YB exercise done on six different days. Protein concentration in raw saliva was determined using the Bio-Rad protein assay based on the Bradford method (Bio-Rad, Hercules, CA). For each sample, 100 μgs protein was diluted in 100 μLs mass spectrometry grade water. To the diluted protein, 100 μLs ammonium bicarbonate (100 mM) was added and the sample was vortexed. Proteins were reduced using 5 mM dithiothreitol and heated to 60°C for 30 minutes. Samples were allowed to cool to room temperature and proteins were alkylated using 12 mM iodoacetamide at room temperature for 30 minutes. Trypsin (Trypsin Gold, Promega) was added to each sample at a ratio of 1 : 50 and incubated at 37°C for 18 hours. Samples were acidified using formic acid to a final concentration to 0.1% and peptides were passed over a conditioned solid phase cartridge (Strata-X, Phenomenex, 60 mg/mL). Peptides were washed with 0.1% formic acid and eluted in 50% acetonitrile/0.1% formic acid. Peptides were dried by centrifugal vacuum and resuspended in 0.1% formic acid. Peptide concentration was estimated by absorbance at 280 nm and all samples were diluted with equal volumes of 0.1% formic acid to a final concentration of 0.4 μg/μL.

Peptides (4 μg) were trapped onto an Acclaim PepMap100 trap column (100 μm ID × 2 cm, C18, 5 μm, 100 Å, Thermo Scientific) using 100% mobile phase A (MPA, 98% water, 0.1% formic acid, 2% acetonitrile) at a flow rate of 5 μL/min, for 5 minutes. Trapped peptides were separated on an Acclaim PepMap100 analytical column (75 μm ID × 15 cm, C18, 3 μm, 100 Å, Thermo Scientific) using an Eksigent NanoLC Ultra System. A gradient of mobile phase B (MPB, 2% water, 0.1% formic acid, 95% acetonitrile) to MPA was increased from 5% to 40% over 40 minutes and then increased from 40% to 80% over 10 minutes. Peptides were introduced into a nanosource and tandem mass spectrometry was performed using an AB SCIEX Triple TOF 5600 mass spectrometer (ABSCIEX, Framingham, MA). Data were collected in information dependent acquisition mode with the following parameters: 250-millisecond MS accumulation time, 100-millisecond product ion accumulation time, 20-ion selected per cycle, total cycle time of 1.3 seconds, charge states for selection = +2 to +4, 6-second exclusion after one occurrence, and rolling collision energy. The scanning windows for the TOF-MS and product ion scans were 300 to 1250 and 100 to 1600 m/z, respectively. Time of flight collision energy was set to 10 and declustering potential was set to 100.

3.5. Protein Identification and Quantification. Acquired raw data (.wiff) was converted to .MGF format using the AB SCIEX converter (version 1.2 beta). MGF files were searched against the 2012_1 release of the Human UniProtKB/Swiss-Prot database (37,303 entries) with addition of proteins from the common Repository of Adventitious Proteins database (cRAP; 2012.01.01; the Global Proteome Machine, 112 entries) using the Mascot search engine. The following parameters were selected: Digestion Enzyme, semitrypsin; parent ion tolerance, 20 ppm; fragment ion tolerance, 0.25 Da; fixed modification, carbamidomethyl(C); variable modification, pyro-Glu(Q), oxidation(M). Mascot search results were uploaded to Scaffold (version 3.1.2, Proteome Software Inc., Portland, OR) and scored by Peptide Prophet and Protein Prophet algorithms. Peptide threshold was set to 80%, protein threshold was set to 99.9%, and minimum 2 peptides were required resulting in a false-discovery rate equal to 0.8%. Protein spectral counts were normalized to total spectral counts using the "quantitative value" tool. Spectral count values of 0 were given a minimum value of 1. The gene ontology tool was utilized in Scaffold to categorize proteins.

3.6. Western Blotting. Western Blotting was performed as previously described [27, 28]. Briefly, 100 μL of saliva samples was mixed with equal volume of 2X SDS-sample buffer and heated at 95°C for 5 min for denaturation. After centrifugation for 5 min at 14,000 rpm at room temperature (RT), 20 μL of the denatured samples was resolved on 4–12% Bis-Tris gel with MOPS running buffer (Life Technologies) and transferred to PVDF membranes. Membranes were blocked with 2% BSA in Tris-buffered saline containing 0.05% Tween (TBST) for 1 h at RT and incubated with 1 : 1000 diluted primary antibodies: DMBT1 (sc-28239, Santa Cruz Biotechnology) and Ig lambda-2 chain C region (MAB219P, Maine Biotechnology Services) overnight at 4°C. After washing and incubation for 1 hour at RT with the secondary antibodies conjugated to horse radish peroxidase (1 : 10,000 dilution), the bands were visualized using enhanced chemiluminescence. The membrane was then stained with Ponceau S (Sigma) to determine protein loading. The scanned images of the Western Blots were quantified using NIH ImageJ. The DMBT1 protein levels were normalized to Ponceau S staining and represented as graph.

3.7. Statistical Analysis. Comparisons were performed between baseline and specific time points (5, 10, 15, and 20 min after YB). Pre- and postmeasurements were analyzed using a paired t-test because all comparisons passed normality testing (Shapiro-Wilk test). Differences were accepted when $P < 0.05$. For Western Blot analysis, a two-way repeated measures ANOVA was utilized. Values were log-transformed prior to statistical analysis. Pairwise post hoc comparisons were made using the Holm-Sidak test. Differences were accepted when $P < 0.05$.

4. Results

All the participants enrolled and randomized completed the trial. There is no dropout or adverse effects.

4.1. Discovery Proteomic Study. Label-free proteomics resulted in a total of 133 proteins identified at a protein false-discovery rate of 0.8%. Gene ontology (GO) annotation categorized 93 out of 133 (70%) proteins under the head node, biological process, in the selected GO term: cellular process. A little more than a quarter of the proteins within this head

Table 1: Differentially abundant proteins based on normalized spectral counts for the pre- and post-Yogic breathing samples. Protein identification was assigned by MASCOT search (FDR < 1%). Uniprot #: accession number from Uniprot for each protein. MW: predicted molecular weight. $\log_2$FC: average ratio of normalized spectral counts after Yoga divided by those before Yoga for each respective time point. *P* value: probability value for paired *t*-test.

Protein identification	Uniprot #	MW	$\log_2$FC	*P* value
Ig lambda-2 chain C regions	P0CG05	11 kDa	1.1	0.000
Mucin-7	Q8TAX7	39 kDa	0.8	0.002
Alpha-2-macroglobulin-like protein 1	A8K2U0	161 kDa	−1.4	0.006
Deleted in malignant brain tumors 1 protein	Q9UGM3	261 kDa	1.1	0.010
Immunoglobulin J chain	P01591	18 kDa	1.8	0.010
Ig alpha-1 chain C region	P01876	38 kDa	1.5	0.012
Ig mu chain C region	P01871	49 kDa	3.8	0.015
Ig heavy chain V-III region BRO	P01766	13 kDa	3.1	0.016
Cystatin-S	P01036	16 kDa	0.5	0.016
Keratin, type I cytoskeletal 10	P13645	59 kDa	−1.7	0.017
Prolactin-inducible protein	P12273	17 kDa	0.7	0.018
Ig alpha-2 chain C region	P01877	37 kDa	1.3	0.018
Keratin, type II cytoskeletal 5	P13647	62 kDa	−1.8	0.022
Glyceraldehyde-3-phosphate dehydrogenase	P04406	36 kDa	−1.1	0.020
Kallikrein-1	P06870	29 kDa	2.9	0.026
UPF0762 protein C6orf58	Q6P5S2	38 kDa	1.5	0.028
Ig kappa chain C region	P01834	12 kDa	1.0	0.029
Cystatin-B	P04080	11 kDa	−1.2	0.033
Ig heavy chain V-III region TUR	P01779	12 kDa	1.6	0.038
Cysteine-rich secretory protein 3	P54108	28 kDa	2.3	0.045
Zymogen granule protein 16 homolog B	Q96DA0	23 kDa	1.1	0.049
Keratin, type II cytoskeletal 6A	P02538	60 kDa	0.1	0.049

node (36/133, 27%) belonged to immune system process. The majority of proteins in the cellular compartment head node (74/133, 56%) were assigned to the extracellular region.

Comparison of proteins by normalized spectral counting revealed significant changes in 22 proteins (Table 1) following YB in a single participant who repeated the study Yogic Breathing exercises on six different days. Five proteins were lower in abundance and 17 proteins were elevated ranging from −1.8 to 3.8 mean fold change. The majority of statistically significant proteins (36%) belong to the immunoglobulin family and every member identified in this group was elevated.

4.2. Targeted Western Blots. Expression of salivary DMBT1 using Western Blot analysis is shown for all of the samples from YB group (Figure 3(a)) and AC group (Figure 4(a)). Elevated expression of DMBT1 was observed in 7 out of 10 subjects from the YB group and none in the AC group. Elevations in DMBT1 level were observed as early as 5 min and sustained through 15 min in all participants who demonstrated elevated DMBT1 following YB. In 4 of the 7 participants with elevated DMBT1, the increase in expression was reversed by 20 min following YB suggesting that the effects of YB on DMBT1 expression may be acute.

Relative DMBT1 levels as determined by densitometry were different between AC and YB groups (Figure 5). There was a significant interaction between groups and time assessed by two-way ANOVA ($P < 0.001$). Both AC and YB groups were similar at baseline (0 min). DMBT1 was elevated by 10-fold and 11-fold at 10 and 15 minutes, respectively, in the YB group compared to the time-matched AC group ($P < 0.05$; Holm-Sidak pairwise comparison). Absolute elevations in DMBT1 expression by Western Blot were comparable in magnitude to elevations noted by LC-MS-MS.

Further Western Blotting analysis on another candidate protein, IGLC2, with high spectral count in MS, fold change, and the level of statistical significance, showed a marked increase upon YB (Figure 6(a)). All of the 10 participants from the YB group showed an increase in IGLC2, where the overall level in two participants (numbers 9 and 10) was low. The increase was evident as early as 5 minutes. The level of IGLC2 returned to near basal by the end of 20 minutes of exercise except in two cases (numbers 1 and 3). This suggests that YB induces mainly a transient increase in IGLC2 level. It is interesting to note that, among AC subjects, two of them have a noticeable increase in IGLC2 level (numbers 15 and 19), whereas the rest of them did not show a market increase (Figure 6(b)). We further analyzed if Carbonic Anhydrase that did not have a significant change in mass spectrometry data could be useful as a loading control. However, due to variations within and between groups, we chose to use Ponceau S stain (Figures 3(b) and 4(b)) as loading control similar to previous studies [29]. Together, our data indicate

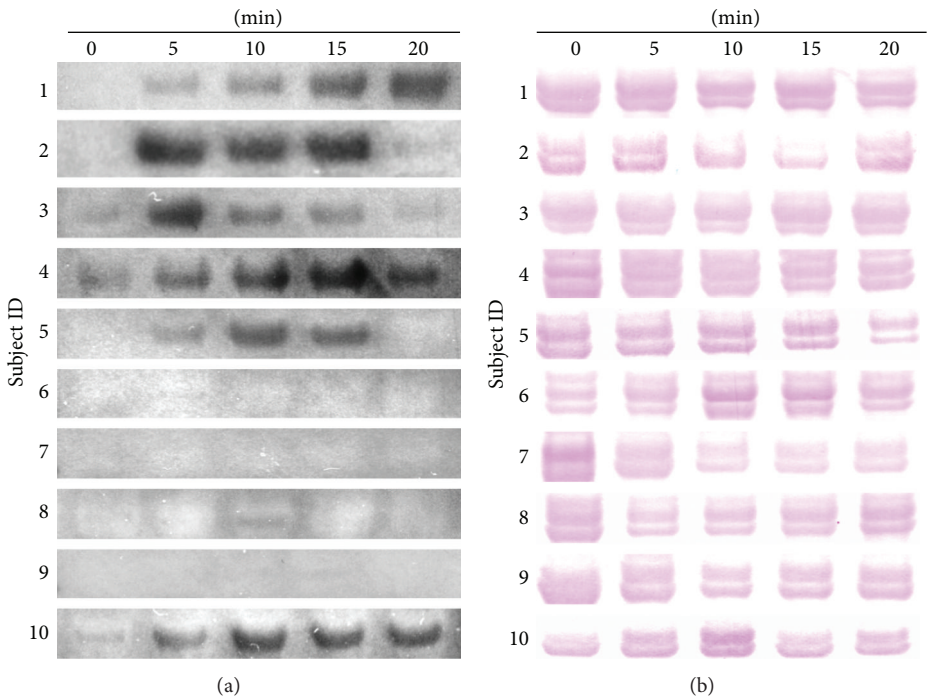

Figure 3: Increased salivary DMBT1 abundance in Yogic breathing participants. Saliva from Yogic breathing group participants (n = 10) was collected at indicated time points. Equal volumes of saliva were loaded and analyzed by Western Blotting with DMBT1 antibody as described under Methods. DMBT1 band around 220 kDa is shown (a). The same membrane was stained with Ponceau S and shown for loading control (b).

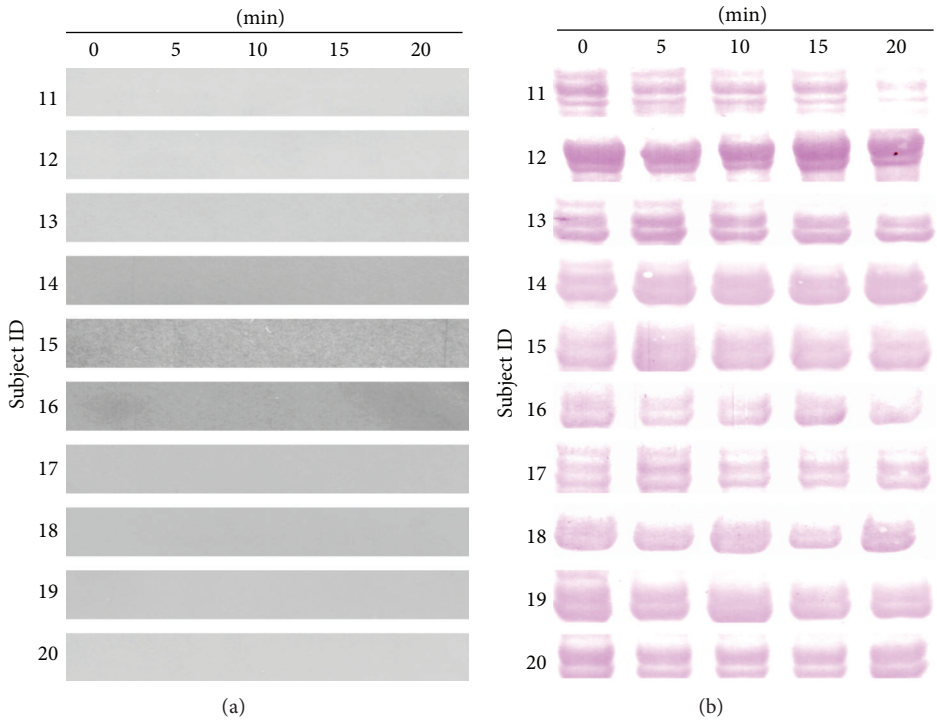

Figure 4: Undetectable salivary DMBT1 level in Attention Control participants. Saliva from Attention Control group participants (n = 10) was collected at indicated time points. Equal volumes of saliva were loaded and analyzed by Western Blotting with DMBT1 antibody as described under Methods. There was no DMBT1 band detected (a). The same membrane was stained with Ponceau S and shown for loading control (b).

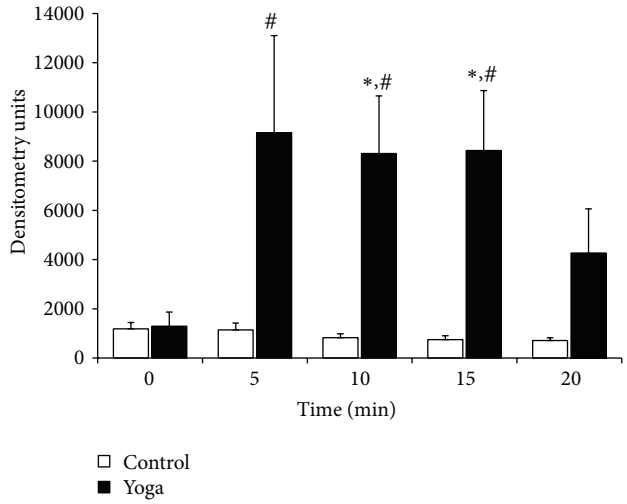

Figure 5: Pooled densitometry data of DMBT1 Western Blots. Protein abundance was quantified by densitometry from Western Blotting (Figures 3(a) and 4(a)) and data are presented as Mean ± Standard Error of relative units. ∗ indicates $P < 0.05$ control versus Yogic breathing group for each respective time point. # indicates $P < 0.05$ for Yogic breathing participants at the indicated time point versus time zero. Statistical differences were determined by two-way ANOVA with Holms-Sidak post hoc test.

that acute single session practice of Yogic Breathing when compared to Attention Control could stimulate alterations in salivary proteome.

5. Discussion

To the best of our knowledge this is the first time a salivary proteomic study has been applied to assess the physiological outcomes of Yogic Breathing. Yoga studies so far have relied mainly on subjective measures (e.g., quality of life questionnaire) and physiological outcomes such as blood pressure to determine the effectiveness of Yoga intervention. Recently, gene expression studies in peripheral blood following Yoga practice have identified a number of genes involved in metabolism, energy regulation, stress, and inflammation [15–18]. Saliva has been used only in the analysis of cortisol as a measure of stress in a recent Yoga study (6 wk Yoga with 1, 3, and 6 months of follow-up) among cancer patients [30]. We hypothesized that YB could acutely produce salivary biomolecules with key biological functions immediately after practice. We have recently reported that the study YB exercises induce nerve growth factor expression in saliva [31]. We expected that YB might alter the status of other biomarkers as well in saliva. Our initial LC-MS-MS analysis was conducted in a trained Yoga instructor before and after 20 min of YB regimen to identify potential markers that could then be analyzed in larger samples. Thus, our initial proteomic analysis showed a significant increase in the acute expression of molecules belonging to GO terms cellular processes, immune response, and those molecules were found mainly in the extracellular space. Of these molecules, several molecules belong to the Ig superfamily, suggesting that YB induces these molecules to promote immune response as a first line of defense in the mucosa. Interestingly, there were four tumor suppressors significantly stimulated after YB, namely, deleted in malignant brain tumor 1 (DMBT1), mucin-7 (MUC7), cysteine-rich secretory protein 3 (CRISP3), and prolactin-inducible protein (PIP). Notably all the above four proteins were found to be downregulated in a recent tumor suppressor gene analysis in oral squamous cell carcinoma using whole-genome analysis [32]. Based on the relatively well-defined multifunctional characteristics including immune regulation, epithelial differentiation, and tumor suppression in a number of tumors, we chose DMBT1 and IGLC2 to analyze further Yogic breathing samples obtained from the clinical trial. The expression data of DMBT1 and IGLC2 strongly indicate that YB significantly induces changes in these proteins in YB group when compared with AC group. The basal level of DMBT1 was different within YB group where only 3 of the YB group participants (numbers 3, 4, and 10) showed a detectable basal DMBT1 level whereas none in the AC group showed a detectable DMBT1 band. This could be due to several reasons including basal physiological variation of DMBT1 level or the psychological induction during randomization or other dietary and/or environmental factors that could not be accounted for in this study protocol.

DMBT1 is a product of *dmbt1* gene, which also codes for gp340/salivary agglutinin (SAG), an alternatively spliced variant from scavenger-receptor cysteine-rich (SRCR) superfamily. This gene also codes for a number of orthologs including Hensin, Ebnerin, CRP-ductin, and BGM/H3 [26]. DMBT1 is expressed in saliva, tears, breast milk, and gastrointestinal, genital, and pulmonary tract (reviewed in [33]). DMBT1 plays an important role in epithelial cell differentiation by binding to galectin-3. This binding is also considered important for activating the Notch signaling pathway and for the angiogenesis at the vascular extracellular matrix [34]. DMBT1 mediates innate immune response by binding to the bacterial and viral antigens. Binding of soluble DMBT1 is known to reduce the infectivity of HIV1 [35] as well as influenza A [36] viruses. DMBT1 has 14 SRCR domains and binds to a broad range of bacteria owing to the presence of common binding motif (RVELYxxxSW) within its SRCR domains [37]. DMBT1 is also shown to activate the complement pathway, further supporting its role in innate immune system [38].

In addition, DMBT1 is significantly downregulated in a number of cancers affecting multiple organs including brain, lungs, pancreas, oral cavity, prostate, cervix, and skin [26]. The reduced level of DMBT1 expression at the tumor site is attributed to the gene deletion of *dmbt1* in tumor cells. Incidentally, *dmbt1* gene is located within Chromosome 10q similar to PTEN, another tumor suppressor, implicating both of these molecules as important biomarkers in cancer prognosis. In fact, *dmbt1* is proposed as a breast cancer causative gene [39]. Stimulating salivary DMBT1 by a nonpharmacologic, noninvasive, behavioral intervention such as YB could hold several health benefits including maintenance of an effective innate immune system and production of tumor suppressors de novo. Although we have shown an increase of DMBT1 in saliva following YB, the possible mechanisms through

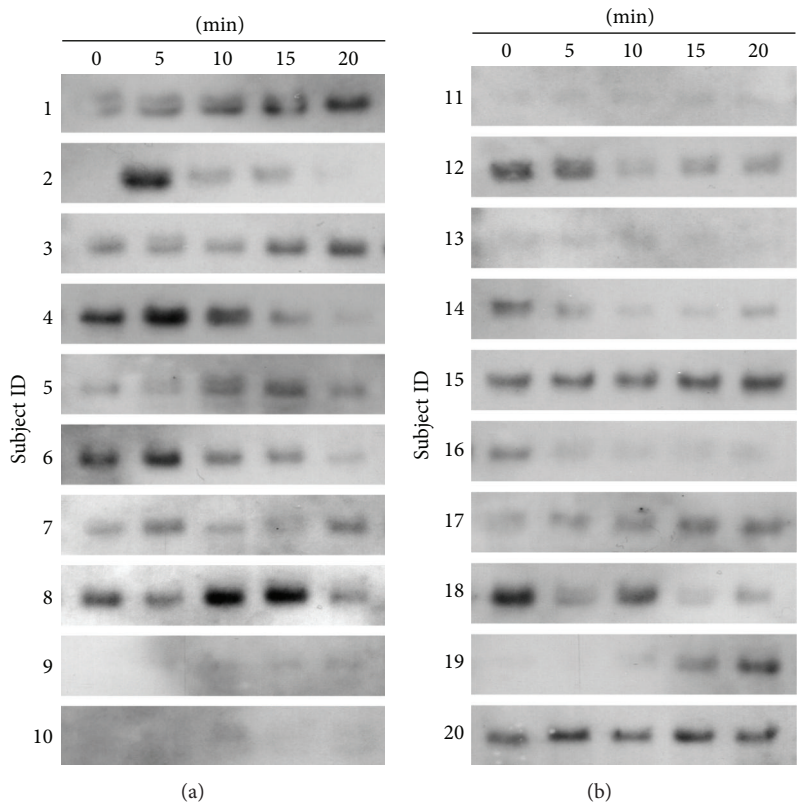

Figure 6: Level of IGLC2 in saliva from Yogic breathing and Attention Control groups. Saliva from Yogic breathing group (a) and Attention Control group (b) participants ($n = 10$ each) was collected at indicated time points. Equal volumes of saliva were loaded and analyzed by Western Blotting with IGLC2 antibody as described under Methods.

which this happens are unknown. Signals emanating from extracellular matrix, epigenetic control (e.g., methylation [40]), and intracellular mechanisms could account for this induction. Moreover, as DMBT1 is a secretory protein, the increased level we observe in 5 minutes after YB could be due to the release from the secretory granules of ductal and acinar cells of the salivary glands.

Similarly, the increase in IGLC2 from our data is the first of its kind for this molecule to be tested in YB setting. IGLC2 level is increased in all the YB participants (although the level is low in two participants) but not in eight of the AC group participants. The reason why two participants from AC group have higher levels of IGLC2 is unclear. One could speculate that mere calming down (sitting and reading) might have an effect on IGCL2 in select participants. It is interesting to note that the majority of proteins (36%) that are significantly altered upon YB belong to the immunoglobulin superfamily. IGLC2 is encoded by chromosome 22 and is increased in several pathological conditions including HIV infection [41], multiple myeloma [42], and influenza A virus infection [43], suggesting that this induction could be involved in protection against infection and immune response. Although serum has higher kappa/lambda ratio, in mucosal secretions, such as saliva, this ratio is significantly reduced [25] suggesting the importance of IGLC2 in mucosal defense. Together, our data indicate that YB could increase salivary secretion that contains proteins with key roles in immune response. Further studies with large population are necessary to further validate these data. As one of the first studies in this area, our study has few limitations: the small number of subjects tested and that this is not a double-blinded study as the participants when informed that they are assigned to YB group might have had some elevation in basal DMBT1 due to psychological stimulation that is not related to the YB exercise per se. Mindful of these limitations, future studies could be focused, for example, to analyze if YB could stimulate DMBT1 in cancer patients and if YB could facilitate the availability of DMBT1 in tumor sites where DMBT1 is downregulated.

In conclusion, for the first time we are showing that an acute Yogic Breathing practice induces changes in levels of salivary proteins of significance to immune response and cancer. Future *Omic* studies using saliva as a source in individuals after both acute and long-term practice of various Yoga techniques could explain molecular mechanisms through which several Yoga techniques may work.

Conflict of Interests

The authors declare that there is no conflict of interests regarding the publication of this paper.

Acknowledgments

This study was supported by Voucher Award (to Sundaravadivel Balasubramanian) from South Carolina Clinical and Translational Research Institute through NIH/NCRR Grant nos. UL1 RR029882 and UL1 TR000062. Sundaravadivel Balasubramanian thanks Dr. Dhandapani Kuppuswamy for providing lab supplies for part of this study. The authors greatly appreciate mass spectrometry technical assistance by Ms. Alison Bland and Dr. John Arthur of the Nephrology Proteomics Laboratory.

References

[1] J. Engebretson, "Culture and complementary therapies," *Complementary Therapies in Nursing and Midwifery*, vol. 8, no. 4, pp. 177–184, 2002.

[2] S. Rajalakshmi and G. Veluchamy, "Kaya Kalpa methods adopted by Siddars: a scientific approach," *Bulletin of the Indian Institute of History of Medicine*, vol. 30, no. 2, pp. 103–110, 2000.

[3] S. Thirumular, *Tirumanthiram English Translation of Tamil Spiritual Classic*, Himalayan Academy Publications, Kapaa, Hawaii, USA.

[4] L. Bernardi, J. Wdowczyk-Szulc, C. Valenti et al., "Effects of controlled breathing, mental activity and mental stress with or without verbalization on heart rate variability," *Journal of the American College of Cardiology*, vol. 35, no. 6, pp. 1462–1469, 2000.

[5] L. Bernardi, C. Porta, L. Spicuzza et al., "Slow breathing increases arterial baroreflex sensitivity in patients with chronic heart failure," *Circulation*, vol. 105, no. 2, pp. 143–145, 2002.

[6] J. Kitko, "Rhythmic breathing as a nursing intervention," *Holistic Nursing Practice*, vol. 21, no. 2, pp. 85–88, 2007.

[7] N. Vallath, "Perspectives on Yoga inputs in the management of chronic pain," *Indian Journal of Palliative Care*, vol. 16, no. 1, pp. 1–7, 2010.

[8] R. Bhargava, M. G. Gogate, and J. F. Mascarenhas, "Autonomic responses to breath holding and its variations following pranayama," *Indian Journal of Physiology and Pharmacology*, vol. 32, no. 4, pp. 257–264, 1988.

[9] A. N. Sinha, D. Deepak, and V. S. Gusain, "Assessment of the effects of pranayama/alternate nostril breathing on the parasympathetic nervous system in young adults," *Journal of Clinical and Diagnostic Research*, vol. 7, no. 5, pp. 821–823, 2013.

[10] A. B. Bhavanani, Madanmohan, Z. Sanjay, and I. V. Basavaraddi, "Immediate cardiovascular effects of pranava pranayama in hypertensive patients," *Indian Journal of Physiology and Pharmacology*, vol. 56, no. 3, pp. 273–278, 2012.

[11] S. Telles, R. Nagarathna, and H. R. Nagendra, "Autonomic changes during 'OM' mediation," *Indian Journal of Physiology and Pharmacology*, vol. 39, no. 4, pp. 418–420, 1995.

[12] B. Kalyani, G. Venkatasubramanian, R. Arasappa et al., "Neurohemodynamic correlates of 'OM' chanting: a pilot functional magnetic resonance imaging study," *International Journal of Yoga*, vol. 4, no. 1, pp. 3–6, 2011.

[13] C. A. Merrill, M. A. G. Jonsson, L. Minthon et al., "Vagus nerve stimulation in patients with Alzheimer's disease: additional follow-up results of a pilot study through 1 year," *The Journal of Clinical Psychiatry*, vol. 67, no. 8, pp. 1171–1178, 2006.

[14] T. Kraus, K. Hösl, O. Kiess, A. Schanze, J. Kornhuber, and C. Forster, "BOLD fMRI deactivation of limbic and temporal brain structures and mood enhancing effect by transcutaneous vagus nerve stimulation," *Journal of Neural Transmission*, vol. 114, no. 11, pp. 1485–1493, 2007.

[15] D. S. Black, S. W. Cole, M. R. Irwin et al., "Yogic meditation reverses NF-κB and IRF-related transcriptome dynamics in leukocytes of family dementia caregivers in a randomized controlled trial," *Psychoneuroendocrinology*, vol. 38, no. 3, pp. 348–355, 2013.

[16] M. K. Bhasin, J. A. Dusek, B.-H. Chang et al., "Relaxation response induces temporal transcriptome changes in energy metabolism, insulin secretion and inflammatory pathways," *PLoS ONE*, vol. 8, no. 5, Article ID e62817, 2013.

[17] S. Qu, S. M. Olafsrud, L. A. Meza-Zepeda, and F. Saatcioglu, "Rapid gene expression changes in peripheral blood lymphocytes upon practice of a comprehensive yoga program," *PLoS ONE*, vol. 8, no. 4, Article ID e61910, 2013.

[18] J. E. Bower, G. Greendale, A. D. Crosswell et al., "Yoga reduces inflammatory signaling in fatigued breast cancer survivors: a randomized controlled trial," *Psychoneuroendocrinology*, vol. 43, pp. 20–29, 2014.

[19] W. M. Edgar, "Saliva: its secretion, composition and functions," *British Dental Journal*, vol. 172, no. 8, pp. 305–312, 1992.

[20] A. Zhang, H. Sun, P. Wang, and X. Wang, "Salivary proteomics in biomedical research," *Clinica Chimica Acta*, vol. 415, pp. 261–265, 2013.

[21] B. L. Schulz, J. Cooper-White, and C. K. Punyadeera, "Saliva proteome research: current status and future outlook," *Critical Reviews in Biotechnology*, vol. 33, no. 3, pp. 246–259, 2013.

[22] J. M. Yoshizawa and D. T. W. Wong, "Salivary microRNAs and oral cancer detection," *Methods in Molecular Biology*, vol. 936, pp. 313–324, 2013.

[23] F. D. Shah, R. Begum, B. N. Vajaria et al., "A review on salivary genomics and proteomics biomarkers in oral cancer," *Indian Journal of Clinical Biochemistry*, vol. 26, no. 4, pp. 326–334, 2011.

[24] G. B. Proctor and G. H. Carpenter, "Salivary secretion: mechanism and neural regulation," *Monographs in Oral Science*, vol. 24, pp. 14–29, 2014.

[25] C. M. Mole, M. C. Bene, P. M. Montagne, E. Seilles, and G. C. Faure, "Light chains of immunoglobulins in human secretions," *Clinica Chimica Acta*, vol. 224, no. 2, pp. 191–197, 1994.

[26] V. G. Martínez, S. K. Moestrup, U. Holmskov, J. Mollenhauer, and F. Lozano, "The conserved scavenger receptor cysteine-rich super family in therapy and diagnosis," *Pharmacological Reviews*, vol. 63, no. 4, pp. 967–1000, 2011.

[27] S. Balasubramanian, L. Quinones, H. Kasiganesan et al., "β3 integrin in cardiac fibroblast is critical for extracellular matrix accumulation during pressure overload hypertrophy in mouse," *PLoS ONE*, vol. 7, no. 9, Article ID e45076, 2012.

[28] S. Balasubramanian, S. K. Mani, H. Kasiganesan, C. C. Baicu, and D. Kuppuswamy, "Hypertrophic stimulation increases β-actin dynamics in adult feline cardiomyocytes," *PLoS ONE*, vol. 5, no. 7, Article ID e11470, 2010.

[29] R. Aviner, T. Geiger, and O. Elroy-Stein, "Genome-wide identification and quantification of protein synthesis in cultured cells and whole tissues by puromycin-associated nascent chain proteomics (PUNCH-P)," *Nature Protocols*, vol. 9, no. 4, pp. 751–760, 2014.

[30] K. D. Chandwani, G. Perkins, H. R. Nagendra et al., "Randomized, controlled trial of yoga in women with breast cancer undergoing radiotherapy," *Journal of Clinical Oncology*, vol. 32, no. 10, pp. 1058–1065, 2014.

[31] S. Balasubramanian, J. E. Mintzer, and A. E. Wahlquist, "Induction of salivary nerve growth factor by Yogic breathing: a randomized controlled trial," *International Psychogeriatrics*, vol. 27, no. 1, pp. 168–170, 2014.

[32] W.-C. Ko, K. Sugahara, T. Sakuma et al., "Copy number changes of CRISP3 in oral squamous cell carcinoma," *Oncology Letters*, vol. 3, no. 1, pp. 75–81, 2012.

[33] A. J. M. Ligtenberg, E. C. I. Veerman, A. V. N. Amerongen, and J. Mollenhauer, "Salivary agglutinin/glycoprotein-340/DMBT1: a single molecule with variable composition and with different functions in infection, inflammation and cancer," *Biological Chemistry*, vol. 388, no. 12, pp. 1275–1289, 2007.

[34] H. Müller, J. Hu, R. Popp et al., "Deleted in malignant brain tumors 1 is present in the vascular extracellular matrix and promotes angiogenesis," *Arteriosclerosis, Thrombosis, and Vascular Biology*, vol. 32, no. 2, pp. 442–448, 2012.

[35] Z. Wu, D. van Ryk, C. Davis et al., "Salivary agglutinin inhibits HIV type 1 infectivity through interaction with viral glycoprotein 120," *AIDS Research and Human Retroviruses*, vol. 19, no. 3, pp. 201–209, 2003.

[36] M. R. White, E. Crouch, J. Vesona et al., "Respiratory innate immune proteins differentially modulate the neutrophil respiratory burst response to influenza A virus," *American Journal of Physiology—Lung Cellular and Molecular Physiology*, vol. 289, no. 4, pp. L606–L616, 2005.

[37] J. T. D. Leito, A. J. M. Ligtenberg, K. Nazmi, J. M. A. de Blieck-Hogervorst, E. C. I. Veerman, and A. V. N. Amerongen, "A common binding motif for various bacteria of the bacteria-binding peptide SRCRP2 of DMBT1/gp-340/salivary agglutinin," *Biological Chemistry*, vol. 389, no. 9, pp. 1193–1200, 2008.

[38] J. T. D. Leito, A. J. M. Ligtenberg, M. van Houdt, T. K. van den Berg, and D. Wouters, "The bacteria binding glycoprotein salivary agglutinin (SAG/gp340) activates complement via the lectin pathway," *Molecular Immunology*, vol. 49, no. 1-2, pp. 185–190, 2011.

[39] C. Gao, K. Devarajan, Y. Zhou, C. M. Slater, M. B. Daly, and X. Chen, "Identifying breast cancer risk loci by global differential allele-specific expression (DASE) analysis in mammary epithelial transcriptome," *BMC Genomics*, vol. 13, no. 1, article 570, 2012.

[40] J. Muñoz and J. S. Castresana, "Silencing of DMBT1 in neuroblastoma cell lines is not due to methylation of CCWGG motifs on its promoter," *Neoplasma*, vol. 53, no. 1, pp. 15–18, 2006.

[41] M. Bibas, P. Lorenzini, A. Cozzi-Lepri et al., "Polyclonal serum-free light chains elevation in HIV-infected patients," *AIDS*, vol. 26, no. 16, pp. 2107–2110, 2012.

[42] A. Bradwell, S. Harding, N. Fourrier et al., "Prognostic utility of intact immunoglobulin Ig′κ/Ig′λ ratios in multiple myeloma patients," *Leukemia*, vol. 27, no. 1, pp. 202–207, 2013.

[43] L. M. Teran, S. Rüggeberg, J. Santiago et al., "Immune response to seasonal influenza A virus infection: a proteomic approach," *Archives of Medical Research*, vol. 43, no. 6, pp. 464–469, 2012.

Hindawi Publishing Corporation
Evidence-Based Complementary and Alternative Medicine
Volume 2015, Article ID 828156, 5 pages
http://dx.doi.org/10.1155/2015/828156

Research Article

Effects of Shengjiang (*Zingiberis Rhizoma Recens*) and Its Processed Products on Nitric Oxide Production in Macrophage RAW 264.7 Cells

Hui Liao

Department of Pharmacy, Shanxi Provincial People's Hospital, 29 Shuangtasi Street, Taiyuan, Shanxi 030012, China

Correspondence should be addressed to Hui Liao; huiliao@263.net

Received 19 August 2014; Revised 19 September 2014; Accepted 19 September 2014

Academic Editor: Ning Wang

In Chinese medicine, Shengjiang (*Zingiberis Rhizoma Recens*) and its processed products, such as Ganjiang (*Zingiberis Rhizoma*), Paojiang (*Zingiberis Rhizoma Preparatum*), and Jiangtan (*Zingiberis Rhizoma Carbonisata*), exert distinct efficacy clinically. This research tried to study the effects of extracts from Shengjiang and its processed products in RAW 264.7 macrophage cells. After incubation of the different ginger types in RAW 264.7 cells for 24 h, an aliquot of the culture was mixed with an equal volume of Griess reagent, and nitric oxide (NO) production was evaluated using a Griess assay. Lipopolysaccharide (LPS) was used as the positive control. Milli-Q water (MQW) was used as the solvent control. The results showed that NO production increased significantly in RAW 264.7 cells following the stimulation of LPS ($0.05\,\mu g\,mL^{-1}$), Shengjiang, Ganjiang, Paojiang, and Jiangtan ($50\,\mu g\,mL^{-1}$, $500\,\mu g\,mL^{-1}$) separately compared with the MQW control ($P < 0.01$). The stimulation effects of Shengjiang and Ganjiang were significantly higher than those of Paojiang and Jiangtan at different concentrations ($P < 0.01$). The conclusion we could get from this research is that Shengjiang and its processed products could induce NO production in RAW 264.7 cells.

1. Introduction

According to the Traditional Chinese Medicine theory, Shengjiang (*Zingiberis Rhizoma Recens*), the fresh rhizome of the Zingiberaceae plant ginger (*Zingiber officinale Rosc*), and its processed products, such as Ganjiang (*Zingiberis Rhizoma*), Paojiang (*Zingiberis Rhizoma Preparatum*), and Jiangtan (*Zingiberis Rhizoma Carbonisata*), can be used as medicines, and each of them exerts a distinct clinical efficacy [1, 2].

Modern studies have demonstrated that Ganjiang and Paojiang, the processed products of Shengjiang, both can inhibit the proliferation of lung cancer A549 cells and gastric cancer SGC-7901 cells [3]. A high concentration of nitric oxide (NO), as an important signaling molecule in organisms, can inhibit the proliferation of tumor cells. A large amount of NO generated after induction of the inducible nitric oxide synthase (iNOS) can cause death of tumor cells and inhibit their growth [4].

Studies have confirmed that stimulating factors such as lipopolysaccharide (LPS), interleukin-1, and the tumor necrosis factor can induce macrophages to highly express iNOS, thereby synthesizing NO [5]. It was found in our previous studies that Shengjiang had an effect of enhancing the generation of NO by LPS-induced mouse macrophage RAW 264.7 cells [6]. Moreover, it has been reported that Shengjiang *per se* had an effect of inducing RAW 264.7 cells to produce NO [7]. This study will further explore whether the aqueous extracts of Shengjiang and its processed products, that is, Ganjiang, Paojiang, and Jiangtan, can induce RAW 264.7 cells to generate NO and what impact the extracts of Shengjiang, Ganjiang, Paojiang, and Jiangtan have on the generation of NO by LPS-induced RAW 264.7 cells.

2. Methods

2.1. Preparation of Shengjiang and Its Processed Products. Shengjiang (*Zingiberis Rhizoma Recens*): the fresh rhizome of the Zingiberaceae plant ginger (*Zingiber officinale Rosc*) was treated by removing fibrous roots, mud, and sand, washed clean, and cut into thick slices upon use. Ganjiang (*Zingiberis Rhizoma*): the fresh rhizome of the plant ginger was treated

Table 1: Standard assay requirements for Shengjiang (*Zingiberis Rhizoma Recens*) and its processed herbs [1].

Different ginger types	Water content	Total ash	Water soluble extractive	Volatile oil	6-Gingerol
Shengjiang (*Zingiberis Rhizoma Recens*)		<2.0%			>0.050%
Ganjiang (*Zingiberis Rhizoma*)	<19.0%	<6.0%	>22%	>0.80%	>0.60%
Paojiang (*Zingiberis Rhizoma Praeparatum*)	<12.0%	<7.0%	>26%		>0.30%
Jiangtan (*Zingiberis Rhizoma Carbonisata*)			<26%		>0.050%

by removing fibrous roots, mud, and sand, was washed clean, and was dried at a low temperature (40–45)°C. Paojiang (*Zingiberis Rhizoma Preparatum*): the Ganjiang was heated with sand until it was plumped up and turned brown at the surface and yellow inside; then, it was sprayed with a small amount of clean water, removed, and dried in the sun. Jiangtan (*Zingiberis Rhizoma Carbonisata*): the Ganjiang was carbonized by stir-frying until the surface turned black and the interior turned brown [1].

All the samples were identified by the Traditional Chinese Herb Division, Pharmacy Department of the Shanxi Provincial People's Hospital. The processing standards for each sample are shown in Table 1 [1].

Three grams of each sample was hermetically pulverized and then placed into a sealed tube. Then, 15 mL of Milli-Q water (MQW) at 100°C was added, sealed, shaken at room temperature for 1 h, and then ultrasonically extracted in a water bath at 60–65°C for 15 min. The extraction was repeated another two times same as above. The extracting solutions were collected, pooled, and centrifuged at 14,000 g for 15 min. The supernatant was removed and freeze-dried *in vacuo* to a constant weight to obtain extracts of Shengjiang, Ganjiang, Paojiang, and Jiangtan, respectively. The extracts were stored at 4°C until use. The extracts were redissolved in MQW at a desired concentration (50 μg mL^{-1} and 500 μg mL^{-1}) upon experiment.

2.2. Reagents and Instruments. Lipopolysaccharide (LPS), sodium nitrite ($NaNO_2$), and Griess reagent (0.1% N-(1-naphthyl)ethylenediamine dihydrochloride, 1% sulfanilamide in 5% phosphoric acid) were all prepared in-house from reagents purchased from Wako Chemicals USA Inc. (Richmond, VA, USA).

The used Victor2 plate reader (Wallac, Turku, Finland), 96-well polystyrene microplates, and Wallac Delfia 1296-003 shaker were purchased from PerkinElmer (Boston, MA, USA).

2.3. Cell Source and Culture. RAW 264.7 cells, a mouse macrophages cell line, were purchased from the American Type Culture Collection (Manassas, VA, USA) and cultured in colorless Dulbecco's modified eagle medium (DMEM) supplemented with heat inactivated fetal bovine serum (10%), D-glucose (3.5 mg mL^{-1}), Na pyruvate (100 mM), L-glutamine (2 mM), penicillin (100 U mL^{-1}), streptomycin (100 μg mL^{-1}), and amphotericin B (250 μg mL^{-1}) at 37°C and 5% CO_2.

2.4. Effects of Shengjiang, Ganjiang, Paojiang, and Jiangtan in RAW 264.7 Cells. The effects of the extracts were determined in RAW 264.7 cells (99 μL, plated at 1×10^6 cells mL^{-1}). The cells were treated with extracts (1 μL). Nitrite, a stable end-product of NO metabolism, was then measured after 24 h using the Griess reaction [8]. The culture media of the RAW 264.7 cells (80 μL) were mixed with an equal volume of Griess reagent, followed by spectrophotometric measurement at 550 nm. The nitrite concentrations in the culture media were determined by comparison with a $NaNO_2$ standard curve. LPS (1 μL, diluted with DMEM, 0.05 μg mL^{-1}) was the positive control, and MQW was the solvent control. Each concentration was assayed 6 times.

2.5. Effects of Shengjiang, Ganjiang, Paojiang, and Jiangtan in LPS-Activated RAW 264.7 Cells. The activities of inducible nitric oxide synthase (iNOS) of the extracts were determined with RAW 264.7 cells (98 μL, plated at 1×10^6 cells mL^{-1}). The extracts (1 μL) were added to the cells, and then, cells were stimulated with LPS (1 μL, diluted with DMEM, 0.05 μg mL^{-1}) after 2 h. Nitrite was measured after another 22 h using the Griess reaction as above. Each concentration was assayed 6 times.

2.6. Statistics. All data are expressed as the mean ± standard deviation. Statistical analyses of the results were performed using SPSS software version12.0 (SPSS Inc., Chicago, IL, USA). Student's t-test was used for intergroup comparison. $P < 0.05$ was considered statistically significant.

3. Results

3.1. Standard Equation of $NaNO_2$. The concentrations of $NaNO_2$ were 0, 1, 2, 5, 10, 50, 100, and 500 μM. The standard equation of $NaNO_2$ was as follows: Y (absorbance) = 0.0018 × (the concentration of $NaNO_2$) + 0.0454, $R^2 = 0.9994$.

3.2. Effects of LPS in RAW 264.7 Cells. NO production was increased significantly by LPS stimulation compared with the MQW solvent control ((14.4 ± 2.2) μM versus (0.8 ± 0.5) μM, $P < 0.001$) (Table 2).

Table 2: Effects of Shengjiang (*Zingiberis Rhizoma Recens*) and its processed herbs in RAW 264.7 cells ($\overline{x} \pm s$).

Group	Concentration (μg mL^{-1})	Nitrite (μM)
Shengjiang (*Zingiberis Rhizoma Recens*)	50	36.1 ± 4.2^{abd}
	500	219.8 ± 7.3^{ace}
Ganjiang (*Zingiberis Rhizoma*)	50	40.8 ± 2.1^{abd}
	500	207.7 ± 28.0^{ace}
Paojiang (*Zingiberis Rhizoma Praeparatum*)	50	12.3 ± 2.9^{a}
	500	17.9 ± 2.7^{a}
Jiangtan (*Zingiberis Rhizoma Carbonisata*)	50	2.3 ± 0.9^{a}
	500	14.1 ± 2.7^{a}
Solvent control		0.8 ± 0.5
LPS positive control	0.05	14.4 ± 2.2^{a}

Notes: $^{a}P < 0.01$, compared with MQW solvent control; $^{b}P < 0.01$, Shengjiang and Ganjiang compared with Paojiang at 50 μg mL^{-1}; $^{c}P < 0.01$, Shengjiang and Ganjiang compared with Paojiang at 500 μg mL^{-1}; $^{d}P < 0.01$, Shengjiang and Ganjiang compared with Jiangtan at 50 μg mL^{-1}; $^{e}P < 0.01$, Shengjiang and Ganjiang compared with Jiangtan at 500 μg mL^{-1}.

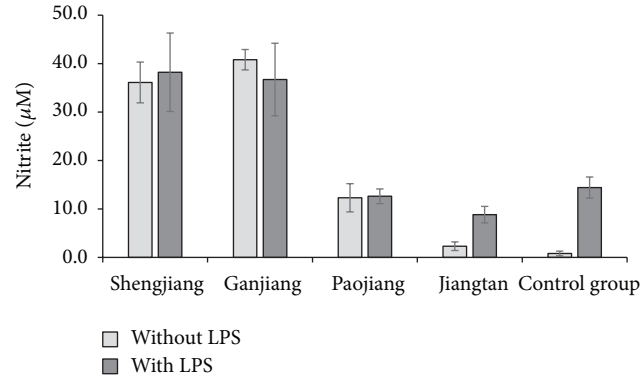

Figure 1: The effects of Shengjiang (*Zingiberis Rhizoma Recens*) and its processed herbs in RAW 264.7 cells at 50 μg mL^{-1}. LPS control compared with solvent control ((14.4±2.2) μM versus (0.8±0.5) μM, $P < 0.001$). "Jiangtan with LPS" compared with "Jiangtan without LPS" ((8.8 ± 1.7) μM versus (2.3 ± 0.9) μM, $P < 0.001$) and "Jiangtan with LPS" compared with "LPS control" ((8.8±1.7) μM versus (14.4± 2.2) μM, $P < 0.001$).

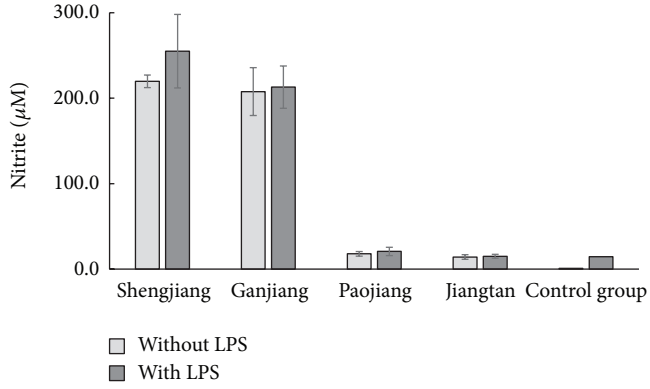

Figure 2: The effects of Shengjiang (*Zingiberis Rhizoma Recens*) and its processed herbs in RAW 264.7 cells at 500 μg mL^{-1}. "Paojiang with LPS" compared with "Paojiang without LPS" ((20.7 ± 4.8) μM versus (17.9 ± 2.7) μM, $P = 0.029$). "Paojiang with LPS" compared with "LPS control" ((20.7 ± 4.8) μM versus (14.4 ± 2.2) μM, $P = 0.014$).

3.3. Effects of Shengjiang, Ganjiang, Paojiang, and Jiangtan in RAW 264.7 Cells. The extracts from Shengjiang, Ganjiang, Paojiang, and Jiangtan could stimulate NO production significantly as compared with the MQW solvent control at 50 μg mL^{-1} and 500 μg mL^{-1} (Jiangtan at 50 μg mL^{-1} $P = 0.008$; others: $P < 0.001$). Shengjiang and Ganjiang displayed significant effects compared with Paojiang and Jiangtan at different concentrations ($P < 0.001$) (Table 2).

3.4. Effects of Shengjiang, Ganjiang, Paojiang, and Jiangtan in LPS-Activated RAW 264.7 Cells. When Shengjiang and Ganjiang at 50 μg mL^{-1} and 500 μg mL^{-1}, Paojiang at 50 μg mL^{-1}, and Jiangtan at 500 μg mL^{-1} were coadministered with LPS, no addition or synergy effects were observed (without LPS versus with LPS, resp., $P > 0.05$) (Figures 1 and 2).

When Paojiang at 500 μg mL^{-1} was coadministered with LPS, the content of NO production was significantly higher than the test group without LPS ((20.7 ± 4.8) μM versus (17.9 ± 2.7) μM, $P = 0.029$) and also higher than LPS positive control significantly ((20.7 ± 4.8) μM versus (14.4 ± 2.2) μM, $P = 0.014$) (Figure 2).

When Jiangtan was coadministered with LPS at 50 μg mL^{-1}, the results showed that NO production was significantly higher than the test group without LPS ((8.8 ± 1.7) μM versus (2.3 ± 0.9) μM, $P < 0.001$), but lower than LPS control significantly ((8.8 ± 1.7) μM versus (14.4 ± 2.2) μM, $P < 0.001$) (Figure 1).

4. Discussion

Modern pharmacological studies have found that a high concentration of NO mainly has a cytotoxic effect and inhibits and kills tumor cells through mechanisms including mediating the activation of macrophages to achieve an antitumor effect. The results of the study in which chemotherapy with 5-fluorouracil (5-FU), together with supplementation of the NO precursor L-arginine (L-Arg), was administered to a nude mice model of human liver cancer revealed that 5-FU could induce an increase in the expression and activity of iNOS *in vivo*, and after combination with L-Arg 5-FU could significantly enhance the expression and activity of iNOS and significantly increase the concentration of NO in tumor tissues, suggesting that endogenous NO plays an important role in the *in vivo* antitumor effect of 5-FU combined with L-Arg [9].

Research data indicates that transfection of the iNOS gene into highly metastatic mouse malignant melanoma cells results in the high expression of iNOS activity, which causes a loss of tumor metastasis. Moreover, clinical data

has confirmed that the concentration of NO in the serum of the patients with large intestine cancer was significantly increased after supplementation with L-Arg, indicating that the L-Arg-NO pathway is an action mechanism by which L-Arg inhibits tumor growth [10].

NO, which has a short half-life of 6 to 60 seconds, can be oxidized to nitrite immediately after its generation and exists in intracellular and extracellular fluids in the form of nitrite. Thus, in experiments, the content of nitrite, a stable product of NO, is usually measured to reflect the amount of NO [8]. At present, the model has been widely used in experimental studies on NO.

RAW 264.7 macrophages cell lines are thought to be very sensitive to the induction of mRNA expression by various cytokines via LPS stimulation [11]. In macrophages, macrophage-inducible NO synthase is mainly responsible for NO production in response to various stimuli [12]. Reverse transcription-polymerase chain reaction (RT-PCR) and Western Blotting were used to determine the change in iNOS after the stimulation of RAW 264.7 cells with LPS. The results demonstrated that, after 24-hour stimulation with 0.1 μg mL^{-1} LPS, the levels of iNOS mRNA and protein expression in the cells were significantly increased and exhibited a dose-effect relationship within a concentration range of 0.01–10 μg mL^{-1}. It was considered that LPS could induce RAW 264.7 cells to produce iNOS, thereby increasing the NO content [13].

Our previous study showed that extracts from Shengjiang seemed to stimulate the NO production at 500 μg mL^{-1} but had no effect at 50 μg mL^{-1} [6]. It was interesting to see in another report that 100 μg mL^{-1} extracts from Shengjiang could induce macNOS mRNA expression, but induction effects at a dose below 10 μg mL^{-1} were weak or negligible [7]. In our study, Shengjiang was mixed with water and sonicated at room temperature [6], but samples were extracted by boiling in distilled water in another research [7]. Some research has demonstrated that Yanshanjiang (*Alpinia zerumbet*), another herb of the Zingiberaceae plant, could promote NO secretion. The active ingredient was its volatile oil [14]. It has been reported that some volatile oils in Ganjiang are significantly decreased when the drying temperature was 65°C [15]. It seemed that the extraction temperature is an important factor in the research. In this study, we extracted samples ultrasonically in a water bath at 60–65°C in sealed tubes and tried the concentrations of Shengjiang and its processed herbs at 500 μg mL^{-1} and 50 μg mL^{-1}.

The results of this study indicate that the content of nitrite in RAW 264.7 cell culture after LPS induction was significantly increased from 0.8 ± 0.5 μM to 14.4 ± 2.2 μM, as compared with the solvent control group. At the action concentration of 500 μg mL^{-1} and 50 μg mL^{-1}, the content of nitrite in the cell culture of each experimental group of Shengjiang, Ganjiang, Paojiang, and Jiangtan was significantly increased as compared with the solvent control group.

At the same concentration, the stimulation effects of Shengjiang and Ganjiang to produce nitrite, a product of NO, were significantly higher than those of Paojiang and Jiangtan. The main chemical components in Shengjiang are volatile oils and phenols, such as gingerol and shogaol [16]. The processing temperature plays an important role in determining the content of volatile oils in processed herbs. The high processing temperature might be responsible for the inducible effects of Paojiang and Jiangtan being significantly lower than Ganjiang and Shengjiang in this study.

When the doses of Shengjiang and Ganjiang were 500 μg mL^{-1} and 50 μg mL^{-1}, the nitrite levels were significantly higher than that of the positive LPS control. Under the action of 500 μg mL^{-1} of Shengjiang and Ganjiang, the nitrite content levels were 15 and 14 times as high as that of LPS, respectively. Most likely because the effects of Shengjiang and Ganjiang were significantly much higher than that of LPS, when Shengjiang and Ganjiang were coadministered with LPS, no additional or synergistic effect was demonstrated.

Even though the inducible effect of Shengjiang and Ganjiang did not display significant differences at the same concentration, Shengjiang and Ganjiang possessed both similarities and obvious differences in drug properties and efficacies and also had significant differences in clinical applications. There were significant differences in chromatographic peaks on their UPLC fingerprint chromatograms before and after processing [17], demonstrating that the ingredients in Shengjiang were "qualitatively" and "quantitatively" changed after the processing. It has been reported that over 60 compounds have been extracted from Ganjiang, and 40 of those compounds have been identified. In addition, over 50 compounds from Shengjiang have been extracted, and 33 of those compounds have been identified. There are 10 compounds in Ganjiang that Shengjiang does not have, and there are 3 compounds in Shengjiang that have not been detected in Ganjiang [18].

When Paojiang at 500 μg mL^{-1} was coadministered with LPS, the content of NO production was significantly higher than single Paojiang, and also single LPS. It seemed there had been the synergistic effect of Paojiang at 500 μg mL^{-1} and LPS in RAW 264.7 cells. Another interesting result was when Jiangtan was coadministered with LPS at 50 μg mL^{-1}. The data showed that NO production was significantly higher than single Jiangtan, but lower than single LPS. We are not sure that there is some inhibition effect after their combination and need more analytical research.

Accordingly, our further studies will focus on which ingredients play the role in the significant higher levels of nitrite treated with Shengjiang and Ganjiang compared to positive LPS control in RAW 264.7 cells. We are also interested in Paojiang and Jiangtan: How did the main active component change after high processed temperature? Will they have different pharmacological effect on RAW 264.7 cells compared with Shengjiang and Ganjiang? We will give further research on these questions.

Conflict of Interests

The author declares that there is no conflict of interests regarding the publication of this paper.

References

[1] Chinese pharmacopoeia commission, *Pharmacopoeia of People's Republic of China*, China Medical Science Press, Beijing, China, 2010.

[2] Z. W. Xie, *Chinese Herbal Medicine Name Dictionary*, Beijing Science and Technology Press, Beijing, China, 2004.

[3] Z. Y. Tao, *The Experiment on the Effect of Ginger Class Chinese Medicine on Inhibiting Cell Growth and Apoptosis Cell Induction*, Nanjing University of Chinese Medicine, Nanjing, China, 2011.

[4] R. Cui, H. Ji, and Y. S. Lai, "Research progress of nitric oxide donor/nitric oxide donor compounds on anti-tumor treatment," *Chinese Journal of Clinical Rational Drug Use*, vol. 5, no. 6B, pp. 175–177, 2012.

[5] M. Lepoivre, H. Boudbid, and J. F. Petit, "Antiproliferative activity of γ-interferon combined with lipopolysaccharide on murine adenocarcinoma: dependence on an L-arginine metabolism with production of nitrite and citrulline," *Cancer Research*, vol. 49, no. 8, pp. 1970–1976, 1989.

[6] H. Liao, L. K. Banbury, and D. N. Leach, "Elucidation of Danzhixiaoyao Wan and its constituent herbs on antioxidant activity and inhibition of nitric oxide production," *Evidence-Based Complementary and Alternative Medicine*, vol. 4, no. 4, pp. 425–430, 2007.

[7] N. Imanishi, N. Mantani, S. Sakai et al., "Inducible activity of ginger rhizome (Zingiber offifinale Rosc.) on the mRNA expression of macrophage-inducible nitric oxide (NO) synthase and NO production in a macrophage cell line, RAW264.7 cells," *The American Journal of Chinese Medicine*, vol. 32, no. 5, pp. 727–735, 2004.

[8] L. C. Green, D. A. Wagner, J. Glogowski, P. L. Skipper, J. S. Wishnok, and S. R. Tannenbaum, "Analysis of nitrate, nitrite, and [^{15}N]nitrate in biological fluids," *Analytical Biochemistry*, vol. 126, no. 1, pp. 131–138, 1982.

[9] X. Y. Yin, J. M. Jiang, J. Y. Liu, and J. R. Zhu, "Effects of endogenous nitric oxide induced by 5-FU and L-Arg on the human liver carcinoma in nude mice," *Chinese Journal of Cancer Prevention and Treatment*, vol. 14, no. 22, pp. 1690–1693, 2007.

[10] J. W. Hui, X. P. Gao, Q. Y. Ma, and Y. J. Wang, "The effects of L-arginine on the cell proliferation in patients with colorectal tumor and its mechanisms," *Journal of Shannxi Medicine*, vol. 40, no. 6, pp. 666–668, 2011.

[11] N. Pennanen, S. Lapinjoki, A. Palander, A. Urtti, and J. Monkkonen, "Macrophage-like RAW 264 cell line and time-resolved fluoroimmunoassay (TRFIA) as tools in screening drug effects on cytokine secretion," *International Journal of Immunopharmacology*, vol. 17, no. 6, pp. 475–480, 1995.

[12] C. J. Lowenstein, E. W. Alley, P. Raval et al., "Macrophage nitric oxide synthase gene: Two upstream regions mediate induction by interferon γ and lipopolysaccharide," *Proceedings of the National Academy of Sciences of the United States of America*, vol. 90, no. 20, pp. 9730–9734, 1993.

[13] Y. Hu, Y. L. Lou, Y. Wang, A. Xie, and F. Guo, "Effects of lipopolysaccharide induction on inducible nitric oxode synthase in RAW 264.7 macrophages," *Jiangxi Journal of Medical Laboratory Sciences*, vol. 25, no. 6, pp. 525–527, 2007.

[14] X. C. Shen, W. K. Li, and L. Tao, "Ameliorating effectsof essential oil from Fructus Apliniae zerumbet (EOFAZ) on NOS-NO system in human umbilical vein endothelial cells injury (HUVECs) induced by oxidized-low density lipoprotein (ox-LDL) in vitro," *Chinese Journal of Hospital Pharmacy*, vol. 32, no. 24, pp. 1937–1940, 2012.

[15] W. Xu, J. Ding, Y. Zhao, and X. X. Yang, "GC/MS analysis of volatile oil from fresh ginger after different dried conditions," *Chinese Traditional Patent Medicine*, vol. 30, no. 3, pp. 399–401, 2008.

[16] J. P. Li, Y. S. Wang, H. Ma, J. D. Hao, and H. Yang, "The comparison of the main chemical component of dried ginger and fresh ginger," *China Journal of Chinese Materia Medica*, vol. 26, no. 11, pp. 748–751, 2001.

[17] Y. Q. Han, Y. Hong, J. Gui, J. R. Gao, Y. Z. Wang, and L. Z. Xia, "UPLC fingerprint comparison among fresh, dried and processed ginger from different habitats," *Chinese Traditional Patent Medicine*, vol. 35, no. 2, pp. 356–359, 2013.

[18] X. H. Wang, Y. F. Wei, L. Y. Li, F. Long, and Y. J. Zhang, "Analysis of chemical constituents of volatile oil in Qianwei - grown dry ginger and fresh ginger by gas chromatography-mass spectrometry," *Journal of Chengdu University of Traditional Chinese Medicine*, vol. 29, no. 3, pp. 54–55, 2006.

Hindawi Publishing Corporation
Evidence-Based Complementary and Alternative Medicine
Volume 2015, Article ID 842091, 9 pages
http://dx.doi.org/10.1155/2015/842091

Research Article

Gambogic Acid Lysinate Induces Apoptosis in Breast Cancer MCF-7 Cells by Increasing Reactive Oxygen Species

Yong-Zhan Zhen,[1] Ya-Jun Lin,[2] Kai-Ji Li,[1] Xiao-Shan Yang,[2] Yu-Fang Zhao,[1] Jie Wei,[2] Jing-Bo Wei,[1] and Gang Hu[2]

[1]*Department of Histology and Embryology, Basic Medical College of Hebei United University, Tangshan 063000, China*
[2]*The Key Laboratory of Geriatrics, Beijing Hospital & Beijing Institute of Geriatrics, Ministry of Health, No. 1 Dahua Road, Dongdan, Dongcheng District, Beijing 100730, China*

Correspondence should be addressed to Gang Hu; huganglys2010@126.com

Received 8 August 2014; Revised 2 December 2014; Accepted 15 December 2014

Academic Editor: Senthamil R. Selvan

Gambogic acid (GA) inhibits the proliferation of various human cancer cells. However, because of its water insolubility, the antitumor efficacy of GA is limited. *Objectives.* To investigate the antitumor activity of gambogic acid lysinate (GAL) and its mechanism. *Methods.* Inhibition of cell proliferation was determined by MTT assay; intracellular ROS level was detected by staining cells with DCFH-DA; cell apoptosis was determined by flow cytometer and the mechanism of GAL was investigated by Western blot. *Results.* GAL inhibited the proliferation of MCF-7 cells with IC_{50} values 1.46 μmol/L comparable with GA (IC_{50}, 1.16 μmol/L). GAL promoted the production of ROS; however NAC could remove ROS and block the effect of GAL. GAL inhibited the expression of SIRT1 but increased the phosphorylation of FOXO3a and the expression of p27Kip1. At knockdown of FOXO3a, cell apoptosis induced by GAL can be partly blocked. In addition it also enhanced the cleavage of caspase-3. *Conclusions.* GAL inhibited MCF-7 cell proliferation and induced MCF-7 cell apoptosis by increasing ROS level which could induce cell apoptosis by both SIRT1/FOXO3a/p27Kip1 and caspase-3 signal pathway. These results suggested that GAL might be useful as a modulation agent in cancer chemotherapy.

1. Introduction

Breast cancer represents the most common cancer in women in western countries. One in 8 women in the United States will develop breast cancer in her lifetime, while its incidence rate constantly increases in developing countries [1, 2]. Over the past decade, although the introduction of new drugs, including paclitaxel and Herceptin, has improved the treatment landscape for breast cancer patients, some patients continue to experience drug resistance and disease relapse [3, 4]. Therefore, further investigations to find a novel anti-breast-cancer drug should be conducted.

Gambogic acid (GA) is the principal active component of gamboge, the resin from various *Garcinia* species including *G. Morella and G. hanburyi* [5]. It was reported in traditional Chinese medical documents that GA possessed diverse biological effects such as anti-inflammatory and antipsoriatic efficacy [6, 7], anti-invasive effect [8], inhibiting angiogenesis [9], and inducing cell apoptosis [10]. One of the major barriers for GA clinical application is its insolubility in water. GA could only dissolve in DMSO [11], and DMSO is rather harmful to cells. Even though it dissolves in DMSO, if diluted by water, it will precipitate. Thus it impedes the uses of GA. In the present study, we prepared gambogic acid lysinate (GAL), which can dissolve in water, and the solubility of GAL in water is 1.16 g. No report about the manufacture of GAL and its antitumor activity has been found yet. In this study, we investigated the antitumor activity of GAL.

2. Materials and Methods

2.1. Chemicals and Antibodies. Gambogic acid (98%) was purchased from Nanjing Jingzhu Bio-technology Ltd. (Nanjing, Jiangsu, China). Lysine was purchased from Beijing

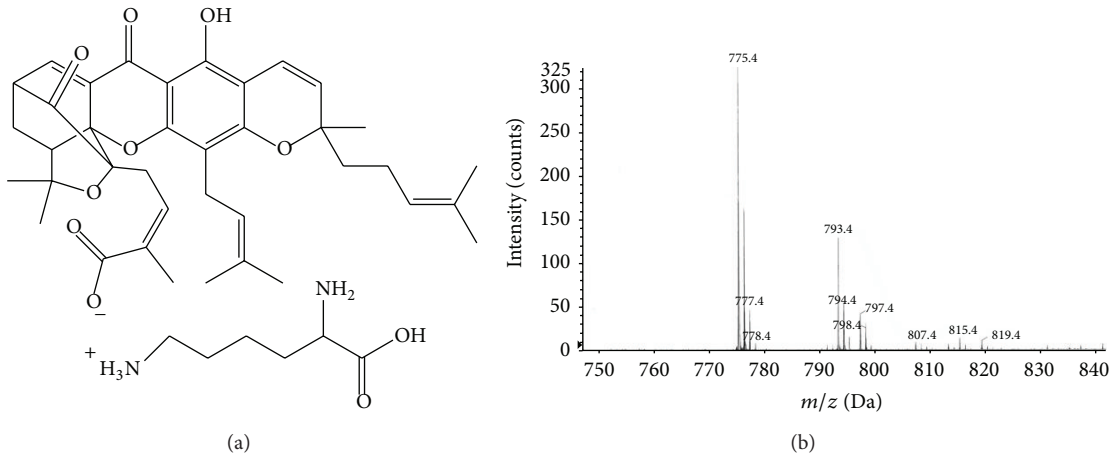

(a) (b)

Figure 1: The structure and the determination of gambogic acid lysinate. Gambogic acid and lysine combine together through ionic bond. It is determined by Matrix-Assisted Laser Desorption/Ionization Time of Flight Mass Spectrometry and the peak value (755.4 Da) is gambogic acid lysinate.

Solarbio Science and Technology Co. (Beijing, China). Gambogic acid lysinate (GAL) was made in our department. 3-(4,5-Dimethylthiazol-2-yl)-2,5-diphenyltetrazolium bromide (MTT) and dimethyl sulfoxide (DMSO) were obtained from Sigma Aldrich (Shanghai, China). FOXO3a siRNA and the scrambled siRNA (NC siRNA) control were supplied by Santa Cruz Technology (Dallas, TX, USA). Antibodies against SIRT1, FOXO3a, p-FOXO3a (s294), p27Kip1, caspase-3 and cleaved-caspase-3 (C-caspase-3) were purchased from Cell Signaling Technology (Beverly, MA, USA). Antibody against β-actin was purchased from Santa Cruz Technology (Dallas, TX, USA). Secondary antibodies were purchased from Cell Signaling Technology.

2.2. The Protocol of GAL Preparation and Matrix-Assisted Laser Desorption/Ionization Time of Flight Mass Spectrometry (MALDI-TOF MS) Analysis. Lysine (29.2 mg) was dissolved in distilled water and then gambogic acid (62.9 mg) was added to lysine solution. After lysine reacted with gambogic acid at 30°C for 24 hours, the solution was frozen and dried in freeze-drier (SCIENTZ, Ningbo, China) for 12 hours. An Agilent 6500 MS system (Agilent Technologies, CA, USA) was used to analyze the molecular weight of new product. The analysis method is following. Ionization is achieved using electrospray in the positive mode with the spray voltage set at 4.0 kV. The fragmentor voltage and collision energy were optimized during tuning as 150, 18 eV for GAL. Analysis was carried out in electrospray positive ionization using multiple reaction monitoring modes. The mass transition ion pair was selected as m/z 840 → 750 for GAL. The ion spectra of product are represented in Figure 1(b). The data acquisition software used was MassHunter software (Agilent Corporation, MA, USA).

2.3. Cell Culture and Cytotoxicity Assay. Human breast cancer cell lines MCF-7 were used in this study. MCF-7 cells were maintained in DMEM medium supplemented with 10% fetal bovine serum (Hyclone, Logan, UT, USA). Cells were grown in a humidified atmosphere of 5% CO_2 at 37°C. In vitro cytotoxicity of GAL was determined using 3-(4,5-dimethylthiazol-2-yl)-2,5-diphenyltetrazolium bromide (MTT) assay. Briefly, MCF-7 cells were transferred to 96-well tissue culture plates at a density of 3×10^3 cells per well, 24 hours prior to treatment. The medium was then replaced with fresh medium containing GAL at different concentrations. The culture medium without any drug formulation was used as the control. After 48 hours of incubation, medium was removed and cells were washed once with sterile phosphate buffered saline (PBS). Then 20 μL of MTT solution (5 mg/mL) was added to each well and further incubated for 4 hours. Medium was removed and 150 μL DMSO was added to each well to dissolve the purple formazan crystal converted from MTT. Optical density at 570 nm was determined with a SpectraMax 190 Absorbance Microplate Reader (Sunnyvale, CA, USA) and the concentration at which 50% of growth is inhibited (IC_{50}) was calculated by GraphPad Prism 5.0 (GraphPad, La Jolla, CA, USA).

2.4. Examination of Intracellular Reactive Oxygen Species (ROS) Accumulation. Intracellular hydrogen peroxide levels were monitored by fluorescence microscopy and fluorescence spectrophotometer after staining with DCFH-DA (dichlorodihydro-fluorescein diacetate; Molecular Probes, Eugene, OR, USA). Briefly, cells in a logarithmic growth phase (2×10^5 cells per well in a 25 mm^2 polystyrene culture flask) were treated with GAL for 24 h and and then labeled with 10 μmol/L DCFH-DA for 1 h. Next, the cells were monitored by Olympus inverted fluorescence microscope (Tokyo, Japan) and fluorescence spectrophotometer (Cary Eclipse, Palo Alto, CA, USA). The percentage of cells displaying increased dye uptake was used to reflect an increase in ROS levels.

2.5. Hoechst 33258 Staining. The nuclear fragmentation in MCF-7 cells treated with different concentrations of GAL

Table 1: The apoptosis ratio of different groups.

Groups	Normal (%)	Necrosis (%)	Early apoptosis (%)	Late apoptosis (%)
Control	96.20	0.50	1.00	2.30
GAL 0.5 μmol/L	75.84	1.09	5.45	17.62
GAL 1.0 μmol/L	68.92	2.17	5.95	22.95
GAL 2.0 μmol/L	47.62	9.14	5.90	37.35

(0, 0.5, 1, and 2 μmol/L) for 24 h was visualized using Hoechst 33258 staining. MCF-7 cells were plated in 6-well plates at a density of 5×10^4 cells per well and incubated with GAL. After 24 h, the cells were incubated with Hoechst 33258 (5 μg/mL) for 30 min at room temperature. Following washing with PBS, the cells were visualized and photographed under an Olympus inverted fluorescence microscope (Tokyo, Japan).

2.6. Flow Cytometric Analysis of Cell Apoptosis. Apoptosis was determined using an annexin V-FITC apoptosis kit (BD Pharmingen, Franklin Lakes, NJ, USA) according to manufacturer's instructions. After treatment with GAL (0, 0.5, 1, and 2 μmol/L) for 24 h, cells were washed with ice-cold PBS and resuspended in binding buffer (10 mmol/L HEPES, pH 7.4, 140 mmol/L NaCl, and 2.5 mmol/L $CaCl_2$) at a concentration of 1×10^6 cells/mL. Cells were stained with annexin V-FITC and propidium (PI) for 15 min in dark before being analyzed with flow cytometer (Beckman Coulter Inc., Miami, FL, USA).

2.7. Western Blotting Analysis. MCF-7 cells were treated with various concentrations of GAL (0, 0.25, 0.5, 1, and 2 μmol/L) for 24 h in 25 cm^2 flask. The cells were collected, washed twice with PBS, and then lysed with RIPA buffer and protease and phosphatase inhibitors cocktail (Roche, Beijing, China) for 20 min on ice. The cell lysates were cleared by centrifugation at 12,000 g for 20 min. Protein concentrations were determined by Bradford assay. Equal amounts of lysate (40 μg) were resolved by SDS-PAGE and transferred to polyvinylidene difluoride membrane (Millipore Corp., Bedford, MA, USA). Membranes were blocked in TBST containing 5% non-fat skim milk at room temperature for 2 h and probed with primary antibodies overnight at 4°C. Then membranes were blotted with an appropriate horseradish peroxidase-linked secondary antibody. Proteins were visualized using enhanced chemiluminescence Western blotting detection reagents (Amersham Pharmacia Biotech, Inc., Piscataway, NJ, USA).

2.8. RNA Interference. FOXO3a (FKHRL1) small interfering RNA (siRNA) and the scrambled siRNA were purchased from Santa Cruz Technology (Dallas, TX, USA). After FOXO3a siRNA or NC siRNA was transfected into MCF-7 cells using silMPORTER (Upstate, Virginia, USA) for 24 h, 1 μmol/L GAL was added for 24 h. After GAL treatment for 24 h, the cells were harvested. Then, cells apoptosis was checked through Hoechst staining and protein expression correlated with apoptosis was detected by Western blotting analysis.

2.9. Statistical Analysis. Data are presented as mean ± standard deviation (SD). Statistical analysis was performed using SPSS 11.5 software (SPSS Inc., Chicago, Illinois, USA). Comparison between groups was performed with Student's t-test. A P value of ≤ 0.05 was considered statistically significant.

3. Results

3.1. The Molecular Structure and the Identification of GAL. The molecular weight of GAL is 775 and molecular formula is $C_{44}H_{58}N_2O_{10}$ (Figure 1(a)). GAL is determined by Matrix-Assisted Laser Desorption/Ionization Time of Flight Mass Spectrometry and the peak value is 755.4 Da (Figure 1(b)).

3.2. GAL Inhibited the Proliferation of MCF-7 Cells and NAC Could Block Its Inhibition. The proliferation inhibitory effect of GAL in human MCF-7 cells was examined with MTT assay as described in Section 2. Cells were cultured for 48 h (Figure 2(a)) in the presence of various concentrations of GAL. MCF-7 cells showed a decreased cell proliferation after treatment with GAL. The IC_{50} value of GAL for MCF-7 cells is 1.46 μmol/L comparable with GA (IC_{50}, 1.16 μmol/L). Cells were cultured for different times (0, 6, 12, 24, 36, 48, and 60 h) in the presence of 2 μmol/L GAL. MCF-7 cells showed a decreased cell proliferation over time (Figure 2(b)). In addition, the proliferation inhibitory effect of GAL in human MCF-7 cells was blocked, when NAC (0, 1, 2, and 4 mmol/L) was added in combination with GAL (Figure 2(c)).

3.3. Induction of Oxidative Stress in MCF-7 Cells. The intracellular ROS level was stained with DCFH-DA and determined by fluorescence microscopy and fluorescence spectrophotometer as described in Section 2. GAL could increase ROS level in dose dependent manner; however NAC could decrease the increase of ROS induced by GAL (Figure 3).

3.4. Induction of Apoptosis by GAL in MCF-7 Cells. By Hoechst 33258 staining the nuclei of untreated cells were normal in appearance and showed diffused staining of the chromatin. After exposure to GAL for 24 h, most cells presented typical morphological changes of apoptosis such as chromatin condensation, cell shrinkage, chromatin margination, or apoptotic bodies (Figure 4(a)). Induction of apoptosis by GAL was further confirmed by annexin V-FITC/PI staining. GAL (0.5, 1, 2 μmol/L) induced apoptosis in MCF-7 cells in dose dependent manner and the ratio of apoptosis was 23.07%, 28.9%, and 43.25%, respectively (Figure 4(b), Table 1). It suggested that apoptosis was the predominant mode of GAL-induced cell death.

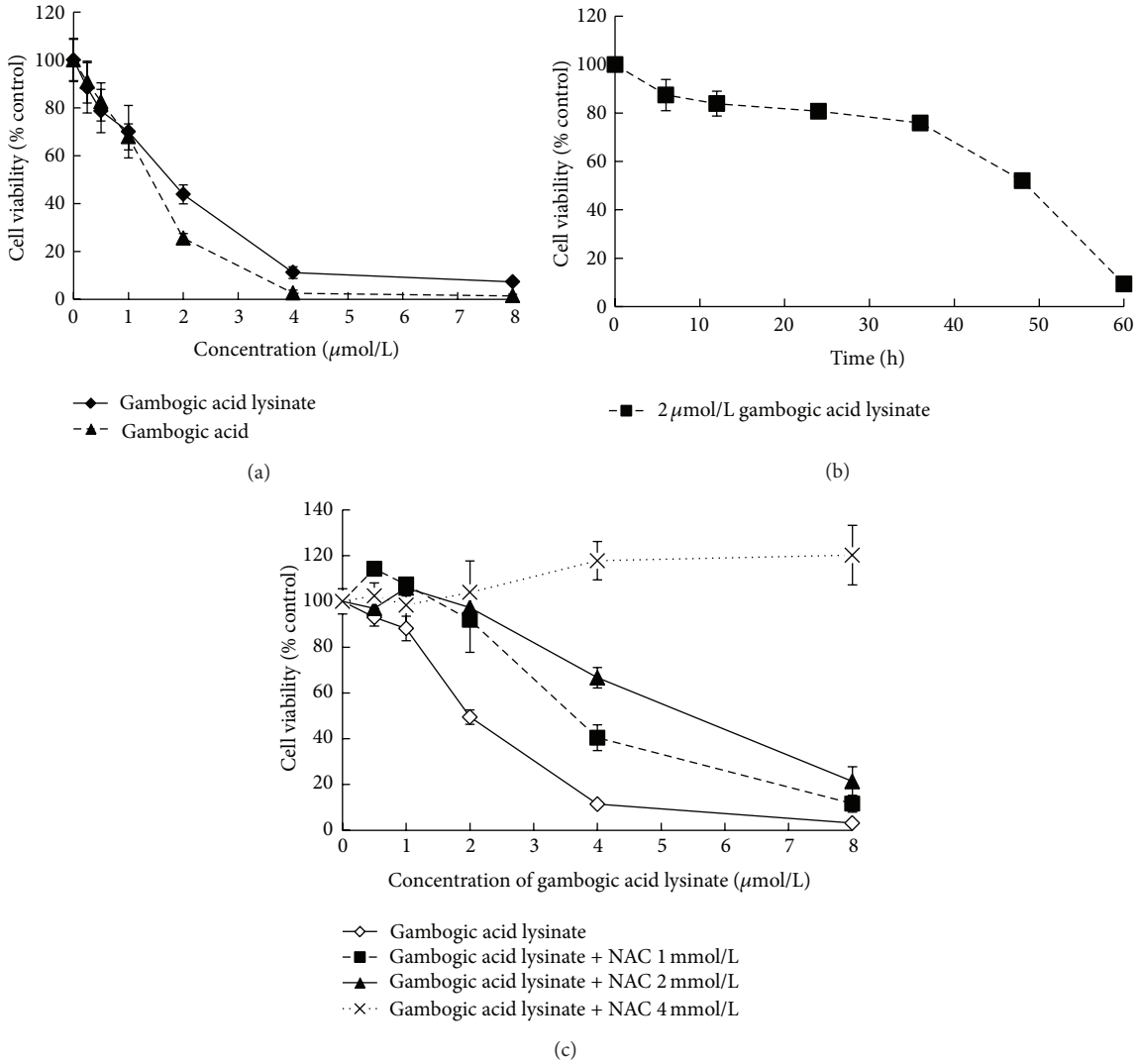

Figure 2: Gambogic acid lysinate can inhibit MCF-7 cell proliferation; however NAC can block it. (a) Exponential growth MCF-7 cells were treated with various concentrations of gambogic acid lysinate (0, 0.25, 0.5, 1, 2, 4, and 8 μmol/L) for 48 h; (b) exponential growth MCF-7 cells were treated with 2 μmol/L gambogic acid lysinate for different times (0, 6, 12, 24, 36, 48, and 60 h); (c) exponential growth MCF-7 cells were treated with various concentrations of gambogic acid lysinate (0, 0.25, 0.5, 1, 2, 4, and 8 μmol/L) plus various concentrations of NAC (0, 1, 2, and 4 mmol/L) for 48 h, and cell viability was detected by MTT method.

3.5. Downregulation of SIRT1 and Upregulation of C-Caspase-3 in GAL-Induced Apoptosis in MCF-7 Cells. In order to investigate the role of apoptosis, the activity of SIRT1 and caspase-3 in response to GAL treatment was determined. SIRT1 expression was decreased by GAL in a dose dependent manner. However, the phosphorylation of FOXO3a and the expression p27Kip1 were increased by GAL in a dose dependent manner. In addition the expression of cleaved caspase-3 also increased in a dose dependent manner; however the expression of caspase-3 decreased at GAL 2 μmol/L treated group (Figure 5). There is no change of the expression of Bcl-2 and Bax.

3.6. FOXO3a siRNA Partly Blocked Cell Apoptosis Induced by GAL in MCF-7 Cells. Compared with control group, after exposure to GAL+NC siRNA for 24 h, most cells presented typical morphological changes of apoptosis such as chromatin condensation, cell shrinkage, chromatin margination, or apoptotic bodies. Compared with GAL+NC siRNA group, GAL+FOXO3a siRNA group partly blocked the effect of GAL (Figure 6(a)). By Western blot analysis we found that FOXO3a siRNA decreased the expression of FOXO3, the phosphorylation of FOXO3, and the expression of p27Kip1, but with no effect on the expression of SIRT1, caspase-3, Bax, and Bcl-2 (Figure 6(b)).

4. Discussion and Conclusions

Breast cancer is the most common cancer among women in China and western countries. It is also the principal cause of cancer death for females. As a result of "westernized lifestyles" and exogenous estrogen exposure, there is an increasing trend

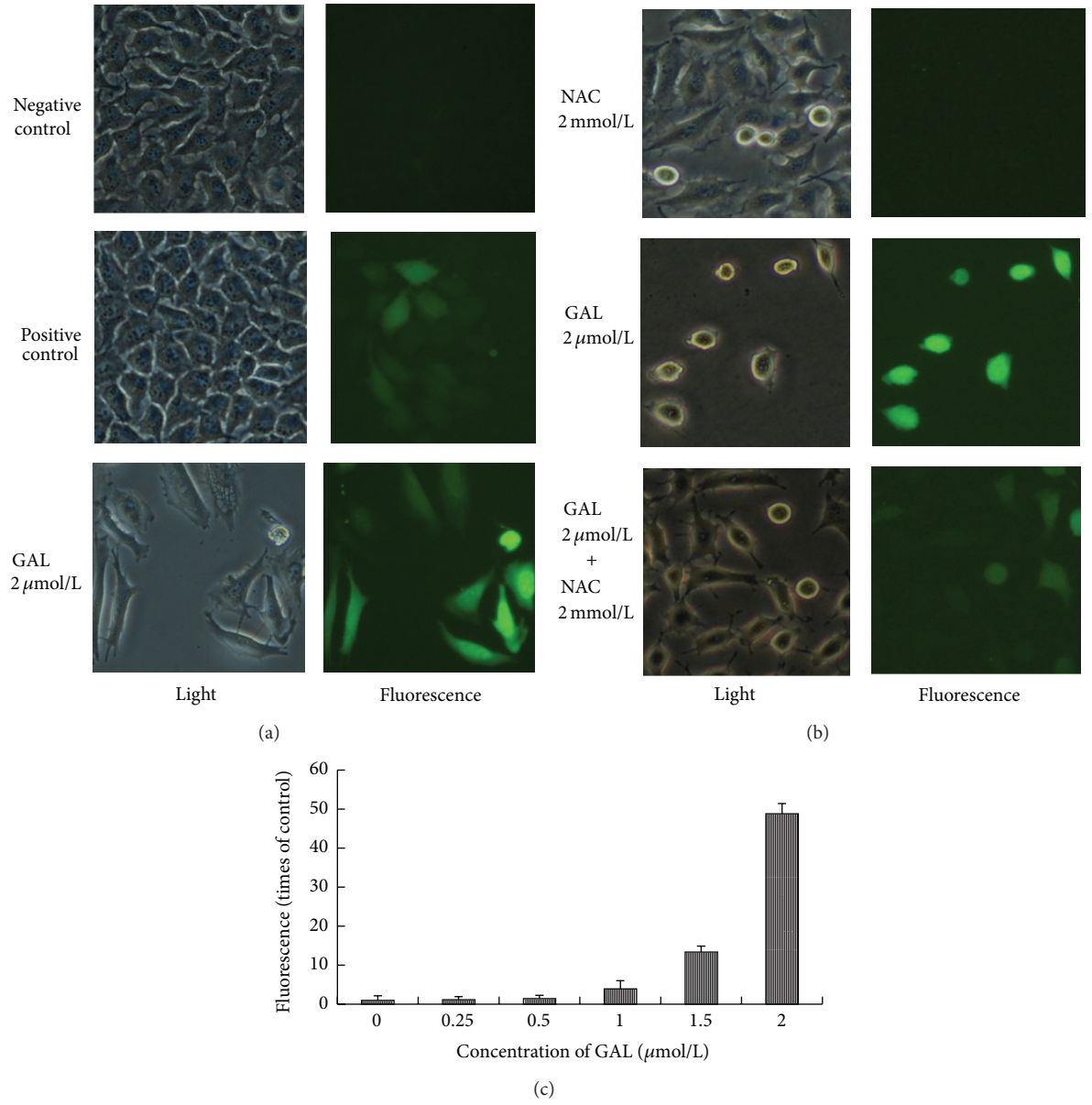

Figure 3: Gambogic acid lysinate can increase intracellular ROS level and NAC can block it. Exponential growth MCF-7 cells were treated with PBS (negative control), Rosup 100 mg/L (positive control), gambogic acid lysinate 2 μmol/L, NAC 2 mmol/L, and gambogic acid lysinate 2 μmol/L + NAC 2 mmol/L for 24 h. After treatment MCF-7 cells were stained with DCFH-DA and were determined by fluorescence microscopy (a, b) and fluorescence spectrophotometer (c).

of breast cancer incidence in China in the latest decades [1, 12]. SIRT1 physiologically interacts with p53 and attenuates its functions through deacetylation at its C-terminal Lys382 residue [13]. The expression of SIRT1 protein was seen in most human breast cancer specimens, and its expression was significantly associated with distant metastasis and poor prognosis [14–16] and reported to function as a tumor promoter. Recently, SIRT1 has emerged as a potent therapeutic target to cancer treatment. Therefore, identification of potent and unique SIRT1 inhibitor for cancer treatment is urgently needed.

GAL is the salt of lysine and gambogic acid, which has antitumor activities in a broad range of human cancer cells [17]. The difference between GAL and GA is that GAL can dissolve in water; however GA cannot. In this study, we observed that the inhibition of GAL to MCF-7 cell proliferation was comparable to that of GA and the IC_{50} values of GAL and GA were 1.46 and 1.16 μmol/L, respectively. GAL could inhibit MCF-7 cell proliferation in dose and time dependent manner (Figures 2(a) and 2(b)). We also found that NAC can block the activity of GAL, when GAL was administrated in combination with NAC (1, 2, and 4 mmol/L). The block of NAC to the activity of GAL was increased with the increase of the concentration of NAC (Figure 2(c)). It is well known that NAC is an ROS scavenger and is frequently used as a precursor to GSH, which supports the synthesis of GSH, and

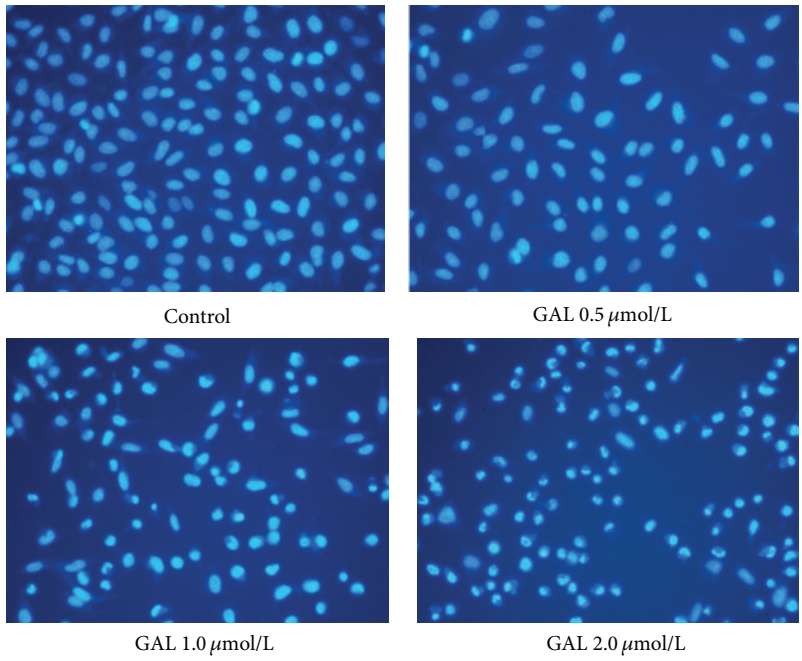

(a)

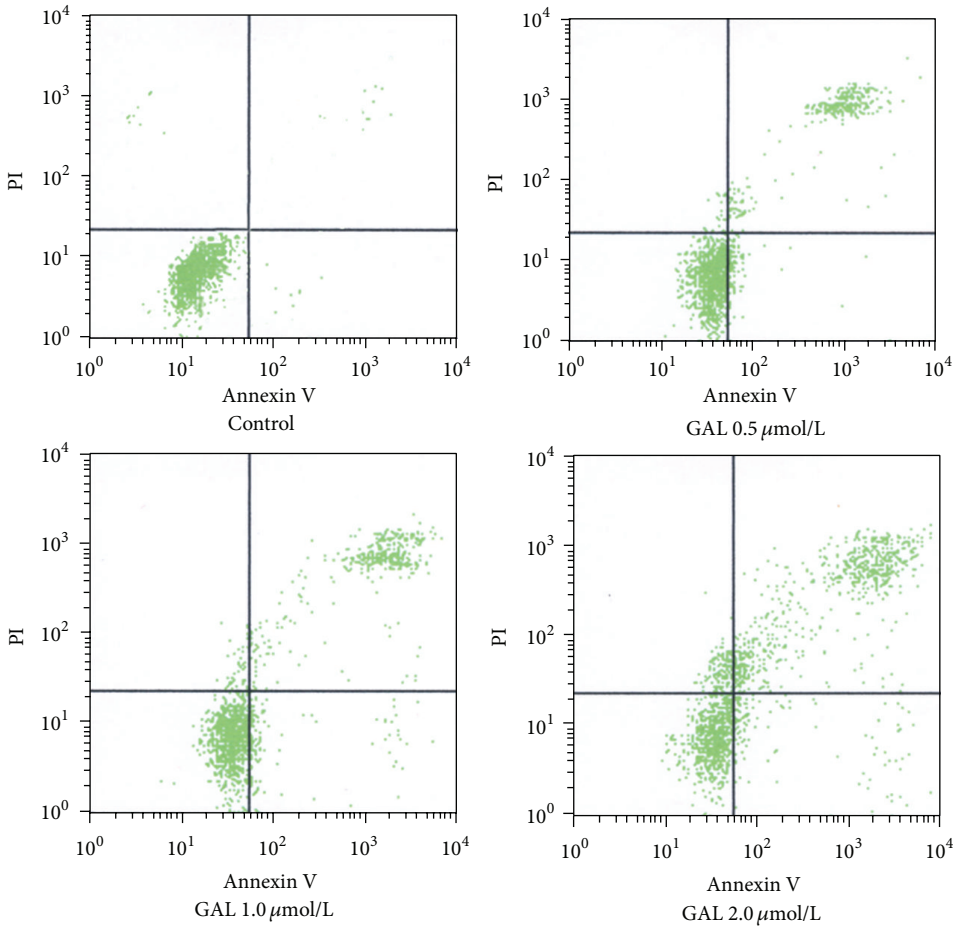

(b)

Figure 4: Gambogic acid lysinate can induce MCF-7 cell apoptosis. Exponential growth MCF-7 cells were treated with GAL (0, 0.5, 1, 1.5, and 2 μmol/L) for 24 h. (a) After treatment MCF-7 cells were stained with Hoechst 33258 and observed by fluorescence microscope. (b) After treatment MCF-7 cells were stained with annexin V-FITC and PI and analyzed with flow cytometer.

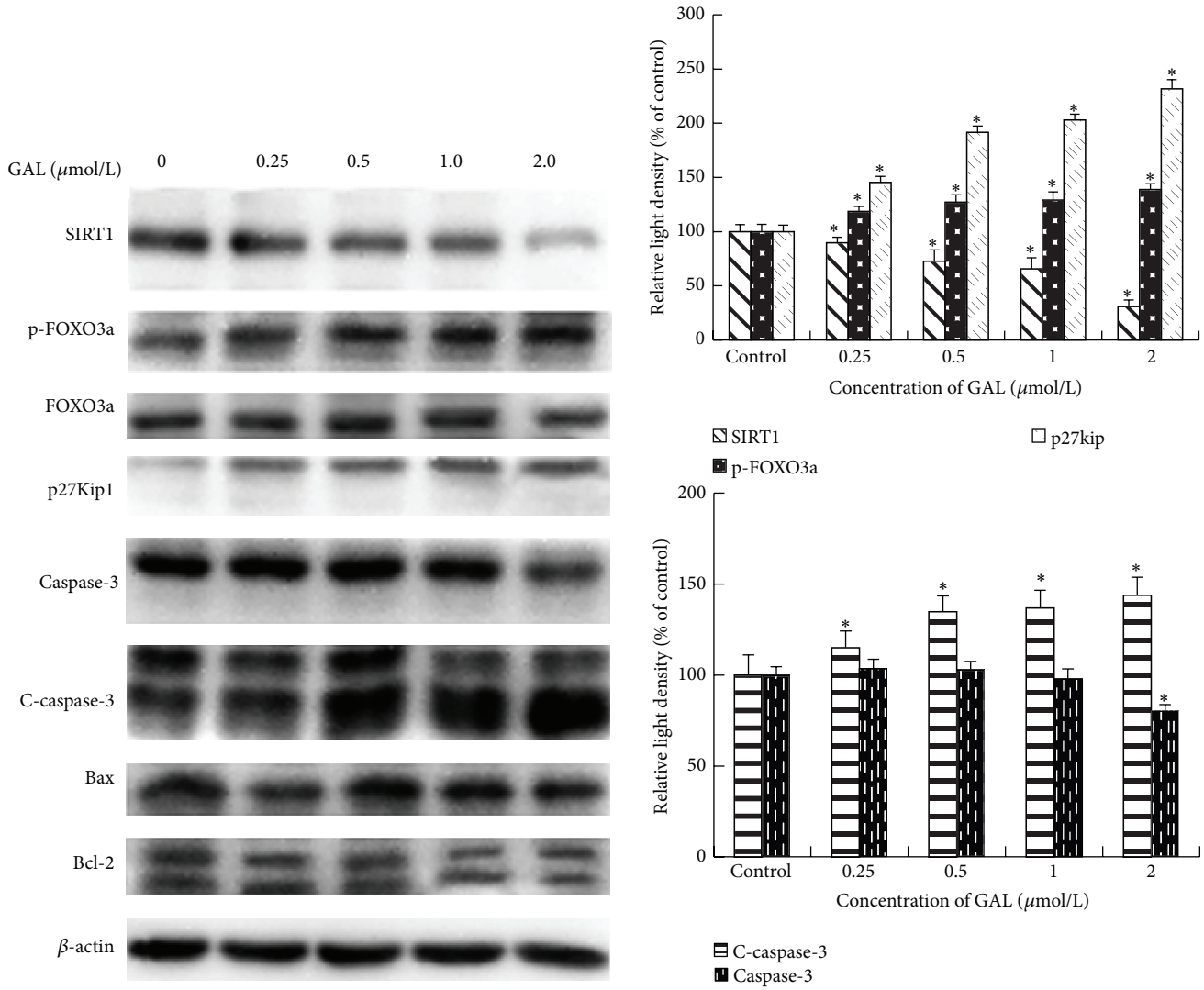

Figure 5: Gambogic acid lysinate can induce MCF-7 cells apoptosis by SIRT1 and caspase-3 signal pathway. MCF-7 cells were treated with the indicated concentrations of GAL for 24 h, and the cell extracts were prepared and analyzed by Western blotting with corresponding antibodies. The blots were quantified by densitometry with Scion Image (Scion Corporation, Frederick, MD, USA), and the relative ratio of target protein to β-actin was calculated and expressed as the mean ± SD from three experiments. $^{*}P < 0.05$ versus the control group.

assists in replenishing GSH when stores are compromised during oxidative or electrophilic stress [18, 19]. It can be deduced that GAL can inhibit MCF-7 cell proliferation by increasing ROS level, and NAC can remove the ROS induced by GAL. It is further confirmed by fluorescence microscope and fluorescence spectrophotometer by which intracellular ROS can be determined.

It is well known that ROS can induce cell apoptosis by various signal pathways including targeting cytosolic thioredoxin reductase [20], JNK/ATF2 pathway [21], p53-mitochondrial pathway [22], and AMPK/SIRT1/PGC-1α signal pathway [23]. It has been reported that GA has the ability to activate apoptotic signaling in numerous types of cancer cells. Herein, we also demonstrated that GAL kills MCF-7 cells predominantly through induction of apoptosis (Figure 4). GAL triggers apoptotic cell death in dose dependent manner. In Western blot analysis we also observed that SIRT1 expression was decreased in dose dependent manner. SIRT1 is one of the cytoplasmic NAD^{+}-dependent histone deacetylases and deacetylates histone H3 lysine 56 (H3K56) and a-tubulin. It also shares nonhistone substrates of FOXO1, FOXO3, and p53 with SIRT1 [24]. In previous study it is reported that forkhead transcription factors can be inhibited by the deacetylase SIRT1 [25], and increased expression of any FOXO member results in the activation of the cell cycle inhibitor p27Kip1 [26]. In this study we investigated the change of FOXO3a and p27Kip1. We found that the phosphorylation of FOXO3a and the expression of p27Kip1 increased with the decrease of SIRT1 expression. It can be concluded that SIRT1/FOXO3a/p27Kip1 signal pathway is one of the pathways by which GAL induced MCF-7 cell apoptosis. In the meantime we also observed that GAL enhanced the expression of cleaved caspase-3. It can be inferred that caspase-3 signal pathway also takes part in the apoptotic process induced

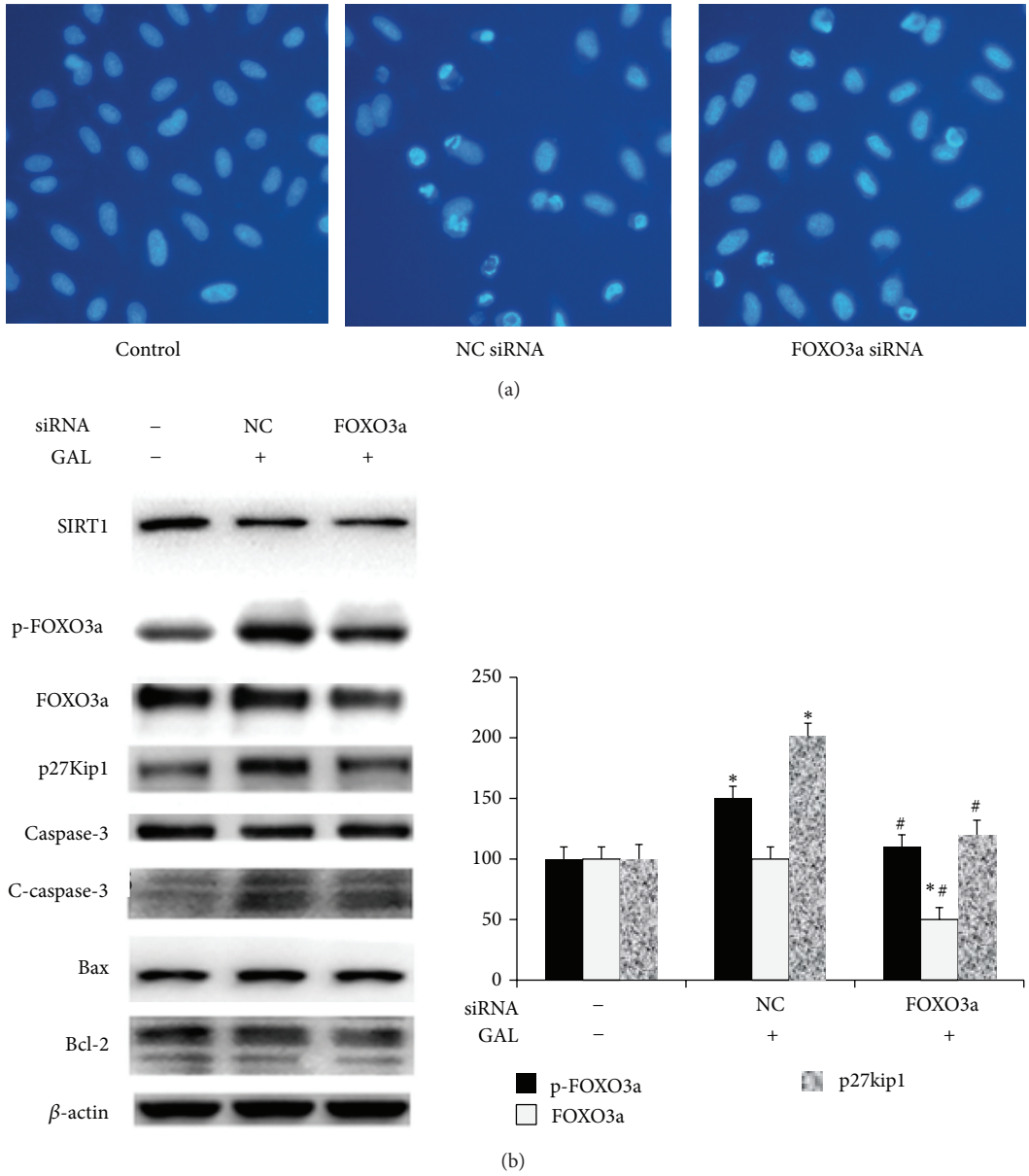

Figure 6: FOXO3a siRNA partly blocked cell apoptosis induced by GAL in MCF-7 cells. MCF-7 cells were transfected with NC or FOXO3a siRNA for 24 h; then 1 μmol/L GAL was added for 24 h. After GAL treatment for 24 h, (a) MCF-7 cells were stained with Hoechst 33258 and observed by fluorescence microscope; (b) MCF-7 cells were harvested and cell extracts were prepared and analyzed by Western blotting with corresponding antibodies. The blots were quantified by densitometry with Scion Image (Scion Corporation, Frederick, MD, USA), and the relative ratio of target protein to β-actin was calculated and expressed as the mean ± SD from three experiments. $^{*}P < 0.05$ versus the control group; $^{\#}P < 0.05$ versus the GAL+NC siRNA group.

by GAL. At knockdown of FOXO3a, we found the expression of FOXO3, the phosphorylation of FOXO3, and the expression of p27Kip1 were decreased and cell apoptosis induced by GAL was partly blocked; however the expression of SIRT1, caspase-3, Bax, and Bcl-2 did not change (Figure 6(b)). It was further confirmed that SIRT1/FOXO3a/p27Kip1 signal pathway is only one of the pathways by which GAL induced MCF-7 cell apoptosis.

In conclusion these results suggested that GAL inhibited MCF-7 cells proliferation and induced MCF-7 cells apoptosis by increasing ROS level which could induce cell apoptosis by both SIRT1/FOXO3a/p27Kip1 and caspase-3 signal pathway. GAL may be a new chemotherapy drug for breast cancer.

Conflict of Interests

The authors declare that they have no conflict of interests regarding the publication of this paper.

Authors' Contribution

Yong-Zhan Zhen and Ya-Jun Lin contributed equally to this work.

Acknowledgment

This work was financially supported by a grant from the National Natural Science Foundation of China (no. 81001439).

References

[1] C. Desantis, J. Ma, L. Bryan, and A. Jemal, "Breast cancer statistics, 2013," *CA Cancer Journal for Clinicians*, vol. 64, no. 1, pp. 52–62, 2014.

[2] G. Fountzilas, U. Dafni, C. Papadimitriou et al., "Dose-dense sequential adjuvant chemotherapy followed, as indicated, by trastuzumab for one year in patients with early breast cancer: first report at 5-year median follow-up of a Hellenic Cooperative Oncology Group randomized phase III trial," *BMC Cancer*, vol. 14, no. 1, p. 515, 2014.

[3] L. Amiri-Kordestani, G. M. Blumenthal, Q. C. Xu et al., "FDA approval: ado-trastuzumab emtansine for the treatment of patients with HER2-positive metastatic breast cancer," *Clinical Cancer Research*, vol. 20, no. 17, pp. 4436–4441, 2014.

[4] H. Wang, T. Vo, A. Hajar et al., "Multiple mechanisms underlying acquired resistance to taxanes in selected docetaxel-resistant MCF-7 breast cancer cells," *BMC Cancer*, vol. 14, no. 1, article 37, 2014.

[5] X. Wang and W. Chen, "Gambogic acid is a novel anticancer agent that inhibits cell proliferation, angiogenesis and metastasis," *Anti-Cancer Agents in Medicinal Chemistry*, vol. 12, no. 8, pp. 994–1000, 2012.

[6] R. Cascão, B. Vidal, H. Raquel et al., "Potent anti-inflammatory and antiproliferative effects of gambogic acid in a rat model of antigen-induced arthritis," *Mediators of Inflammation*, vol. 2014, Article ID 195327, 7 pages, 2014.

[7] J. Wen, H. Pei, X. Wang et al., "Gambogic acid exhibits anti-psoriatic efficacy through inhibition of angiogenesis and inflammation," *Journal of Dermatological Science*, vol. 74, no. 3, pp. 242–250, 2014.

[8] Q. Qi, N. Lu, C. Li et al., "Involvement of RECK in gambogic acid induced anti-invasive effect in A549 human lung carcinoma cells," *Molecular Carcinogenesis*, 2014.

[9] N. Lu, H. Hui, H. Yang et al., "Gambogic acid inhibits angiogenesis through inhibiting PHD2-VHL-HIF- 1α pathway," *European Journal of Pharmaceutical Sciences*, vol. 49, no. 2, pp. 220–226, 2013.

[10] D. Duan, B. Zhang, J. Yao et al., "Gambogic acid induces apoptosis in hepatocellular carcinoma SMMC-7721 cells by targeting cytosolic thioredoxin reductase," *Free Radical Biology and Medicine*, vol. 69, pp. 15–25, 2014.

[11] H. Zhang, Y. Lei, P. Yuan et al., "ROS-mediated autophagy induced by dysregulation of lipid metabolism plays a protective role in colorectal cancer cells treated with gambogic acid," *PLoS ONE*, vol. 9, no. 5, Article ID e96418, 2014.

[12] H. Zeng, R. Zheng, S. Zhang, X. Zou, and W. Chen, "Female breast cancer statistics of 2010 in China: estimates based on data from 145 population-based cancer registries," *Journal of Thoracic Disease*, vol. 6, no. 5, pp. 466–470, 2014.

[13] L. R. Saunders and E. Verdin, "Sirtuins: critical regulators at the crossroads between cancer and aging," *Oncogene*, vol. 26, no. 37, pp. 5489–5504, 2007.

[14] S. Proietti, A. Cucina, G. Dobrowolny et al., "Melatonin downregulates MDM2 gene expression and enhances p53 acetylation in MCF-7 cells," *Journal of Pineal Research*, vol. 57, no. 1, pp. 120–129, 2014.

[15] B. J. Hwang, A. Madabushi, J. Jin, S. Y. Lin, and A. L. Lu, "Histone/protein deacetylase SIRT1 is an anticancer therapeutic target," *American Journal of Cancer Research*, vol. 4, no. 3, pp. 211–221, 2014.

[16] H. Yuan, L. Su, and W. Y. Chen, "The emerging and diverse roles of sirtuins in cancer: a clinical perspective," *OncoTargets and Therapy*, vol. 6, pp. 1399–1416, 2013.

[17] X. Shi, X. Chen, X. Li et al., "Gambogic acid induces apoptosis in imatinib-resistant chronic myeloid leukemia cells via inducing proteasome inhibition and caspase-dependent bcr-abl down-regulation AC," *Clinical Cancer Research*, vol. 20, no. 1, pp. 151–163, 2014.

[18] I. Downs, J. Liu, T. Y. Aw, P. A. Adegboyega, and M. N. Ajuebor, "The ROS scavenger, NAC, regulates hepatic Vα14iNKT cells signaling during Fas mAB-dependent fulminant liver failure," *PLoS ONE*, vol. 7, no. 6, Article ID e38051, 2012.

[19] F. Zhang, S. S. Lau, and T. J. Monks, "The cytoprotective effect of N-acetyl-L-cysteine against ROS-induced cytotoxicity is independent of its ability to enhance glutathione synthesis," *Toxicological Sciences*, vol. 120, no. 1, pp. 87–97, 2011.

[20] D. Duan, B. Zhang, J. Yao, Y. Liu, and J. Fang, "Shikonin targets cytosolic thioredoxin reductase to induce ROS-mediated apoptosis in human promyelocytic leukemia HL-60 cells," *Free Radical Biology and Medicine*, vol. 70, pp. 182–193, 2014.

[21] J. J. An, K. J. Shi, W. Wei et al., "The ROS/JNK/ATF2 pathway mediates seleniteinduced leukemia NB4 cell cycle arrest and apoptosis in vitro and in vivo," *Cell Death and Disease*, vol. 4, no. 12, article e973, 2013.

[22] M.-J. Xie, Y.-H. Ma, L. Miao et al., "Emodin-provoked oxidative stress induces apoptosis in human colon cancer HCT116 cells through a p53-mitochondrial apoptotic pathway," *Asian Pacific Journal of Cancer Prevention*, vol. 15, no. 13, pp. 5201–5205, 2014.

[23] B. Huang, X. Cheng, D. Wang et al., "Adiponectin promotes pancreatic cancer progression by inhibiting apoptosis via the activation of AMPK/Sirt1/PGC-1α signaling," *Oncotarget*, vol. 5, no. 13, pp. 4732–4745, 2014.

[24] S. Hirai, S. Endo, R. Saito et al., "Antitumor effects of a sirtuin inhibitor, tenovin-6, against gastric cancer cells via death receptor 5 up-regulation," *PLoS ONE*, vol. 9, no. 7, Article ID e102831, 2014.

[25] Y. Yang, H. Hou, E. M. Haller, S. V. Nicosia, and W. Bai, "Suppression of FOXO1 activity by FHL2 through SIRT1-mediated deacetylation," *The EMBO Journal*, vol. 24, no. 5, pp. 1021–1032, 2005.

[26] G.-Z. Tao, N. Lehwald, K. Y. Jang et al., "Wnt/β-catenin signaling protects mouse liver against oxidative stress-induced apoptosis through the inhibition of forkhead transcription factor $FoxO_3$," *The Journal of Biological Chemistry*, vol. 288, no. 24, pp. 17214–17224, 2013.

Hindawi Publishing Corporation
Evidence-Based Complementary and Alternative Medicine
Volume 2015, Article ID 865714, 9 pages
http://dx.doi.org/10.1155/2015/865714

Research Article

Antitumor Activities of Ethyl Acetate Extracts from *Selaginella doederleinii* Hieron *In Vitro* and *In Vivo* and Its Possible Mechanism

Jia-zhi Wang, Juan Li, Ping Zhao, Wen-tao Ma, Xie-he Feng, and Ke-li Chen

Hubei University of Traditional Chinese Medicine, Key Laboratory of TCM Resource and TCM Compound Co-Constructed by Hubei Province and Ministry of Education, Wuhan 430065, China

Correspondence should be addressed to Juan Li; lz198207@126.com and Ke-li Chen; kelichen@126.com

Received 28 July 2014; Accepted 30 November 2014

Academic Editor: Senthamil R. Selvan

The antitumor activities of ethyl acetate extracts from *Selaginella doederleinii* Hieron (SD extracts) *in vitro* and *in vivo* and its possible mechanism were investigated. HPLC method was developed for chemical analysis. SD extracts were submitted to 3-(4,5-dimethylthiazol-2-yl)-2,5-diphenyl tetrazolium bromide (MTT) assay on different cells, flow cytometry, and RT-PCR analysis using HepG2 cell and antitumor activity *in vivo* using H-22 xenograft tumor mice. Six biflavonoids from SD extracts were submitted to molecular docking assay. The results showed that SD extracts had considerable antitumor activity *in vitro* and *in vivo* without obvious toxicity on normal cells and could induce cell apoptosis. The mechanisms of tumorigenesis and cell apoptosis induced by SD extracts may be associated with decreasing the ratio of bcl-2 and bax mRNA level, activating caspase-3, suppressing survivin, and decreasing the gene expression of COX-2, 5-LOX, FLAP, and 12-LOX mRNA. The main active component in SD extracts is biflavonoids and some exhibited strong interactions with COX-2, 5-LOX, 12-LOX, and 15-LOX. These results offering evidence of possible mechanisms of SD extracts suppress cell proliferation and promote apoptosis and provide the molecular theoretical basis of clinical application of *S. doederleinii* for cancer therapy.

1. Introduction

Selaginella doederleinii Hieron is a traditional Chinese folk herb which belongs to the family *Selaginellaceae* and is abundant in South and Southwestern China at low altitude [1]. It has been used as folk medicine for the therapy of sore throat, rheumatoid arthritis, and different tumors with a long history, especially for nasopharyngeal carcinoma, choriocarcinoma, lung cancer, and cervical cancer [2–4].

Lian et al. reported that the ethanol extract of *S. doederleinii* can induce mitochondria-related apoptosis in human nasopharyngeal carcinoma CNE cells [5, 6]. Also, researches on the cytotoxic activity against HCT, NCI-H358, K562, and CNE cells of *S. doederleinii* have been reported [1, 6, 7]. Compounds from this herb such as several biflavonoids, lignans, and alkaloids have been reported [7–9]. However, ethyl acetate extracts had stronger antitumor activities than ethanol extract for their abundant biflavonoids, such as amentoflavone, robustaflavone, 2″,3″-dihydro-3′,3‴-biapigenin, 3′,3‴-binaringenin, heveaflavone, and 7,4′,7″,4‴-tetra-O-methyl-amentoflavone [10, 11].

Aberrant arachidonic acid (AA) metabolism is involved in the inflammatory and carcinogenic processes. The effects of biflavonoid mixture from *S. doederleinii* on cyclooxygenase (COX) and lipoxygenase- (LOX-) dependent AA expression in hepatocellular carcinoma were investigated and their effects on cell proliferation and apoptosis were also studied.

2. Materials and Methods

2.1. Plant Materials. The Chinese herbal *S. doederleinii* was collected from Nanning (Guangxi, China). Identification of specimen was confirmed by Dr. Dingrong Wan, South-Central University for Nationalities (Wuhan, China), and a voucher specimen was deposited in the herbarium of Hubei University of Chinese Medicine, China.

SD extract was obtained by the previously described method [8]. Briefly, the air-dried and powdered samples were

extracted twice with petroleum ether and then were filtered. The residues were extracted twice with ethyl acetate and then were filtered. Then the solution was dried using a rotary evaporator, and it was lyophilized and transformed into a power before dissolved in DMSO (dimethyl sulfoxide). The purity of SD extract was about 9.3%.

2.2. HPLC Analysis. The detailed method of HPLC analysis could be seen in the literature [11, 12]. Briefly, HPLC analysis was performed on a Dionex HPLC system with P680 Pump, a DiamonsilTM C18 column (250 mm × 5.6 mm, 5 μm), and a UVD 170 U variable wavelength UV-Vis detector. Data were collected and processed using "Chromeleon version 6.0" software. The mobile phase consisted of acetonitrile (A) and water (B). The gradient program was as follows: 25% A in 0–5 min, 25–35% A in 5–12 min, 35–45% A in 12–17 min, 45–50% A in 17–25 min, 50–55% A in 25–40 min, 55–70% A in 40–45 min, 70–100% A in 45–50 min, 100% A in 50–55 min, and 100–25% A in 55–60 min. The flow rate was 1.0 mL/min and column temperature was maintained at 30°C. The injection volume was 10 μL. The detector was set at 330 nm for acquiring chromatograms.

2.3. Reagents and Cell Culture. MTT, Trizol, and DMSO were obtained from Sigma (St. Louis, MO, USA). DMEM medium, trypsin, penicillin, and streptomycin were purchased from Gibco (USA). FBS (fetal bovine serum) was bought from Hyclone (USA). All chemicals and reagents were of analytical reagent grade.

HepG2 (hepatocellular carcinoma), Hela (cervical carcinoma), A549 (lung cancer), DU145 (prostatic carcinoma), PC12 (pheochromocytoma), and Vero (African green monkey kidney) cells were obtained from China Center for Type Culture Collection of Wuhan University. The cells were incubated in a humidified atmosphere of 95% air and 5% CO_2 at 37°C and maintained in DMEM culture medium with 10% FBS plus 100 U/mL streptomycin and 100 U/mL penicillin. The cells were subcultured with 0.25% trypsin when they were 80% confluent. Then, the cells in exponential growth phase were collected for the following experiments.

2.4. MTT Assay. Evaluation of antitumor activity *in vitro* was determined with MTT assay which was performed as described before [13]. Briefly, the cells were seeded in 96-well culture plates at a density of 2×10^3 cells per well and then allowed to attach for 24 h before treated with varying concentrations of SD extracts (0, 12.5, 25, 50, 75, 100, and 200 μg/mL) for 72 h. Subsequently, 50 μL MTT of 1 mg/mL was added to each well to react 4 h. The absorbance was determined using the 96-well microplate reader at 570 nm after the formed purple formazan crystals dissolved in 100 μL DMSO. The growth inhibitory ratio was calculated by the following formula: rate of growth inhibition (%) = $(1 - OD_{treated}/OD_{control}) \times 100\%$ [14]. The IC_{50} value (concentration of 50% inhibition) was obtained from the dose-response plots of three independent repetitive trials.

2.5. Morphology Observation. HepG2 cells were seeded into 24-well plates at a density of 10^4 cells per well and then exposed to different concentrations of SD extracts for 48 h. The morphological changes of cells were observed and photographed using inverted light microscopy (IX70; Olympus Optical Co., Tokyo, Japan).

2.6. Annexin V-FITC/PI Double Staining Assay. Exponentially growing HepG2 cells were placed down in 6-well plate and cultured as above. Then the cells were treated with SD extracts at different concentrations for 24 h. After the drug incubation time, all cells were harvested with trypsin and washed twice with PBS, followed by resuspended in 400 μL Annexin V binding buffer. Then the cells were stained with 5 μL Annexin V-FITC for 15 minutes and 10 μL PI for 5 minutes at 4°C. This assay was performed exactly as the manufacturers' instruction of the Annexin V-FITC cell apoptosis detection kit (BestBio, china). A FACSCalibur flow cytometer was used to detected fluorescence and the percentage of apoptotic cells was calculated by the internal software system of the FACSCalibur. Approximately 10^4 cells were analyzed for each trail.

2.7. RNA Extraction and Real-Time PCR. The mRNA levels of COX-2, FLAP, 5-LOX, 12-LOX, 15-LOX, bcl-2, bax, caspase-3, and survivin were quantified by real-time RT-PCR assays. The β-actin was internal reference gene. HepG2 cells were placed down in 6-well plate at a concentration of 5×10^5 cells/mL. After 60% confluency, the cells were exposed to SD extracts at the concentration of IC_{50} for different times (0, 1.5, 3, 6, 9, and 12 h). Then, the cells were harvested to SD extract total RNA using Trizol reagent. A UV spectrophotometer was used to estimate RNA concentration at 260 nm. The purity of RNA was assessed by the ratio of absorbance at 260 and 280 nm (A260/A280 between 1.8 and 2.0). After quantification, 2 μg RNA was used for the synthesis of cDNA in each reverse transcription reaction via TIANScript RT Kit. We conducted PCR to amplify the target genes with reagents and protocols from the SYBR Green PCR Master Mix kit by Invitrogen (Carlsbad, CA, USA). The 20 μL reaction system contained 1 μL generated cDNA template, 1 μL of specific sense primer (Table 1), 1 μL of specific antisense primer, 10 μL 2 × SYBR Green PCR Master Mix, and 7 μL double distilled water. The thermal cycling conditions were 95°C for 15 min, followed by 40 cycles of 95°C for 10 s, 59–63°C (annealing temperature) for 20 s, and 72°C for 30 s and a final incubation at 72°C for 5 min. The relative expression of each gene was normalized to the amount of β-actin in the same dosage of cDNA, and the relative quantification method was $2^{-\Delta\Delta CT}$ method [15]. All RT-PCR reactions for each sample were done in triplicate.

2.8. Molecular Docking. We performed a series of molecular docking experiments to estimate the binding affinity of some biflavonoids with COX-2, LOX-5, LOX-12, and LOX-15.

2.8.1. Preparing Protein and Ligands. The three-dimensional structure of biflavonoids was downloaded from PubChem (http://pubchem.ncbi.nlm.nih.gov/) database [16] and refined with the help of Discovery Studio Visualizer (http://accelrys.com/products/discovery-studio/visualization.html). Then, these ligands were converted to MOL2 format using

Table 1: Primer list.

Gene	Forward primer (5′ to 3′)	Reverse primer (5′ to 3′)
5-LOX	GCCTCCCTGTGCTTTCC	ACCTGGTCGCCCTCGTA
FLAP	GCTGCGTTTGCTGGACTGATGTA	TAGAGGGGAGATGGTGGTGGAGAT
12-LOX	CTTCCCGTGCTACCGCTG	TGGGGTTGGCACCATTGAG
15-LOX	CTGGAGCCTTCCTAACCT	GTGACAAAGTGGCAAACC
COX-2	TATGAGTGTGGGATTTGACCAG	TCAGCATTGTAAGTTGGTGGAC
bcl-2	GTGGAGGAGCTCTTCAGGGA	AGGCACCCAGGGTGATGCAA
bax	GGCCCACCAGCTCTGAGCAGA	GCCACGTGGGCGTCCCAAAGT
caspase-3	ATGGAGAACACTGAAAACTCAGT	TTAGTGATAAAAATAGAGTTCTTTTGT
survivin	ATGGGTGCCCCGACGTTGCCCCCT	TCAATCCATGGCAGCCAGCTGCTCG
β-actin	TGACGTGGACATCCGCAAAG	CTGGAAGGTGGACAGCGAGG

this software. Finally, these mol2 files are optimized by "Prepare Ligands" in Autodock Tools [17] and converted to PDBQT files. The 3D structure of COX-2 (PDBID: 1CX2) [18], LOX-5 (PDBID: 2Q7M) [19], LOX-12 (PDBID: 3RDE) [20], and LOX-15 (PDBID: 1LOX) [21] was obtained from Protein Data Bank, based on their resolution and chemical similarity between bioflavonoids of *S. doederleinii* and the cocrystalled ligands. Protein structure was imported to Autodock Tools. After deleting duplicated chains, removing water and other ligands, and adding hydrogen, the preprocessed structure was assigned with AMBER force field [22] and converted to PDBQT files automatically.

2.8.2. Docking Methodology. Docking procedure can be divided into two parts: grid generation and docking. In the AutoGrid procedure, the target enzyme was embedded on a three-dimensional grid point [17]. The energy of interaction of each atom in the ligand was encountered. In the following phase, Autodock 4.2 was employed in this study. This software uses Lamarckian genetic algorithm (LGA) to perform ligand conformational searching. This algorithm first builds a population of individuals (genes), and then each individual is mutated to acquire a slightly different translation and rotation. The individuals with the low resulting energy after energy minimization process are transferred to the next generation and the process is repeated to obtain the best scored one. For each, binding energy of each pose was calculated using AutoDock 4.2 scoring functions [23].

In the present study, three-dimensional affinity grids of size $60 \times 60 \times 60$ Å with 0.6 Å spacing which centered on the geometric center of cocrystalled ligand were calculated for each of the following atom types: HD, C, A, N, OA, and SA, which represent all possible atom types in a protein and ligand. Additionally, an electrostatic map and a desolvation map were also calculated. Rapid energy evaluation was achieved by precalculating atomic affinity potentials for each atom in the ligand molecule. We have selected important docking parameters for the LGA as follows: population size of 150 individuals, 5 million energy evaluations, maximum of 30000 generations, number of top individuals to automatically survive to next generation of 1, mutation rate of 0.02, crossover rate of 0.8, 10 docking runs, and random initial positions and conformations. The probability of performing local search on an individual in the population was set to 0.06. Top-scored conformation of each ligand was analyzed by AutoDock Tools and Pymol.

2.9. Antitumor Activity of SD Extracts In Vivo. Kunming mice (male, 20 ± 2 g) were procured from the Center of Experimental Animals in Wuhan University, Wuhan, China. In order to evaluate the antitumor effect of SD extracts *in vivo*, the mice were injected with H-22 (mice hepatoma) cells in the armpit for subcutaneous xenograft tumor models, respectively, except the normal group mice. Then the tumor bearing mice were divided into five groups randomly of which each group has 12 mice. The negative and normal control group mice received only 0.9% normal saline. 5-Fu intraperitoneal injection was taken as positive control. The low-dose, medial-dose, and high-dose drug group were orally administrated with 4, 8, and 16 g/kg/d SD extracts separately. All samples were administrated once every day for 10 days except positive group mice which administrated every other day (10 mg/kg/2d). On the 11th day, all mice were sacrificed, and tumors were excised and weighed for evaluating the tumor growth inhibition. The spleen and thymus were also segregated and weighed to calculate the spleen index and thymus index.

2.10. Statistical Analysis. The statistical analysis was evaluated by Student's t-test. All data were expressed as mean ± SD. Variance of P values obtained was calculated by means of a single-factor ANOVA test. The values of P less than 0.05 were considered to be significantly different from each control.

3. Results

3.1. Fingerprints Analysis. HPLC chromatogram was applied for examining biflavonoids from ethyl acetate extracts. As reported in literature [10], the peaks of amentoflavone, robustaflavone, 2″,3″-dihydro-3′,3‴-biapigenin, 3′,3‴-binaringenin, heveaflavone, and 7,4′,7″,4‴-tetra-O-methyl-amentoflavone were marked in Figure 1.

3.2. Growth Inhibitory Effects of SD Extract on Different Cells. It was widely assumed that MTT has become one of the most widely used methods for measuring cell proliferation

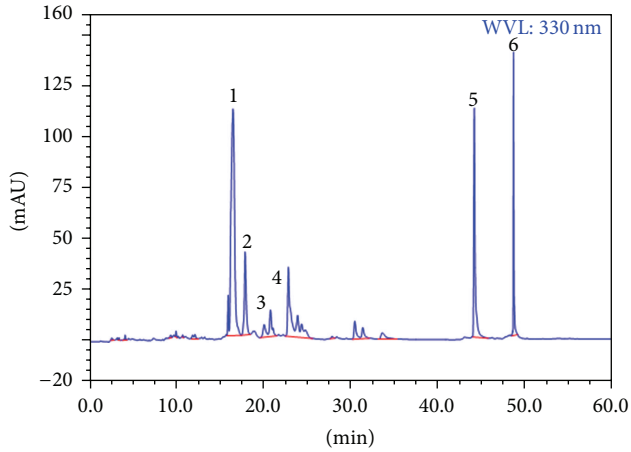

Figure 1: HPLC chromatogram of ethyl acetate extracts. 1: amentoflavone; 2: robustaflavone; 3: 2″,3″-dihydro-3′,3‴-biapigenin; 4: 3′,3‴-binaringenin; 5: heveaflavone; 6: 7,4′,7″,4‴-tetra-O-methylamentoflavone.

Table 2: IC_{50} values for SD extracts on the proliferation of different cells (μg/mL).

	DU145	HeLa	A549	HepG2	PC12	Vero
SD extracts	70.5 ± 2.6	76.1 ± 1.9	51.9 ± 1.5	65.8 ± 4.4	>150	>150

Values are means ± SD (n = 5).

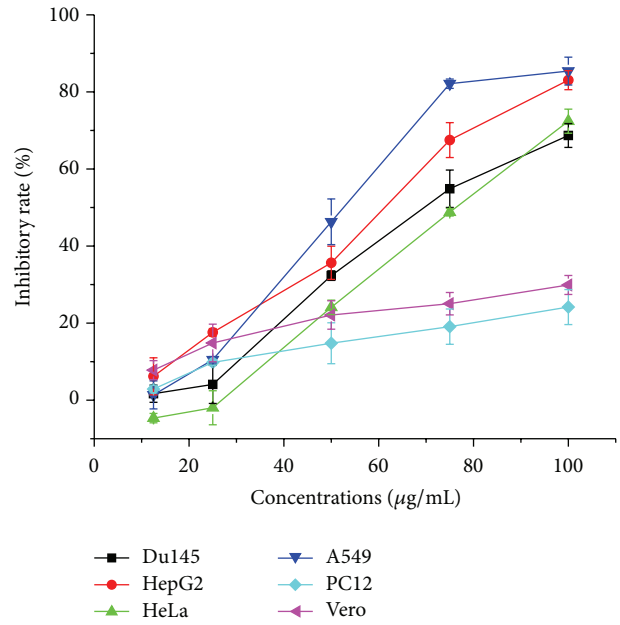

Figure 2: Inhibitory effect of SD extracts on the proliferation of Du145, HepG2, HeLa, A549, PC12, and Vero cells. Cells were treated with different concentrations of SD extracts for 72 h. Values are means ± SD (n = 5).

and viability. In our study, inhibitory activities against five different tumor cells (DU145, HepG2, HeLa, A549, and PC12) and one normal cell (Vero) were evaluated by MTT method. The data from Table 2 suggested that extracts had definite cytotoxic effect on various cancer cells with a close IC_{50} value except for PC12, which have similar structure and function to the nerve cell and (but) a higher chance of surviving, so it is often used as a cell model to study the nervous system [24]. For this reason, the higher IC_{50} value of SD extracts against PC12 indicated that SD extracts (with little damage to) hurt the central nervous system little and that was also revealed in Figure 2.

As shown in Figure 2, SD extracts caused the tumor cells death in a dose-dependent manner and exhibited apparent cytotoxicity to cancer cells. In addition, for normal cells Vero, SD extracts lead to a growth inhibition rate less than 30%, even at the concentration of 100 μg/mL. The level of cytotoxicity of SD extracts against Vero cells was much lower than cancer cells (Figure 2). The results identified that SD extracts had considerable antitumor activity and low cytotoxicity on normal cells.

3.3. Morphological Changes of HepG2 Cells Induced by SD Extracts under Inverted Microscope. As shown in Figure 3, morphological changes of HepG2 cells which were treated with SD extracts at different concentrations (25, 50, and 100 μg/mL) were observed as compared with the untreated control cells. Untreated HepG2 cells attached closely on the culture surface in polygon or rotundity with a good refraction and some of them contacted each other to form colonies (Figure 3). However, after treatment with SD extracts, the cells lost their surface morphology significantly and become small and round, made fewer cellular contacts, reduced in size and number. It also can be seen that cell number is depressed obviously. Also these cell morphological changes were in a dose- and time-dependent manner.

3.4. Apoptosis Analysis by Flow Cytometry. To determine whether SD extracts-induced cell death was related to apoptosis, Annexin V-FITC/PI staining assay was conducted. Display of phosphatidylserine on the surface of cells, considered as the hallmark of apoptosis in early phase, was determined by PI/Annexin V staining assay. When cells were treated with 25 to 200 μg/mL SD extracts for 24 h, cell populations in late apoptotic phases increased from 5.76% to 14.29%, compared with 2.8% of apoptotic cells in the control (Figure 4).

3.5. SD Extracts Changed mRNA Expression of Proinflammatory Factors and Apoptosis-Related Genes. We preformed RT-PCR assay to determine whether SD extracts treatment changed expression of several proinflammatory genes and apoptosis-related genes, which have been verified relevant to cell proliferation, apoptosis, invasion, metastasis, and angiogenesis [25]. As seen in Figure 5, the level of COX-2, 5-LOX, FLAP, and 12-LOX mRNA was markedly decreased by SD extracts in HepG2 cells compared with untreated cells, which implied SD extracts might restrain proinflammatory cytokines production at gene level. In the meanwhile, the mRNA expression of 15-LOX which was generally thought to present tumor inhibition effect increased significantly up to

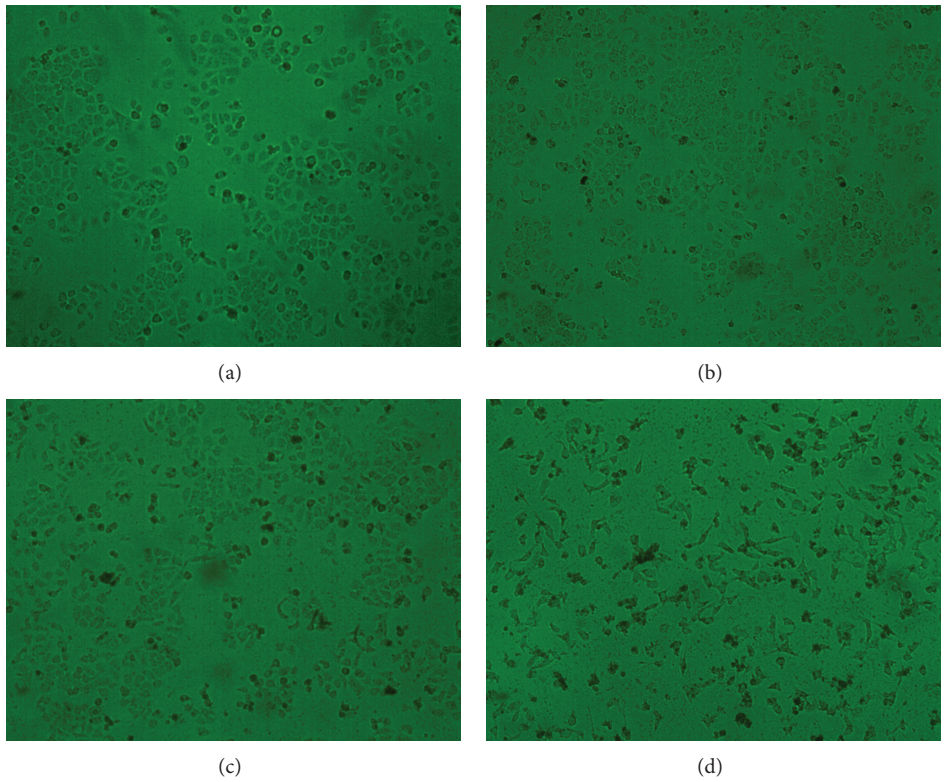

Figure 3: Morphological changes of HepG2 cells induced by different concentration of SD extracts. Changes of cellular morphology were examined at 24 h with 400 magnification. (a) Control; (b) 25 μg/mL; (c) 50 μg/mL; (d) 100 μg/mL.

5.51 times higher than control group (data was not shown). In addition, the expression of COX-2, 5-LOX, FLAP, 12-LOX, and 15-LOX mRNA levels changes regularly with the action time of SD extracts extending in 12 h. The treatment of SD extracts on HepG2 cells for 12 h inhibited COX-2, 5-LOX, FLAP, and 12-LOX mRNA production up to 74.22%, 67.1%, 71.3%, and 83.03%, respectively. These results demonstrated that SD extracts treated for indicated time would resulted in regression of inflammatory in a time-dependent manner, and its effect of inhibiting cell proliferation and promoting cell apoptosis were related with down-regulation of COX-2, 5-LOX, FLAP and 12-LOX and up-regulation of 15-LOX.

In another aspect, bcl-2 and bax are a pair of momentous apoptosis genes, the ratio of bax to bcl-2 determines whether a cell undergoes apoptosis [26], and survivin can prevent and attenuate cell apoptosis markedly [27]. mRNA expression levels of antiapoptotic genes bcl-2 and survivin, proapoptotic gene bax, and caspase-3 were also determined by RT-PCR. Survivin and bcl-2 mRNA expression were decreased, whereas that of bax and caspase-3 were increased in time-dependent manner after SD extracts treatment (Figure 6). As shown in Figure 6, bax and caspase-3 genes were observed to be induced by about 1.92- and 2.62-fold, respectively, whereas bcl-2 and survivin were repressed by about 73.9% and 71.8% after SD extracts treatment compared to untreated cells. These results demonstrated that one of the possible mechanisms of SD extracts induced apoptosis was associated with expression changes of bax, bcl-2, caspase-3, and survivin.

3.6. Molecular Docking. The docking process was accomplished by AutoDock (version 4.2) and the docking results were quantified by AutoDock 4.2 scoring functions. The docking score for biflavonoids could be seen in Figure 7, 3′,3‴-binaringenin exhibited strong interactions with COX-2, all compounds showed good interactions with LOX-5, and amentoflavone, 2″,3″-dihydro-3′,3‴-biapigenin, 3′,3‴-binaringenin, and heveaflavone might have potential better binding ability with LOX-12, while all compounds showed weak interactions with LOX-15. However, robustaflavone exhibited no interactions with COX-2 and LOX-15, and 7,4′,7″,4‴-tetra-O-methylamentoflavone exhibited no interactions with LOX-12 and LOX-15. The binding mode analysis of amentoflavone with COX-2 could be seen in Figure 8.

3.7. Antitumor Activity In Vivo. Due to the good antitumor activities *in vitro* of SD extracts, they were examined for animal studies. As daily observation, no mice dead when treated with SD extracts. The effects of SD extracts on mice transplanted with H-22 were presented in Table 3. The results revealed that SD extracts significantly decreased the tumor weights of H-22 tumor-bearing mice. The inhibitory rates were 23.8%, 39.8%, and 57.7% at the dosages of 4, 8, and 16 g/kg/day, respectively. Furthermore, SD extracts could decrease the spleen and thymus index of the tumor-bearing mice (Table 3).

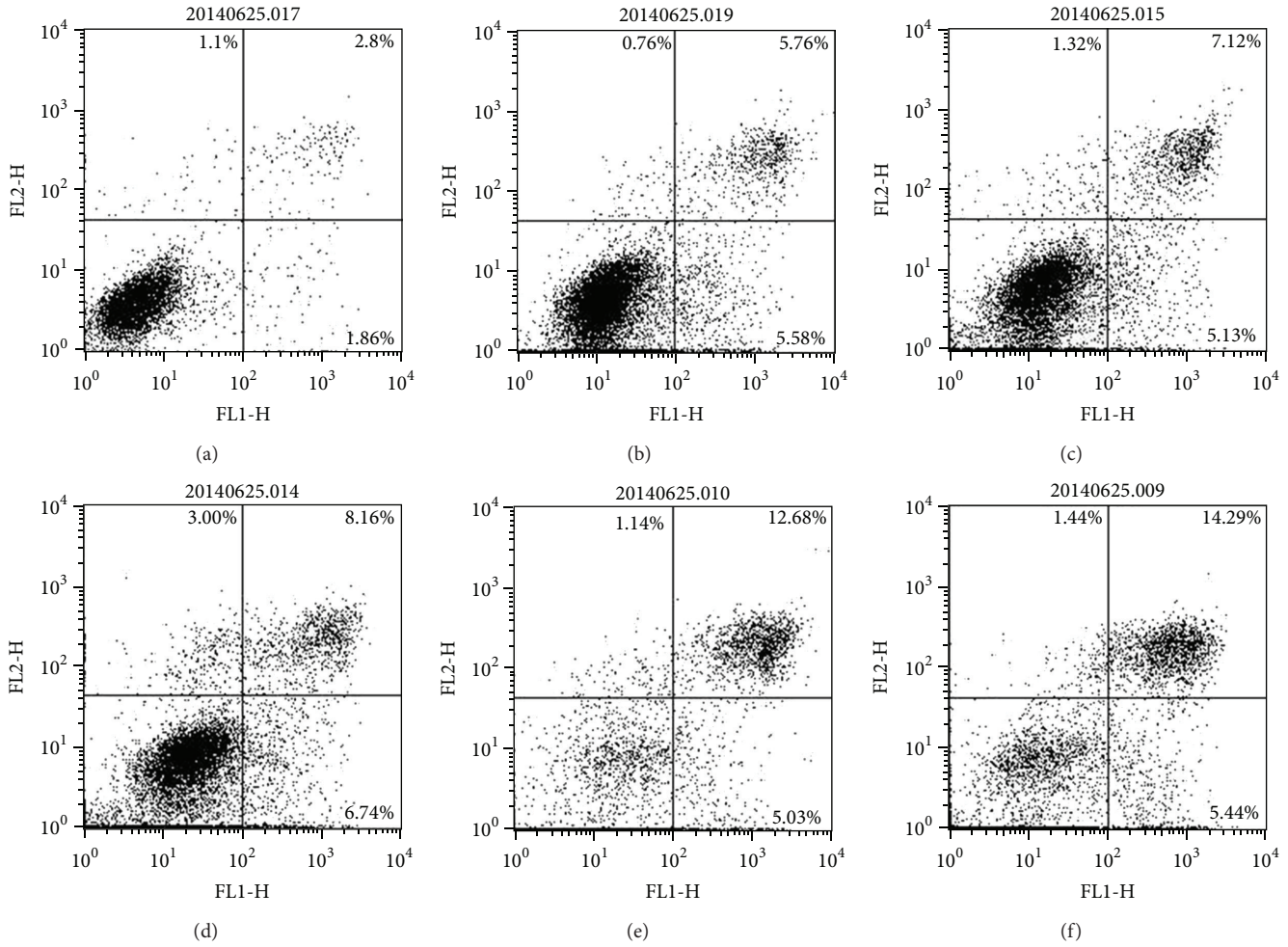

Figure 4: Apoptosis induction by SD extracts in HepG2 cells. Phosphatidylserine translocation of HepG2 cells after SD extracts treatment for 24 h. The population in the region of PI^-/Annexin V^- was considered to be normal cells, the population in the region of PI^-/Annexin V^+ was considered to be early apoptotic cells, while that of PI^+/Annexin V^+ was considered to be late apoptotic cells. (a) Control; (b) 25 μg/mL; (c) 50 μg/mL; (d) 75 μg/mL; (e) 100 μg/mL; (f) 150 μg/mL.

4. Discussion

In the present study, we investigated the anticancer effects of SD extracts on tumor cells and the possible mechanisms. MTT assay proved that SD extracts significantly exhibited antiproliferation activity on various carcinoma cells with a low IC_{50} value and had little damage on Vero and PC12 cells, demonstrating its selective antitumor action to some degree and potential practical valuableness in the therapy for cancer. However, more in-depth research on the detailed mechanisms of SD extracts killing tumor cells rather than normal cells is needed.

Several proinflammatory mediators have been confirmed to play a significant role in inhibition of angiogenesis, apoptosis, proliferation, and metastasis [28]. Both COX and LOX pathway function as a crucial mediator of cell survival and apoptosis [29–31]. COX-2 has been implicated in the growth and progression of a variety of human cancers, 5-LOX and FLAP play a vital role in tumor cells growth related signal transduction and can stimulate oncogene expression, and 12-LOX may be responsible for the adhesion, invasion, and metastasis of cancer cells and also can promote tumor angiogenesis [30]. However, 15-LOX is now considered to be a tumor-inhibiting factor and mainly inhibit carcinoma cells growth. Our RT-PCR results indicated that the mRNA expression of COX-2, 5-LOX, FLAP, and 12-LOX decreased and 15-LOX increased in HepG2 cells after SD extracts treatment. The susceptibility to apoptosis by SD extracts is associated with the level of COX-2 and LOXs in HepG2 cells, which present high COX-2 expression spontaneously. Therefore, SD extracts, as agents which bring the gene expression of COX-2, 5-LOX, FLAP, and 12-LOX mRNA down, should play an inhibitory role in tumorigenesis and metastasis and induce carcinoma cells apoptosis.

The main active component in SD extracts is biflavonoids, and different biflavonoids exhibited interactions with COX-2, 5-LOX, 12-LOX, and 15-LOX in varying degrees. This study just analyzed six biflavonoids, and there were other compounds in SD extracts, and more works are needed.

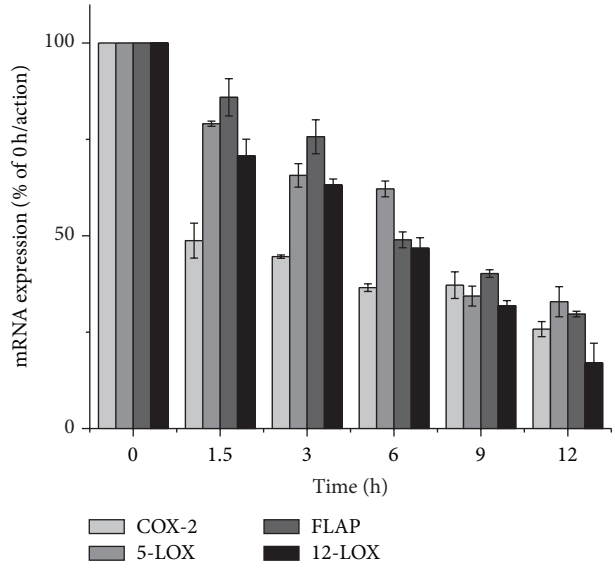

Figure 5: Effects of SD extracts on COX-2, 5-LOX, FLAP, and 12-LOX mRNA expression. HepG2 cells were treated with SD extracts (65.8 μg/mL) for 0, 1.5, 3, 6, 9, and 12 h. COX-2, 5-LOX, FLAP, and 12-LOX mRNA levels were determined by RT-PCR. Values are means ± SD ($n = 5$).

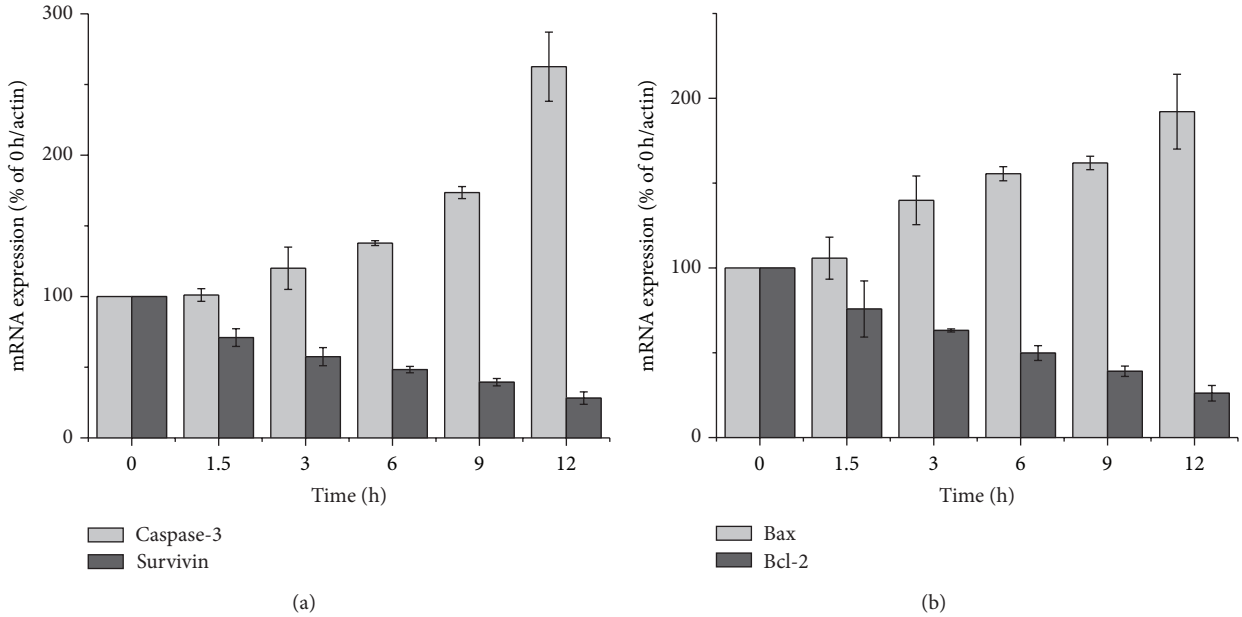

Figure 6: Effects of SD extracts on mRNA expression of apoptosis-related genes. (a) mRNA expression of caspase-3 and survivin genes in HepG2 cells treated with SD extracts (65.8 μg/mL) for 0, 1.5, 3, 6, 9, and 12 h. Values are means ± SD ($n = 5$). (b) mRNA expression of bax and bcl-2 genes in HepG2 cells treated with SD extracts for 0, 1.5, 3, 6, 9, and 12 h. Values are means ± SD ($n = 5$).

Table 3: Antitumor effects of SD extracts against tumor growth on H-22 tumor-bearing mice.

		Tumor weight (g)	Tumor growth inhibition (%)	Spleen index (mg/10 g)	Thymus index (mg/10 g)
H22	Control	1.46 ± 0.30		5.62 ± 0.83	2.02 ± 0.42
	16 g/kg	0.62 ± 0.27**	57.7	4.96 ± 0.72	1.64 ± 0.24*
	8 g/kg	0.88 ± 0.28*	39.8	5.30 ± 1.02	1.79 ± 0.38
	4 g/kg	1.12 ± 0.40	23.3	5.55 ± 0.95	1.90 ± 0.32
	5-Fu	0.60 ± 0.15**	58.9	4.76 ± 0.72*	1.42 ± 0.2**

Values represent mean ± SE. * $P < 0.05$ compared to the control group; ** $P < 0.01$ compared to the control group.

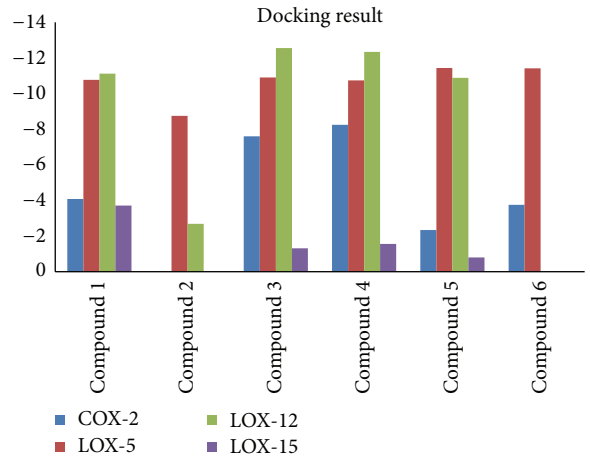

Figure 7: Quantify the interaction between biflavonoids and COX-2, LOX-5, LOX-12, and LOX-15 by AutoDock program. 1: amentoflavone; 2: robustaflavone; 3: 2″,3″-dihydro-3′,3‴-biapigenin; 4: 3′,3‴-binaringenin; 5: heveaflavone; 6: 7,4′,7″,4‴-tetra-O-methylamentoflavone.

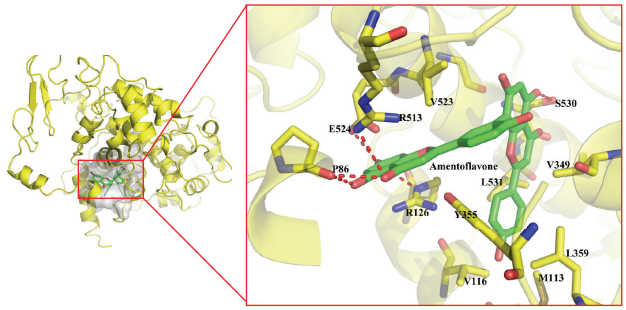

Figure 8: The binding mode analysis of amentoflavone with COX-2. The interactions were analyzed by Pymol.

We also utilized an RT-PCR method to quantitate the expression of both bcl-2, bax, caspase-3, and survivin mRNA expression. The results showed that one of the mechanisms of cell apoptosis induced by SD extracts may decrease the ratio of bcl-2 and bax mRNA level, activate caspase-3, and suppress survivin to promote cell apoptosis.

5. Conclusion

In summary, SD extracts had considerable antitumor activity *in vitro* and *in vivo* without obvious toxicity on normal cells and could induce cell apoptosis. The mechanisms of tumorigenesis and carcinoma cell apoptosis induced by SD extracts may be associated with decreasing the ratio of bcl-2 and bax mRNA level, activating caspase-3, suppressing survivin, and decreasing the gene expression of COX-2, 5-LOX, FLAP, and 12-LOX mRNA. The main active component in SD extracts is biflavonoids, and some exhibited strong interactions with COX-2, 5-LOX, 12-LOX, and 15-LOX.

Abbreviations

AA:	Aberrant arachidonic acid
IC_{50}:	Concentration of 50% inhibition
COX:	Cyclooxygenase
DMSO:	Dimethyl sulfoxide
FBS:	Fetal bovine serum
HEp-2:	Human laryngeal carcinoma cells
LOX:	Lipoxygenase
MTT:	3-(4,5-Dimethylthiazol-2-yl)-2,5-diphenyl tetrazolium bromide
PI:	Propidium iodide
SD extracts:	Ethyl acetate extract of *Selaginella doederleinii*.

Conflict of Interests

The authors declare that there is no conflict of interests regarding the publication of this paper.

Authors' Contribution

Jia-zhi Wang and Juan Li contributed equally to the work.

Acknowledgment

This work was supported by the Scientific Research Foundation Project of the Education Department of Hubei Province (Q20142007).

References

[1] R. C. Lin, A. L. Skaltsounis, E. Seguin, F. Tillequin, and M. Koch, "Phenolic constituents of *Selaginella doederleinii*," *Planta Medica*, vol. 60, no. 2, pp. 168–170, 1994.

[2] T. C. Zhou, X. D. Lin, X. L. Song et al., "Long term treatment outcome of radiation combined with the Chinese herbal *Selaginella* for terminal Nasopharyngeal Carcinoma," *China Journal of Hospital Pharmacy*, vol. 28, no. 24, pp. 2122–2123, 2008.

[3] T. C. Zhou, X. D. Lin, X. L. Song et al., "Clinical observation of *Selaginella* combined with radiotherapy for terminal nasopharyngeal carcinoma," *Chinese Journal of Cancer Prevention and Treatment*, vol. 13, no. 10, pp. 772–773, 2006.

[4] H. Zhong and C. Ben, *Editorial Committee of Chinese Materia Medica*, Shanghai Science and Technology Press, Shanghai, China, 1999.

[5] R. Lian, J. Li, H. M. Ma et al., "Effect of ethanol extract of *Selaginella doederleinii* Hieron on the proliferation of nasopharyngeal carcinoma CNE-1 and C666-1 cells," *African Journal of Traditional Complementary and Alternative Medicines*, vol. 10, no. 6, pp. 490–493, 2013.

[6] H. Liu, H. Peng, Z. Ji et al., "Reactive oxygen species-mediated mitochondrial dysfunction is involved in apoptosis in human nasopharyngeal carcinoma CNE cells induced by *Selaginella doederleinii* extract," *Journal of Ethnopharmacology*, vol. 138, no. 1, pp. 184–191, 2011.

[7] N.-Y. Lee, H.-Y. Min, J. Lee et al., "Identification of a new cytotoxic biflavanone from *Selaginella doederleinii*," *Chemical and Pharmaceutical Bulletin*, vol. 56, no. 9, pp. 1360–1361, 2008.

[8] S. Li, R. Zhu, M. Zhong et al., "Effects of ultrasonic-assistant extraction parameters on total flavones yield of *Selaginella doederleinii* and its antioxidant activity," *Journal of Medicinal Plants Research*, vol. 4, no. 17, pp. 1743–1750, 2010.

[9] S. Li, H. Yao, M. Zhao, Y. Li, L. Huang, and X. Lin, "Determination of seven biflavones of *Selaginella doederleinii* by high performance liquid chromatography," *Analytical Letters*, vol. 46, no. 18, pp. 2835–2845, 2013.

[10] S. Li, M. Zhao, Y. Li et al., "Preparative isolation of six antitumour biflavonoids from *Selaginella Doederleinii* Hieron by high-speed counter-current chromatography," *Phytochemical Analysis*, vol. 25, no. 2, pp. 127–133, 2014.

[11] J. Li, X. Lei, K. L. Chen et al., "Comparison of cytotoxic activities of extracts from *Selaginella* species," *Pharmacognosy Magazine*, vol. 10, no. 40, pp. 529–535, 2014.

[12] X. L. Fan, D. R. Wan, and K. L. Chen, "Studies on HPLC fingerprint characteristics from *Selaginella* plants," *Zhongguo Zhong Yao Za Zhi*, vol. 32, no. 11, pp. 1094–1095, 2007.

[13] T. Mosmann, "Rapid colorimetric assay for cellular growth and survival: application to proliferation and cytotoxicity assays," *Journal of Immunological Methods*, vol. 65, no. 1-2, pp. 55–63, 1983.

[14] F. Liu, J. G. Wang, S. Y. Wang, Y. Li, Y. P. Wu, and S. M. Xi, "Antitumor effect and mechanism of *Gecko* on human esophageal carcinoma cell lines *in vitro* and xenografted sarcoma 180 in Kunming mice," *World Journal of Gastroenterology*, vol. 14, no. 25, pp. 3990–3996, 2008.

[15] M. L. Wong and J. F. Medrano, "Real-time PCR for mRNA quantitation," *BioTechniques*, vol. 39, no. 1, pp. 75–85, 2005.

[16] D. L. Wheeler, T. Barrett, D. A. Benson et al., "Database resources of the National Center for Biotechnology Information," *Nucleic Acids Research*, vol. 35, no. 1, pp. D5–D12, 2007.

[17] G. M. Morris, H. Ruth, W. Lindstrom et al., "AutoDock4 and AutoDockTools4: automated docking with selective receptor flexibility," *Journal of Computational Chemistry*, vol. 30, no. 16, pp. 2785–2791, 2009.

[18] R. G. Kurumbail, A. M. Stevens, J. K. Gierse et al., "Structural basis for selective inhibition of cyclooxygenase-2 by anti-inflammatory agents," *Nature*, vol. 384, no. 6610, pp. 644–648, 1996.

[19] A. D. Ferguson, B. M. McKeever, S. Xu et al., "Crystal structure of inhibitor-bound human 5-lipoxygenase-activating protein," *Science*, vol. 317, no. 5837, pp. 510–512, 2007.

[20] S. Xu, T. C. Mueser, L. J. Marnett, and M. O. Funk Jr., "Crystal structure of 12-Lipoxygenase catalytic-domain-inhibitor complex identifies a substrate-binding channel for catalysis," *Structure*, vol. 20, no. 9, pp. 1490–1497, 2012.

[21] S. A. Gillmor, A. Villaseñor, R. Fletterick, E. Sigal, and M. F. Browner, "The structure of mammalian 15-lipoxygenase reveals similarity to the lipases and the determinants of substrate specificity," *Nature Structural Biology*, vol. 4, no. 12, pp. 1003–1009, 1997.

[22] E. Darian and P. M. Gannett, "Application of molecular dynamics simulations to spin-labeled oligonucleotides," *Journal of Biomolecular Structure and Dynamics*, vol. 22, no. 5, pp. 579–593, 2005.

[23] R. Huey, G. M. Morris, A. J. Olson, and D. S. Goodsell, "Software news and update a semiempirical free energy force field with charge-based desolvation," *Journal of Computational Chemistry*, vol. 28, no. 6, pp. 1145–1152, 2007.

[24] T. J. Shafer and W. D. Atchison, "Ion channel and receptor properties of pheochromocytoma (PC12) cells: a model for neurotoxicological studies," *Neurotoxicology*, vol. 12, no. 3, pp. 473–492, 1990.

[25] D. G. Tang, Y. Q. Chen, and K. V. Honn, "Arachidonate lipoxygenases as essential regulators of cell survival and apoptosis," *Proceedings of the National Academy of Sciences of the United States of America*, vol. 93, no. 11, pp. 5241–5246, 1996.

[26] H.-K. Chang, M.-S. Shin, H.-Y. Yang et al., "Amygdalin induces apoptosis through regulation of Bax and Bcl-2 expressions in human DU145 and LNCaP prostate cancer cells," *Biological and Pharmaceutical Bulletin*, vol. 29, no. 8, pp. 1597–1602, 2006.

[27] N. Zaffaroni and M. G. Daidone, "Survivin expression and resistance to anticancer treatments: perspectives for new therapeutic interventions," *Drug Resistance Updates*, vol. 5, no. 2, pp. 65–72, 2002.

[28] J. K. Kundu and Y.-J. Surh, "Emerging avenues linking inflammation and cancer," *Free Radical Biology and Medicine*, vol. 52, no. 9, pp. 2013–2037, 2012.

[29] G. P. Pidgeon, J. Lysaght, S. Krishnamoorthy et al., "Lipoxygenase metabolism: roles in tumor progression and survival," *Cancer and Metastasis Reviews*, vol. 26, no. 3-4, pp. 503–524, 2007.

[30] B. B. Aggarwal, S. Shishodia, S. K. Sandur, M. K. Pandey, and G. Sethi, "Inflammation and cancer: how hot is the link?" *Biochemical Pharmacology*, vol. 72, no. 11, pp. 1605–1621, 2006.

[31] K. Hasegawa, Y. Ohashi, K. Ishikawa et al., "Expression of cyclooxygenase-2 in uterine endometrial cancer and antitumor effects of a selective COX-2 inhibitor," *International Journal of Oncology*, vol. 26, no. 5, pp. 1419–1428, 2005.

Hindawi Publishing Corporation
Evidence-Based Complementary and Alternative Medicine
Volume 2014, Article ID 719437, 7 pages
http://dx.doi.org/10.1155/2014/719437

Research Article

Balance Performance in Irradiated Survivors of Nasopharyngeal Cancer with and without Tai Chi Qigong Training

Shirley S. M. Fong,[1] Louisa M. Y. Chung,[2] William W. N. Tsang,[3] Joyce C. Y. Leung,[4] Caroline Y. C. Charm,[4] W. S. Luk,[5] Lina P. Y. Chow,[2] and Shamay S. M. Ng[3]

[1] *Institute of Human Performance, The University of Hong Kong, Pokfulam, Hong Kong*
[2] *Department of Health and Physical Education, The Hong Kong Institute of Education, Hong Kong*
[3] *Department of Rehabilitation Sciences, The Hong Kong Polytechnic University, Hong Kong*
[4] *Division of Nursing and Health Studies, Open University of Hong Kong, Hong Kong*
[5] *The Association of Licentiates of the Medical Council of Hong Kong, Hong Kong*

Correspondence should be addressed to Shirley S. M. Fong; smfong@hku.hk

Received 11 July 2014; Revised 21 August 2014; Accepted 24 August 2014; Published 11 September 2014

Academic Editor: Senthamil R. Selvan

This cross-sectional exploratory study aimed to compare the one-leg-stance time and the six-minute walk distance among TC Qigong-trained NPC survivors, untrained NPC survivors, and healthy individuals. Twenty-five survivors of NPC with TC Qigong experience, 27 survivors of NPC without TC Qigong experience, and 68 healthy individuals formed the NPC-TC Qigong group, NPC-control group, and healthy-control group, respectively. The one-leg-stance (OLS) timed test was conducted to assess the single-leg standing balance performance of the participants in four conditions: (1) standing on a stable surface with eyes open, (2) standing on a compliant surface with eyes open, (3) standing on a stable surface with eyes closed, and (4) standing on a compliant surface with eyes closed. The six-minute walk test (6MWT) was used to determine the functional balance performance of the participants. Results showed that the NPC-control group had a shorter OLS time in all of the visual and supporting surface conditions than the healthy control group ($P < 0.05$). The OLS time of the TC Qigong-NPC group was comparable to that of the healthy control group in the somatosensory-challenging condition (condition 3) ($P = 0.168$) only. Additionally, there was no significant difference in the 6MWT distance among the three groups ($P > 0.05$). TC Qigong may be a rehabilitation exercise that improves somatosensory function and OLS balance performance among survivors of NPC.

1. Introduction

Nasopharyngeal cancer (NPC) is a rare malignancy in North America and Europe (incidence rate: 1 per 100,000) but is common in endemic areas that include the southern part of China, Southeast Asia, and North Africa. The incidence rate ranges from 25 to 50 per 100,000 in these endemic regions [1]. In terms of the medical management of NPC, radiotherapy has so far been the mainstay of treatment [2]. Although it is generally believed that the inner ear is not affected by radiation at the dosage commonly used for therapy [3], evidence suggests that radiation-induced inner ear damage does occur in animals [4] and human beings treated for NPC [5]. As the vestibular apparatus located in the inner ear is responsible for body balance [6], it is possible that survivors of NPC after radiotherapy have vestibular dysfunction and postural control deficits. To date, only one study has examined the standing balance performance of irradiated NPC patients. Using posturography and a standard Romberg position, postural sway in bipedal stance was quantified, and the results revealed that postural control was preserved in patients with NPC [5]. However, the authors adopted a double-leg standing posture, which may not have been challenging enough for the participants because of the large base of support [7]. Postural control and sensory deficits might be manifested when NPC survivors stood on one leg (with a smaller base of support). Indeed, chemotherapy could also affect functional balance performance and sensory organization (i.e., visual,

somatosensory, and vestibular senses) in postural control [8]. Therefore, our first hypothesis was that the one-leg-stance (OLS) balance in sensorially challenging conditions (achieved by changing the visual input or support surface stability) and the functional balance performance of NPC survivors would be inferior to those of healthy controls.

Tai Chi (TC) Qigong, which integrates the essence of TC and Qigong, is a Chinese physiotherapeutic approach that consists of breathing exercises coordinated with slow body movements and balance training in an upright posture. It is a type of mind-body exercise and is particularly suitable for patient populations because it is relatively simpler and more repetitive than the traditional TC forms [9, 10]. According to a recent comprehensive review, a growing body of evidence suggests that these mind-body exercises, TC/Qigong/TC Qigong, can improve body balance (e.g., OLS) in patient populations [11]. Therefore, our second hypothesis was that NPC survivors undergoing TC Qigong training would have better OLS balance performance in different sensory conditions than, and superior functional balance performance to, their nontrained counterparts. Their balance ability might even reach the level of healthy individuals. Based on these hypotheses, the main purpose of this cross-sectional study was to compare (1) the one-leg-stance time in different visual and support surface conditions and (2) the six-minute walk distance among TC Qigong-trained NPC survivors, untrained NPC survivors, and healthy individuals.

2. Methods

2.1. Participants. This is a cross-sectional study. One hundred and twenty senior adults participated in the study voluntarily. Survivors of NPC with TC Qigong experience ($n = 25$) were recruited from a Qigong Association that provides TC and Qigong training for cancer survivors. Survivors of NPC without TC Qigong experience ($n = 27$) were recruited from a medical clinic and a cancer self-help group. The inclusion criteria were the following: (1) having a history of NPC (i.e., positive Epstein-Barr virus-DNA and biopsy test results) but being cancer-free during the study period; (2) having finished all cancer treatments in hospital (radiotherapy with or without chemotherapy); (3) being medically stable; (4) being between 40 and 85 years old; (5) being Hong Kong Cantonese; (6) having normal cognitive function and being able to follow instructions; and (7) having been trained in the 18 forms of Tai Chi Internal Qigong [10] for at least six months continuously (for the NPC-TC Qigong group participants only). The exclusion criteria were the following: (1) receiving alternative and complementary therapies such as acupuncture; (2) significant medical conditions such as diabetes mellitus; (3) known sensorimotor, neurological, musculoskeletal, cardiopulmonary, or vascular disorders limiting locomotion or balance performance; (4) walking with assistive device or being wheelchair-dependent; and (5) being engaged in regular exercise such as morning TC.

Sixty-eight healthy senior adults were recruited from two local community centers. They followed the same inclusion and exclusion criteria mentioned above except that they did not have any history of NPC and TC Qigong experience. Written informed consent was obtained from each participant before the data collection. All of the procedures were conducted according to the Declaration of Helsinki, and all of the experimental work was carried out with the approval of the ethics review committee of the administering institution.

2.2. Outcome Measures. Demographic characteristics and medical history were first obtained by interviewing the participants (Table 1). Each participant then underwent the following evaluations of balance and functional outcomes in sequence. A one-minute break was allowed between the tests to avoid fatigue.

2.2.1. One-Leg-Stance Time. The one-leg-stance timed test was conducted to assess standing balance. The participants were instructed to stand barefoot on their dominant leg (1) on a stable surface (ground) with eyes open; (2) on a compliant surface (Stability Trainer, The Hygienic Corporation, Ohio, USA) with eyes open; (3) on a stable surface (ground) with eyes closed; and (4) on a compliant surface (Stability Trainer) with eyes closed. Their arms were at rest on either side of the trunk. In the two eyes-open trials, the participants were instructed to focus on a spot on a nearby wall in front of them. Close guarding was provided to prevent falls during the trials. A stopwatch was used to record the duration of standing (in seconds). The OLS time commenced when the nondominant foot left the ground and ended if the same foot touched the ground or rested against the other leg or the participants hopped on the weight-bearing leg or shifted on the weight-bearing foot or opened their eyes in the eyes-closed trials or when a 60-second OLS duration was reached [12]. A maximum of two trials was allowed for each testing condition for the participants to achieve the 60-second goal. If the participants reached the goal of 60 seconds in the first trial, no further trial was conducted for that particular testing condition. The time of the better trial of each testing condition was recorded. A longer duration indicated better balance ability [12].

2.2.2. Six-Minute Walk Distance. The six-minute walk test (6MWT) was used to determine the functional balance performance of the participants [13]. In accordance with the American Thoracic Society guidelines [14], the participants were instructed to cover as much distance as possible at a self-paced walking velocity in a 30-meter unobstructed walkway within six minutes. They were allowed to rest during the test if necessary but were instructed to resume walking as soon as possible. The total distance walked, to the nearest meter, in a single trial was documented. A longer distance covered indicated a higher level of functional mobility, better balance performance, and better cardiovascular fitness [13, 15]. This test has been found to have good test-retest reliability when used in older adults ($0.88 < r < 0.94$) [16].

2.3. Statistical Analysis. The Statistical Package for the Social Sciences (SPSS) version 20.0 software was used to perform

Table 1: Characteristics of the participants.

	NPC-TC Qigong group ($n = 25$)	NPC-control group ($n = 27$)	Healthy-control group ($n = 68$)	P
Age (year)	55.4 ± 7.5	58.7 ± 9.5	58.8 ± 11.1	0.331
Sex (male : female)	12 : 13	16 : 11	50 : 18	0.057
Weight (kg)	58.2 ± 15.8	55.1 ± 10.6	63.5 ± 12.7	0.014*
Height (cm)	163.2 ± 9.1	161.5 ± 8.1	159.1 ± 8.9	0.124
Body mass index (kg/m^2)	21.8 ± 5.1	21.1 ± 3.2	25.0 ± 4.3	<0.001*
	Reported NPC stage at diagnosis [27]			
Stage I (n, %)	5 (20%)	2 (7.4%)	—	
Stage II (n, %)	5 (20%)	7 (25.9%)	—	
Stage III (n, %)	11 (44%)	15 (55.6%)	—	
Stage IV (n, %)	4 (16%)	3 (11.1%)	—	
Post-NPC duration (year)	12.5 ± 7.1	8.4 ± 9.7	—	0.094
	NPC treatment received			
Radiotherapy (n, %)	17 (68%)	9 (33.3%)	—	
Radiotherapy and chemotherapy (n, %)	7 (28%)	18 (66.6%)	—	
Radiotherapy, chemotherapy, and surgery (n, %)	1 (4%)	0 (0%)	—	

The mean ± standard deviation is presented for the continuous variables.
* $P < 0.05$.

the statistical analyses. All of the demographic and outcome variables were presented using descriptive statistics. The normality of the continuous data was checked using the Kolmogorov-Smirnov test. One-way analysis of variance (ANOVA) was used to compare the age, weight, height, and body mass index of the three groups. A Chi-squared test was used to compare the sex ratio of the groups. In addition, an independent t-test was used to compare the post-NPC duration of the two NPC groups. If significant between-group differences were found in any of the demographic variables, these outstanding outcomes were treated as covariates in the subsequent balance and functional outcome analyses.

For the analyses of the balance and functional outcomes, one-way analysis of covariance (ANCOVA) was used to compare the differences among the three groups. Bonferroni tests were used to analyze the data post hoc as necessary. A significance level of 0.05 (two-tailed) was set for all of the statistical tests.

3. Results

3.1. Demographic Characteristics. The characteristics of the three groups of participants are presented in Table 1. As there were significant between-group differences ($P < 0.05$) in weight and body mass index (BMI), these demographic variables were entered as covariates in the univariate analysis. The sex ratio was also entered as a covariate because it was marginally significant ($P = 0.057$) and, clinically, gender differences can affect balance performance [17, 18].

3.2. Condition 1: One-Leg-Stance on Stable Surface with Eyes Open. The results revealed a significant difference in OLS time among the three groups ($F(2, 117) = 11.912$, $P < 0.001$). Post hoc analysis found that both the NPC-TC Qigong ($P = 0.013$) and the NPC control ($P = 0.003$) groups had a shorter OLS time than the healthy control group. However, no significant difference in OLS time was found between the two NPC groups ($P = 1.000$) (Table 2).

3.3. Condition 2: One-Leg-Stance on a Compliant Surface with Eyes Open. An overall significant difference among the three groups was found ($F(2, 117) = 11.505$, $P < 0.001$). The healthy control group stood longer on one leg than the NPC-TC Qigong ($P = 0.023$) and the NPC control ($P = 0.004$) groups. The OLS time of the two NPC groups was similar ($P = 1.000$) (Table 2).

3.4. Condition 3: One-Leg-Stance on a Stable Surface with Eyes Closed. The ANCOVA result was significant ($F(2, 117) = 6.854$, $P = 0.002$). The NPC control group stood for a shorter duration than the healthy control group ($P = 0.007$) when the eyes were closed. However, the OLS time was similar between the NPC-TC Qigong and the healthy control groups ($P = 0.168$) and between the NPC-TC Qigong and the NPC control groups ($P = 1.000$) (Table 2).

3.5. Condition 4: One-Leg-Stance on a Compliant Surface with Eyes Closed. The ANCOVA result was also significant ($F(2, 117) = 11.147$, $P < 0.001$) in this most challenging condition. The healthy control group stood for longer on one leg than the NPC-TC Qigong ($P = 0.018$) and the NPC control ($P = 0.001$) groups. No significant difference in OLS time was found between the two NPC groups ($P = 1.000$) (Table 2).

Table 2: Comparison of the balance outcomes of the three groups.

	Useful sensory inputs [19]	NPC-TC Qigong group ($n = 25$)	NPC-control group ($n = 27$)	Healthy-control group ($n = 68$)	P values NPC-TC Qigong group versus NPC-control group	P values NPC-TC Qigong group versus healthy-control group	P values NPC-control group versus healthy-control group
One-leg-stance times							
(1) On ground with eyes open (s)	Somatosensory, visual, and vestibular	12.53 ± 8.40	11.74 ± 11.80	19.80 ± 10.87	1.000	0.013*	0.003*
(2) On stability trainer with eyes open (s)	Visual and vestibular	10.08 ± 10.52	9.00 ± 11.13	16.57 ± 9.71	1.000	0.023*	0.004*
(3) On ground with eyes closed (s)	Somatosensory and vestibular	4.76 ± 6.52	2.81 ± 4.37	8.19 ± 8.83	1.000	0.168	0.007*
(4) On stability Trainer with eyes closed (s)	Vestibular	2.48 ± 2.97	1.48 ± 2.42	5.97 ± 6.64	1.000	0.018*	0.001*
Six-minute walk distance (m)	—	308.00 ± 62.72	285.19 ± 50.34	302.50 ± 63.02	0.528	1.000	0.629

The mean ± standard deviation is presented for all of the variables.
* denotes a significant difference at $P < 0.05$.

3.6. Six-Minute Walk Test. There was no significant difference among the three groups in the distance covered in the 6MWT ($F(2, 117) = 1.279$, $P = 0.282$) (Table 2). Therefore, post hoc analysis was not undertaken.

4. Discussion

This is the first study to show that participating survivors of NPC had inferior OLS balance performances in all of the visual and supporting surface conditions compared with age-matched healthy counterparts. Given that postural control requires the ability to utilize sensory inputs (i.e., somatosensory, visual, and vestibular inputs) and to generate coordinated motor outputs [19], our results suggest that survivors of NPC might have multiple underlying sensorimotor impairments in OLS balance control. Indeed, a previous study showed that breast cancer patients treated with chemotherapy demonstrated increased postural instability in bipedal stance compared with healthy controls [8]. Chemotherapy-related peripheral nervous system disorders (e.g., sensorimotor neuropathy, somatosensory, visual, and vestibular deficits) may be the contributing factors [8, 20]. In addition, irradiation of the temporal bone during NPC treatment may result in vestibular damage such as canal paresis [5] that may also affect balance performance. All of these sensorimotor impairments (side effects) resulting from radiotherapy or chemotherapy might explain the overall inferior OLS balance performance among survivors of NPC.

With TC Qigong training, the participating survivors of NPC had a similar OLS balance performance in condition 3 (i.e., stood on a stable surface with eyes closed) to that of the healthy individuals, although they were still no better than the NPC controls. As somatosensory input is the dominant sensory input for balance under a stable support surface and eyes closed condition [19], our results suggest that TC Qigong-trained NPC survivors might rely more on their somatosensory input to balance. This reliance might be because the TC Qigong-trained participants had better knee and ankle joint proprioception that might have resulted in better balance control in the OLS [21].

Ample evidence supports that TC and Qigong training can improve the use of vestibular input to balance [22–24]. For example, using the sensory organization test, Tsang et al. [23] reported that long-term TC practice may improve balance control in the elderly when there was increased reliance on the vestibular system during stance. However, in our study, because irradiation-related damage to the vestibular apparatus is irreversible [5], exercise (TC Qigong) training might not be able to remediate the vestibular deficit in survivors of NPC. Therefore, our NPC-TC Qigong group performed similarly to the NPC control group when relying primarily on their vestibular input to balance (i.e., condition 4—stood on a compliant surface with eyes closed). The non-irradiated healthy controls performed much better than the two NPC groups in this vestibularly challenging condition.

When relying primarily on visual input to balance (i.e., condition 2—stood on a compliant surface with eyes open), the healthy control group also outperformed the two NPC groups, while the two NPC groups performed similarly. This suggests that TC Qigong training might not be able to improve the use of visual input for postural control in survivors of NPC, perhaps because the vestibuloocular reflex is also disrupted in survivors of NPC who undergo radiotherapy [5], and exercise (TC Qigong training) might not be able to heal it.

Interestingly, we found that when the three sensory inputs were present and accurate (condition 1), both the NPC-TC Qigong and the NPC control groups had a shorter OLS duration than the healthy control group. In addition, both groups of NPC survivors balanced similarly in the OLS. The TC Qigong-trained NPC survivors might have been unable to match the healthy controls in terms of OLS performance because, typically, dysfunction in any one of the three senses that contribute to balance can be compensated by inputs from the other two sensory systems. For example, dysfunction of the vestibular system may be compensated by enhancing somatosensory awareness and visual attention to better balance [19]. However, two senses (vestibular and visual) out of the three might have been disrupted in our TC Qigong-trained NPC survivors due to the side effects of radiotherapy or chemotherapy, as explained. Therefore, the compensation mechanism might not have worked in this case. The NPC survivors still had an inferior OLS balance performance when they stood on a stable surface with eyes open relative to the healthy controls, even though they trained in TC Qigong regularly. Certainly, further studies should examine the functions of the individual sensory systems to substantiate this hypothesis.

The sensorimotor deficits of postural control among the survivors of NPC, both with and without TC Qigong training, were not reflected in the six-minute walk test result. This result might be because this test is too general as it assesses both the balance ability and the functional aerobic capacity of the participants [15]. Walking distance might, therefore, have been limited by the aerobic capacity rather than by the balance ability of the participants. Further studies should consider using other dynamic balance measurements, such as the Berg Balance Scale, to quantify the functional balance ability of survivors of NPC [25].

Some limitations to this study warrant comment. First, the use of a convenience sample may have introduced a self-selection bias that may threaten the internal validity of the study. In addition, our rather homogenous subject group may limit the generalizability of results [26]. Second, the study was cross-sectional in nature and thus a cause-and-effect relationship between TC Qigong training and balance performance could not be established. Third, both of the NPC groups had a rather small sample size, which may partially explain some of the insignificant findings. Finally, the OLS clinical test was used to assess balance performance. Future studies could consider using more comprehensive, objective, and accurate laboratory measures (e.g., computerized dynamic posturography) [19] to evaluate the balance ability thoroughly of survivors of NPC.

5. Conclusions

Irradiated survivors of NPC had inferior single-leg standing balance performance relatively to the healthy individuals. The survivors of NPC who were trained in TC Qigong might have relied more on their somatosensory input to maintain single-leg standing balance. Their one-leg-stance time on a stable surface with eyes closed was comparable to that of healthy individuals. However, survivors of NPC, both with and without TC Qigong training, had a shorter OLS time than healthy controls when they stood (1) on a stable surface with eyes open, (2) on a compliant surface with eyes open, and (3) on a compliant surface with eyes closed. The six-minute walk distance was comparable among NPC survivors with and without TC Qigong training and healthy controls. Our results hint that TC Qigong might be a potential rehabilitation exercise to improve the somatosensory function and single-leg standing balance performance of survivors of NPC.

Conflict of Interests

The authors declare that there is no conflict of interests regarding the publication of this paper.

Authors' Contribution

Shirley S. M. Fong contributed to the conceptualization of the study, supervised the data collection and analysis processes, and wrote the first draft of the paper. Louisa M. Y. Chung contributed to the conceptualization of the study, was involved in the data collection and analysis process, and contributed to the write-up of the paper. William W. N. Tsang contributed to the conceptualization and revision of the paper. Joyce C. Y. Leung contributed to the conceptualization of the study, was involved in the data collection and analysis process, and contributed to the write-up of the paper. Caroline Y. C. Charm contributed to the conceptualization of the study, cosupervised the data collection process, and contributed to the write-up of the paper. W. S. Luk contributed to the conceptualization of the study, assisted in the recruitment of participants, cosupervised the data collection process, and contributed to the write-up of the paper. Lina P. Y. Chow contributed to the conceptualization of the study, was involved in the data collection process, and contributed to the write-up of the paper. Shamay S. M. Ng contributed to the conceptualization of the study, cosupervised the data collection and analysis processes, and contributed to the write-up of the paper.

Acknowledgments

This study was supported by a Seed Fund for Basic Research for New Staff (201308159012) from the University of Hong Kong and an Internal Research Grant (RG57/2012-2013R) from the Hong Kong Institute of Education.

References

[1] M. Al-Sarraf and M. S. Reddy, "Nasopharyngeal carcinoma," *Current Treatment Options in Oncology*, vol. 3, no. 1, pp. 21–32, 2002.

[2] H. Lu and M. Yao, "The current status of intensity-modulated radiation therapy in the treatment of nasopharyngeal carcinoma," *Cancer Treatment Reviews*, vol. 34, no. 1, pp. 27–36, 2008.

[3] Y.-H. Young, J.-Y. Ko, and T.-S. Sheen, "Postirradiation vertigo in nasopharyngeal carcinoma survivors," *Otology and Neurotology*, vol. 25, no. 3, pp. 366–370, 2004.

[4] J. E. Gamble, E. A. Peterson, and J. R. Chandler, "Radiation effects on the inner ear," *Archives of Otolaryngology*, vol. 88, no. 2, pp. 156–161, 1968.

[5] W.-Y. Chao, H.-Z. Tseng, and S.-T. Tsai, "Caloric response and postural control in patients with nasopharyngeal carcinoma after radiotherapy," *Clinical Otolaryngology and Allied Sciences*, vol. 23, no. 5, pp. 439–441, 1998.

[6] E. N. Marieb and K. Hoehn, *Human Anatomy and Physiology*, Pearson Education, San Francisco, Calif, USA, 8th edition, 2010.

[7] R. C. Briggs, M. R. Gossman, R. Birch, J. E. Drews, and S. A. Shaddeau, "Balance performance among noninstitutionalized elderly women," *Physical Therapy*, vol. 69, no. 9, pp. 748–756, 1989.

[8] M. A. Wampler, K. S. Topp, C. Miaskowski, N. N. Byl, H. S. Rugo, and K. Hamel, "Quantitative and clinical description of postural instability in women with breast cancer treated with taxane chemotherapy," *Archives of Physical Medicine and Rehabilitation*, vol. 88, no. 8, pp. 1002–1008, 2007.

[9] H.-J. Lee, H.-J. Park, Y. Chae et al., "Tai Chi Qigong for the quality of life of patients with knee osteoarthritis: a pilot, randomized, waiting list controlled trial," *Clinical Rehabilitation*, vol. 23, no. 6, pp. 504–511, 2009.

[10] Y. K. Mak, *18 Forms Tai Chi Qigong*, Wan Li Book, Hong Kong, 7th edition, 2012, (Chinese).

[11] R. Jahnke, L. Larkey, C. Rogers, J. Etnier, and F. Lin, "A comprehensive review of health benefits of qigong and tai chi," *The American Journal of Health Promotion : AJHP*, vol. 24, no. 6, pp. e1–e25, 2010.

[12] T. Michikawa, Y. Nishiwaki, T. Takebayashi, and Y. Toyama, "One-leg standing test for elderly populations," *Journal of Orthopaedic Science*, vol. 14, no. 5, pp. 675–685, 2009.

[13] S. R. Lord and H. B. Menz, "Physiologic, psychologic, and health predictors of 6-minute walk performance in older people," *Archives of Physical Medicine and Rehabilitation*, vol. 83, no. 7, pp. 907–911, 2002.

[14] P. L. Enright, "The six-minute walk test," *Respiratory Care*, vol. 48, no. 8, pp. 783–785, 2003.

[15] M. E. Hackney and G. M. Earhart, "Tai Chi improves balance and mobility in people with Parkinson disease," *Gait & Posture*, vol. 28, no. 3, pp. 456–460, 2008.

[16] R. E. Rikli and C. J. Jones, "The reliability and validity of a 6-minute walk test as a measure of physical endurance in older adults," *Journal of Aging and Physical Activity*, vol. 6, no. 4, pp. 363–375, 1998.

[17] L. Wolfson, R. Whipple, C. A. Derby, P. Amerman, and L. Nashner, "Gender differences in the balance of healthy elderly as demonstrated by dynamic posturography," *Journals of Gerontology*, vol. 49, no. 4, pp. M160–M167, 1994.

[18] T. Troosters, R. Gosselink, and M. Decramer, "Six minute walking distance in healthy elderly subjects," *European Respiratory Journal*, vol. 14, no. 2, pp. 270–274, 1999.

[19] L. M. Nashner, "Computerized dynamic posturography," in *Handbook of Balance Function and Testing*, G. P. Jacobson, C. W. Newman, and J. M. Kartush, Eds., pp. 261–307, Mosby, St. Louis, Mo, USA, 1997.

[20] J.-C. Antoine and J.-P. Camdessanché, "Peripheral nervous system involvement in patients with cancer," *The Lancet Neurology*, vol. 6, no. 1, pp. 75–86, 2007.

[21] D. Xu, Y. Hong, J. Li, and K. Chan, "Effect of tai chi exercise on proprioception of ankle and knee joints in old people," *The British Journal of Sports Medicine*, vol. 38, no. 1, pp. 50–54, 2004.

[22] P. S. Lee, M. Jung, A. Abraham, L. Lei-Rivera, and A. H. Kim, "Efficacy of Tai Chi as a technique for vestibular rehabilitation—a preliminary quasi-experimental study," *Journal of Physical Therapy*, vol. 5, no. 1, pp. 6–13, 2012.

[23] W. W. Tsang, V. S. Wong, S. N. Fu, and C. W. Hui-Chan, "Tai Chi improves standing balance control under reduced or conflicting sensory conditions," *Archives of Physical Medicine and Rehabilitation*, vol. 85, no. 1, pp. 129–137, 2004.

[24] Y. Yang, J. V. Verkuilen, K. S. Rosengren, S. A. Grubisich, M. R. Reed, and E. T. Hsiao-Wecksler, "Effect of combined Taiji and Qigong training on balance mechanisms: a randomized controlled trial of older adults," *Medical Science Monitor*, vol. 13, no. 8, pp. CR339–CR348, 2007.

[25] T. M. Steffen, T. A. Hacker, and L. Mollinger, "Age- and gender-related test performance in community-dwelling elderly people: six-minute walk test, Berg balance scale, timed up & go test, and gait speeds," *Physical Therapy*, vol. 82, no. 2, pp. 128–137, 2002.

[26] L. G. Portney and M. P. Watkins, *Foundations of Clinical Research: Applications to Practice*, Pearson Education, Upper Saddle River, NJ, USA, 3rd edition, 2009.

[27] American Joint Committee on Cancer, *AJCC Cancer Staging Manual*, Lippincott Williams & Wilkins, Philadelphia, Pa, USA, 5th edition, 1997.

Hindawi Publishing Corporation
Evidence-Based Complementary and Alternative Medicine
Volume 2014, Article ID 726724, 9 pages
http://dx.doi.org/10.1155/2014/726724

Research Article

Remarkable Anticancer Activity of *Teucrium polium* on Hepatocellular Carcinogenic Rats

Ariyo Movahedi,[1] Rusliza Basir,[2] Asmah Rahmat,[1] Mohammad Charaffedine,[3] and Fauziah Othman[2]

[1] *Department of Nutrition and Dietetics, Faculty of Medicine, Universiti Putra Malaysia, Malaysia*
[2] *Department of Human Anatomy, Faculty of Medicine, Universiti Putra Malaysia, 43400 Serdang, Selangor, Malaysia*
[3] *Diseased Tissue Pathology Laboratory, Tyre, Lebanon*

Correspondence should be addressed to Fauziah Othman; fauziah@upm.edu.my

Received 23 April 2014; Revised 17 July 2014; Accepted 17 July 2014; Published 13 August 2014

Academic Editor: Esra Küpeli Akkol

The term cancer has been concomitant with despair, agony, and dreadful death. Like many other diseases, herbal therapy has been used to prevent or suppress cancer. The present study investigated the capability of the decoction of *Teucrium polium* L. from Lamiaceae family to protect liver cells against hepatocellular carcinoma in carcinogenesis-induced animal model. After 28 weeks of treatment with decoction of *Teucrium polium* L., serum biochemical markers including ALT, AST, AFP, GGT, ALP, HCY, TNF-α, α2MG, and CBG have been regulated auspiciously. Total antioxidant status also has been increased intensely. Liver lesion score in treated group was lessened and glucocorticoid activity has been intensified significantly. In conclusion, *Teucrium polium* L. decoction might inhibit or suppress liver cancer development.

1. Introduction

Hepatocellular carcinoma (HCC), the predominant form of liver cancer, is the sixth most common cancer and the third most frequent cause of cancer-related death worldwide [1, 2]. Patients diagnosed with HCC have a poor prognosis due to the violent nature of the disease [3]. On the other hand, surgical resection or local extirpation therapy is effective only at an early stage of HCC. Hence, any preventive or suppressive method would be vital. Like other diseases, complementary medicine has been commonly considered in cancer. Herbal medicine has been widely used to cure or prevent diseases since ages. Many of the herbs contain phytochemicals, antioxidants, flavonoids, and dietary fibers which have shown anticancer properties [4, 5]. *Teucrium polium* L. (Lamiaceae), known popularly as Golden/Felty germander, is a subshrub and is native to southwest Asia and the Mediterranean region [6, 7]. Its flowers and its leaves are used both in cooking and for medicinal purposes, particularly for the treatment of stomach ailments. *T. polium* has been long used in Iran commonly as decoctions or infusions for its diuretic, antipyretic, diaphoretic, antispasmodic, tonic, anti-inflammatory, antihypertensive analgesic, antibacterial, and antidiabetic effects [8–12]. An infusion of the leaves and flowers of the plant is also consumed as a refreshing beverage [13]. In recent years, *T. polium* has been tested and showed beneficial effects on nonalcoholic steatohepatitis [14] and it has been shown to be considered as an effective and safe chemosensitizer agent for cancer therapy [15]. *In vitro* study on its aqueous extract has shown that it can effectively inhibit oxidative processes and has substantial antioxidant activity [16]. Based on some isolated compounds from this plant such as diterpenoids, flavonoids, iridoids, sterols, and terpenoids [11, 17], it might have cytotoxic activity and antitumor properties. As herbal decoctions are one of the major techniques in herbal medicine and could be drunk as a

part of daily dietary intake, in the present study, the effect of *T. polium* decoction has been investigated on hepatocellular carcinoma in animal model.

2. Materials and Methods

2.1. Plant Material and Preparation of the T. polium Decoction. High quality dried Iranian *T. polium* (Herbarium number US00050655) leaves were purchased from certified herbal marketing in Tehran, Iran (ParsiTeb Co.), and shipped to Malaysia. Dried *T. polium* leaves were weighed and washed 3 times with tap water and then were put into a 10-liter beaker. For each 100 g of dried leaves, 4000 mL of distilled water was added. Then the mixture was heated up to 70°C to reduce the water content to 1000 mL through evaporation. After these phases, the residues were filtered. The liquids were chilled and kept in the fridge at 4°C in hygienic bottles until being used.

2.2. Force-Feed Calculation. As a neutraceutical study, instead of different concentration which is more common in pharmaceutical studies, the usual decoction technique and one concentration has been used. The Institute of Medicine determined that an adequate intake (AI) for men is roughly 3 liters (about 13 cups) of total beverages a day. The AI for women is 2.2 liters (about 9 cups) of total beverages a day [18]. The average daily water intake of Sprague-Dawley rats in chronic studies is about 15 mL/100 g body weight [19, 20]. As average standard human body weight is 65 kg (71 for male and 61 for female) [21], it is possible to drink and recommend two cups of any kind of herbal tea. Hence, to calculate the best amount of force feeding of the decoction of the herb, the following calculation was used: 2 of 13 cups per day are equal to 460 mL $\rightarrow$ $460 \div 65 \cong 7$ mL/kg body weight $\rightarrow$ 0.7 mL/100 g body weight.

2.3. Animals and Experimental Protocols. The present study was designed as a preclinical study [22]. The protocol of the rat hepatocarcinogenesis in this study was according to Solt and Farber method [23]. Forty male rats, 8 ± 1 weeks old, with average weight 243.1 ± 6.7 g, were divided into groups of three and maintained at $60 \pm 5\%$ relative humidity and 22 ± 1°C with a 12 h light/dark cycle. Allrats had free access to the standard rat food pellet based on AIN-76A [24] and tap water during the study. Hepatocarcinoma was induced in 30 of the rats by single intraperitoneal injection of 200 mg/kg diethyl nitrosamine (DEN) dissolved in corn oil and then followed by a cancer promotion period of 2 weeks on food, which was mixed with 2-acetylaminofluorene (0.02% AAF) as a promoter of hepatocarcinogenesis without partial hepatectomy to promote hepatocarcinogenesis. The rats were then left for 2 weeks. A group of 10 rats served as normal group with no DEN injection or hepatocarcinogenesis promoter diet. After the cancer initiation period, the leftover rats were weighed again and divided randomly into two groups with no significant differences in their weight. Both control and *T. polium* groups were allowed free access to AIN76 and water *ad libitum* for 28 weeks, but rats in *T. polium* group were force-fed 0.7 mL/100 g body weight/day of *T. polium* decoction.

2.4. Chemicals and Biochemical Analyses. Alpha-fetoprotein tumor marker (AFP), tumor necrosis factor-alpha (TNF-α), homocysteine (HCY), corticosteroid binding globulin (CBG), and alpha-2-macroglobulin (α2MG) were analyzed using standard commercial ELISA kit (Cusabio Biotech, China). Gamma-glutamyl transpeptidase (GGT) was tested by using Colorimetric Assay Kit (BioVision, USA). Alanine aminotransferase (ALT/SGPT), aspartate aminotransferase (AST/SGOT), alkaline phosphatase (ALP), and total antioxidant status (TAS) were analyzed by Chemical Pathology Lab at FMHS, UPM, using Roche Cobas C-311 analyzer.

2.5. Decoction Characteristic Analysis. Decoction total phenolic content was evaluated with Folin-Ciocalteu's phenol reagent [25, 26] and colorimetric aluminum chloride method was used for flavonoid determination [25]. The antioxidant activities of the decoction were determined based on its ability to scavenge 2,2-diphenyl-1-picrylhydrazyl (DPPH) radicals, based on method of Brand Williams and coworkers (1995) [27]. Butylated hydroxyanisole (BHA), rutin, and α-tocopherol were used as positive control for synthetic and natural antioxidant, respectively. Antioxidant activity was reported as IC_{50}, defined by the concentration of samples required (mg/mL) to scavenge 50% of the free radicals. Based on the literature, rutin and apigenin are two active compounds of *T. polium* and have been analyzed by high-performance liquid chromatography (HPLC) using services from ChromaDex, Inc., CA, USA.

2.6. Histopathological Examinations. Half of the liver tissue of each sample was fixed in 10% formalin and then the paraffin blocks were prepared. The sections from blocks were stained with hematoxylin-eosin. The histopathological evaluations were performed blindly by an expert pathologist using a scoring system. The lesion scoring was done according to the revised method of Batts and Ludwig by Stevens et al. [28, 29]. The rest of the livers were saved in −80°C for liver glucocorticoid receptor analysis. Fluorescent *in situ* hybridization (FISH) was used to analyze glucocorticoid receptor RNA activity by QuantiGene ViewRNA ISH Tissue 2-Plex Assay kit (Affymetrix Inc., USA). For positive control, ACTB and GAPD were used as housekeeping genes. The frozen tissues were cut using rotary cryomicrotome (Leica 1850 UV) at 4–8 microns and pasted on a slide for FISH test. Slides were observed under confocal laser microscope (Olympus FV10, Japan). In order to view fluorescent activity, the following filters have been used. For Fast Red Substrate Cy3/TRITC (filter set: Excitation: 530 ± 20 nm, Emission: 590 ± 20 nm, Dichroic: 562 nm), for Fast Blue Substrate, Cy7-B/Alexa 750 (custom filter set: Excitation: 630 ± 20 nm, Emission: 775 ± 25 nm, Dichroic: 750 nm), and for DAPI filter set (Excitation: 387/11 nm, Emission: 447/60 nm) were used.

2.7. Statistical Analyses. Data were expressed as mean ± SEM. Statistical differences between normal, treated, and control groups were determined using one-way repeated measures analysis of variance (ANOVA) followed by Duncan's multiple

range as post hoc test. Differences between groups were considered significantly different when P value was less than 0.05.

3. Results

Total phenolic and flavonoid content of the used decoction were 2.635 ± 0.001 mg/mL and 0.081 ± 0.002 mg/mL, respectively. DPPH scavenging activity was shown in Table 1. HPLC results of the used *T. polium* of this study failed to find both rutin and apigenin as active compounds. Therefore, the benefits of this herb would be due to other phenolic components.

Throughout the intervention some of the rats in both groups died. Almost one-third of the rats in the control group died, while *T. polium* treated group showed a significantly lower mortality rate ($P < 0.05$) and only 8.3% of them died. After 28 weeks of treatment, based on the present outcomes, rats in the control group showed higher but no significant weight gain as compared to *T. polium* treated group, 490.14 ± 18.77 versus 461.1 ± 15.0 ($P > 0.05$). In spite of the significantly higher liver weight among control groups, 12.25 ± 0.34 versus 10.50 ± 0.49 g ($P < 0.05$), no significant liver weight ratio was observed, 2.47 ± 0.06 versus 2.28 ± 0.10 ($P > 0.05$).

The effect of *T. polium* on serum liver function markers as compared to control has been illustrated in Table 2. Both normal group and *T. polium* treated group showed significantly lower serum ALP ($P < 0.05$) as compared to the control group. Similar results have also been found for AST, ALT, HCY, and α2MG ($P < 0.05$). Despite the lower level of AST/ALT ratio in the normal group, no significant difference was found between groups ($P > 0.05$). Significantly higher level of CBG was found in *T. polium* treated group and the lowest value was detected in normal group ($P < 0.05$). Although *T. polium* group showed significantly higher levels of TNF-α, α2MG, AFP, and GGT as compared to normal ($P < 0.05$), all these markers were significantly lower than control group ($P < 0.05$). The extremely lowest level of TAS was observed in the control group ($P < 0.01$), while *T. polium* treated group showed a considerably higher TAS level than normal group ($P < 0.05$).

As Figure 1 shows, after 28 weeks of treatment with *T. polium* decoction, most of serum liver function and cancer markers have improved and dropped significantly as compared to the control. AFP, ALP, ALT, and AST were reduced significantly by 37.63 ± 1.29%, 31.98 ± 1.02%, 40.18 ± 0.69%, and 41.16 ± 0.51%, respectively ($P < 0.05$). AST/ALT ratio has slightly increased by 1.62 ± 1.24% ($P > 0.05$). CBG has improved and increased significantly by 16.88 ± 0.86% ($P < 0.05$). Moreover, *T. polium* decoction was able to raise TAS drastically by 861.47 ± 0.38%. Serum GGT, HCY, TNF-α, and α2MG in *T. polium* treated group decreased significantly by 32.46 ± 0.25%, 39.72 ± 0.57%, 32.8 ± 1.04%, and 35.92 ± 0.78% ($P < 0.05$).

3.1. Histopathological Findings. Lesion score of different groups is shown in Figure 2. Based on the present findings,

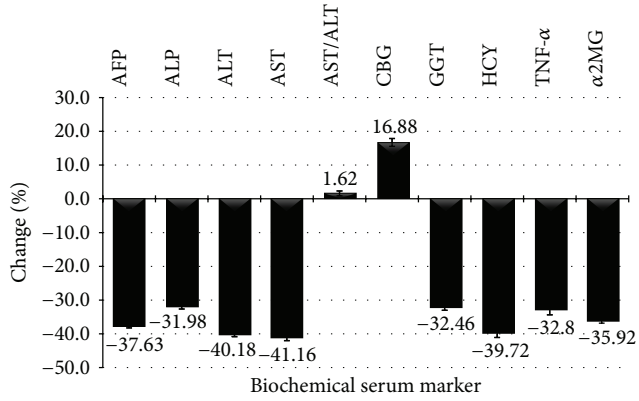

Figure 1: Percentage change of different serum biochemical markers in *T. polium* group as compared to the control group.

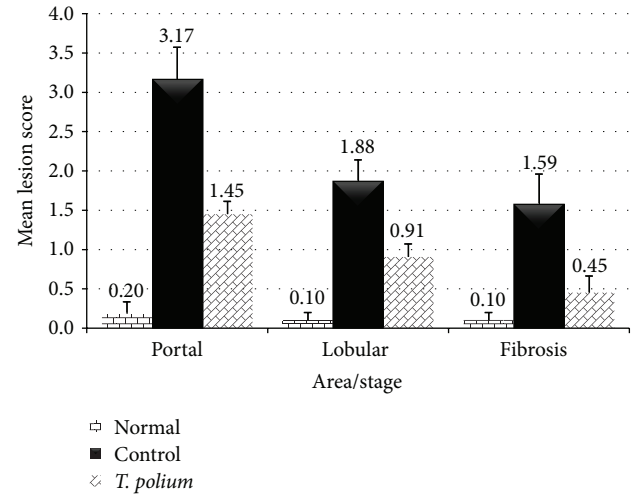

Figure 2: Effect of *T. polium* on mean lesion score of rats' liver tissue as compared to the control.

rats in control group showed a significantly higher lesion score in both portal and lobular region as well as fibrosis stage compared to all other groups ($P < 0.05$). Perceptibly, normal group had the lowest lesion score ($P < 0.05$) due to their health status. *T. polium* treated group showed significantly lower lesion score in all sites as compared to the control group ($P < 0.05$) which was illustrated in Figure 3 as well.

4. Discussion

In this project, the control group had the highest mortality rate, which was expected. Gross histology of *T. polium* group showed no hepatic nodules in this group, unlike the control ones. Differences in the mortality rate with other studies could possibly be explained by either the used dosage of DEN or duration of the study [30]. Unfortunately, there were no comparable data about mortality rate of *T. polium* in a cancer study; however, the mortality rate of both control and treated

Table 1: Comparison of the DPPH scavenging activity of *T. Polium* decoction with standards.

Substance	20	40	80	160	IC_{50}
			Mean ± SEM (μg/mL)		
T. Polium	9.1 ± 0.8[a]	48.4 ± 1.7[a]	83.7 ± 0.5[a]	81.2 ± 1.4[a]	41.5 ± 0.7[a]
α-Tocopherols	46.0 ± 0.4[b]	86.6 ± 1.9[b]	91.6 ± 1.2[b]	91.2 ± 3.5[b]	22.4 ± 0.8[b]
Rutin	41.9 ± 0.3[b]	78.7 ± 1.3[b]	80.2 ± 1.7[a]	80.8 ± 1.0[a]	24.5 ± 0.5[b]
BHA	45.41 ± 0.4[b]	81.9 ± 1.2[b]	85.8 ± 0.4[b]	87.0 ± 5.5[a]	22.5 ± 0.6[b]

[ab]Values in the same column with different superscripts are significantly different at $P < 0.05$ based on one-way ANOVA and Duncan's post hoc test.

Table 2: Effect of *T. polium* on serum biochemical markers as compared to normal and control groups.

Marker	Normal ($n = 10$)	Control ($n = 8$)	*T. polium* ($n = 11$)
ALP (IU/L)	38.78 ± 1.72[a]	77.77 ± 3.74[b]	52.9 ± 3.8[c]
ALT (U/L)	25.84 ± 1.66[a]	67.20 ± 4.91[b]	40.20 ± 3.37[c]
AST (U/L)	56.62 ± 2.53[a]	156.18 ± 10.64[b]	91.89 ± 5.40[c]
AST/ALT ratio	2.24 ± 0.08	2.47 ± 0.25	2.51 ± 0.31
CBG (μg/mL)	10.74 ± 0.26[a]	11.49 ± 0.35[b]	13.43 ± 0.30[c]
HCY (nmol/mL)	0.57 ± 0.03[a]	1.41 ± 0.14[b]	0.85 ± 0.08[c]
TNF-α (pg/mL)	24.03 ± 1.00[a]	49.08 ± 1.12[b]	32.98 ± 1.17[c]
α2MG (ng/mL)	0.71 ± 0.04[a]	1.42 ± 0.09[b]	0.91 ± 0.07[c]
AFP (pg/mL)	47.51 ± 1.05[a]	101.85 ± 2.86[b]	63.52 ± 3.70[c]
TAS (mmol/L)	9.84 ± 0.35[a]	1.09 ± 0.16[b]	10.48 ± 0.06[c]
GGT (mU/mL)	0.68 ± 0.01[a]	1.14 ± 0.04[b]	0.77 ± 0.01[c]

[abc]Values in the same row with different superscripts are significantly different at $P < 0.05$ based on one-way ANOVA and Duncan's post hoc test. Data were presented as mean ± SEM.

groups was rational and similar to other studies [31]. The relationship between HCC and body weight is still not clear and there are many different views on this issue. Usually, weight loss could be seen in a severe level of liver cancer [32]. Apart of many potential underlying variables, which could affect weight changes in liver cancer, two of the major factors are severity and interval of acquiring the disease. Biochemical results of the present study showed promising outcomes. AFP is one of the old but yet the most widely used blood marker tests for liver cancer. High level of AFP among the control group of the present study was similar to previous studies. Many of the studies in the last four decades have shown that AFP was elevated in hepatocarcinogenesis and embryonic carcinomas [33–35]. Beneficial effect of *T. polium* in the present study was supported by previous studies [34, 36]. It was shown that antioxidants can decrease the level of AFP [37, 38]; therefore, phytochemicals or any antioxidant active compounds of *T. polium* which has increased TAS level might affect the AFP level and could express this beneficial effect. Concerning ALP, it has been shown that ALP among liver function tests, in addition to other tumor characters, is an independent factor for disease-free survival and overall survival [39, 40]. Recent studies have suggested that preoperative ALP levels could be utilized to monitor and predict recurrence in high risk HCC patients [41, 42]. Both normal and *T. polium* treated group showed significantly lower serum ALP ($P < 0.05$), which was similar to previous studies [43–45]. Significant elevation of serum AST and ALT activities was seen in a variety of liver conditions, including viral infection, cirrhosis, nonalcoholic steatohepatitis (NASH), drug toxicity, liver tissue degeneration, and necrosis [46]. AST elevations often predominate in patients with cirrhosis and even in liver diseases that typically have increased ALT level [47]. Both normal group and *T. polium* treated group showed significantly lower serum AST and ALT ($P < 0.05$). Beneficial effect of *T. polium* on liver enzymes, including AST and ALT, has been reported previously [43, 45] and the present study supported the previous claims as well. Elevated AST/ALT ratio is clinically accepted as a better marker than assessing individually [48, 49]. Unlike other studies [43], non-significantly higher ratio was found among *T. polium* group. Lack of significant result might be due to the higher standard error of mean in both control and treatment group. Lack of significant result might be due to the higher standard error of mean, among both control and treatment groups.

Glucocorticoids (GCs) are frequently used to support patients suffering from various types of cancers. Their key therapeutic role is based on the GC receptor- (GR-) mediated mechanisms that activate cell death; however, this differs depending on the type of cancer [50]. Glucocorticoids prevent prostaglandin synthesis at the level of phospholipase A2 as well as at the level of cyclooxygenase/PGE isomerase (COX-1 and COX-2) [51]. The latter effect is similar to nonsteroidal anti-inflammatory drugs (NSAIDs), which potentiate the anti-inflammatory effect [52, 53]. COX-2-dependent activity is an essential element for cellular and molecular

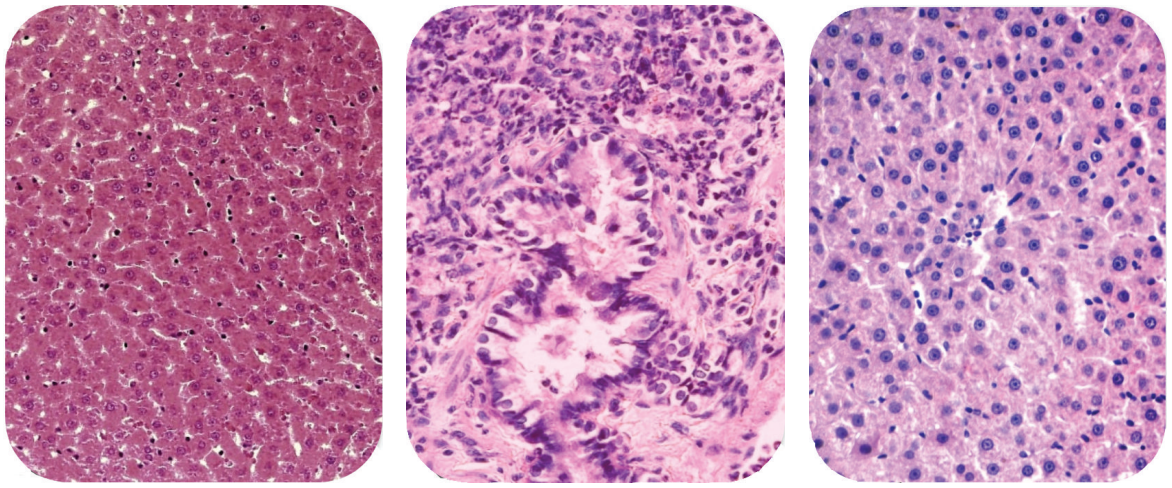

(a) (b) (c)

Figure 3: Light micrograph of liver cell in different groups. (a) Normal liver cell at the lobular region of normal group, lesion score: 0. (b) HCC in control group, lesion score: 4. (c) Hepatitis in *T. polium*, lesion score: 2. H&E, ×400.

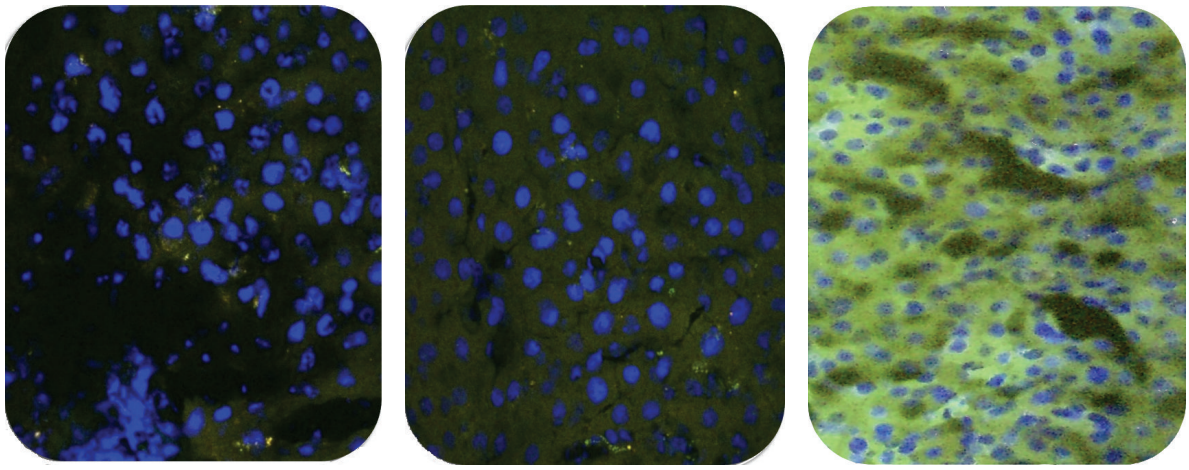

(a) (b) (c)

Figure 4: Fluorescent *in situ* hybridization micrograph of lobular region of protein expression of glucocorticoid receptors in the cytoplasm. (a) Normal. (b) Control. (c) *T. polium* treated group. Blue: nuclei with DAPI; green: protein expression of glucocorticoid receptors in cytoplasm. Frozen section, ×600 magnification.

mechanisms of cancer cell motility and invasion. The COX-2 activity also modulates the expression of matrix metalloproteinase (MMP), which may be a part of the molecular mechanism by which COX-2 promotes cell invasion and migration [52]. Many studies on different types of cancer have shown that cyclooxygenase suppression would decrease cancer cells [52–54]. Therefore, cyclooxygenase suppression by glucocorticoids might decrease risk of cancer or control its metastasis [55]. Glucocorticoids inhibit hepatocellular proliferation and modulate the expression of oncogenes and tumor suppressor genes via mechanisms involving the glucocorticoid receptor. Glucocorticoids also produce a receptor-mediated inhibitory effect on both basal and hormone-stimulated expression of a newly discovered family of molecules important for shutting off cytokine action [56] as well as different caspase pathways [57]. Based on the present study, *T. polium* has glucocorticoids stimulation activity, which might have a positive effect on cancer prevention or treatment. The results of confocal microscopy of fluorescent *in situ* hybridization of liver cells helped us to have a better answer for our findings in both light microscopy and biochemical results. As the FISH result in Figure 4 illustrated, high level of glucocorticoid receptor activity was observed in *T. polium* treated group. Therefore, higher activity of GC receptors and higher level of serum CBG, which have been found in the present study, could also explain the possible anticancer or

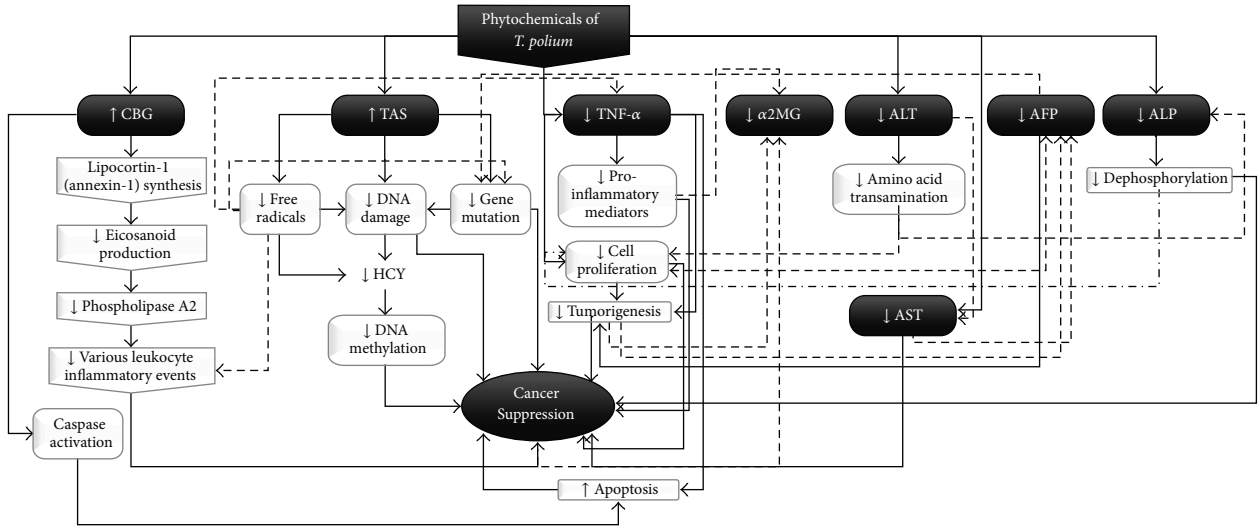

Figure 5: Brief possible beneficial effects of *T. polium* on HCC.

cancer suppressor competences of *T. polium*. Overall, as the present study is the first study in its field, further study would help us to have a better view of the mechanism of action of this herb on glucocorticoids stimulation.

It is well established that the elevated serum GGT activity could be found in diseases of the liver, biliary system, pancreas, and different types of cancers including HCC [58, 59]. In the present study, significantly lower level of GGT was found in *T. polium* treated groupas compared to control group ($P < 0.05$). Both epidemiological and experimental studies found a linkage between hyperhomocysteinemia and a varied range of impaired liver functions like cirrhosis and chronic alcohol consumption [60]. The present results showed significantly higher levels of HCY in the control group and are supported by few studies which have found high levels of HCY in different types of cancer [61] and liver disorders [62]. Recently it has been demonstrated that HCY inhibited hepatocyte proliferation by upregulating protein levels of p53 as well as mRNA and protein levels of p21Cip1 in primary cultured hepatocytes. HCY induced TRB3 expression via endoplasmic reticulum stress pathway, causing Akt dephosphorylation. Knockdown of endogenous TRB3 meaningfully suppressed the inhibitory effect of HCY on cell proliferation and the phosphorylation of Akt. [63]. Significantly lower HCY level in *T. polium* treated group showed vaguely that *T. polium* compounds could possibly suppress tumorigenicity through other possible mechanisms rather than HCY and its mentioned cascade pathway. Unfortunately, like GGT, the present study is the first attempt to observe the effect of this herb on serum level of HCY and further studies are needed to have better insight.

The role of TNF-α in liver cancer looks as a mixed blessing. TNF-α is a pleiotropic cytokine that can make both cell death and cell proliferation. TNF-α-induced cell death is normally blocked by the concurrently activated NF-κB pathway [64]. Deregulated TNF expression within the tumor microenvironment seems to favor malignant cell tissue invasion, migration, and final metastatic formation. On the other side, TNF-α clearly possesses antitumor effects not only in preclinical models, but also in the clinical ones [65]. It has been suggested that TNF-α plays an important role in the progress of different types of cancer including liver cancer [66]. The role of TNF-α has been connected to all steps engaged in tumorigenesis, including cellular transformation, promotion, survival, proliferation, invasion, angiogenesis, and metastasis [67]. Based on the present study, anticancer activity of *T. polium* compounds could possibly suppress TNF-α elevation which also might have either direct or indirect beneficial reciprocal effect on other markers.

Animal studies showed that α2MG is an imperative novel cytochemical marker to identify hepatocellular preneoplastic and neoplastic lesions, particularly amphophilic cell foci, undetectable by establishing cytochemical markers, and is tightly linked to rat hepatocarcinogenesis [68]. Furthermore, a number of authors have reported upregulation of serum α2MG in association with HCC in humans being significantly raised as compared to liver cirrhosis and amoebic liver abscess [69]. In the present study *T. polium* treated group showed significantly lower levels of α2MG as compared to control group. It is shown that cancer cells produce and secrete large amounts of α2MG, which seems to be linked with their tumorigenicity [70]; therefore, *T. polium* might decrease α2MG secretion through cancer tumorigenicity suppression.

Extremely high level of TAS in treated group could be one of the master keys in revealing possible cancer suppressor capabilities of *T. polium*. It has been shown that excessive reactive oxygen species (ROS) cause oxidative damage to biomolecules and lead to cellular alterations and ultimately tumorigenesis and neoplastic transformation [71]. Therefore, high level of TAS not only could act as excess ROS protector, but also might indirectly affect other cancer markers which have been tested. Figure 5 illustrates the possible beneficial effects of *T. polium* on HCC.

Lesion score evaluation of rats' liver also showed *T. polium* decoction successfully reduced the score of inflammation or necrosis at the both portal and lobular area as compared to control group ($P < 0.05$), which was comparable with previous anticancer herbal studies [34, 36].

These beneficial effects of *T. polium* could be explained by the significantly high level of flavonoid compounds and antioxidant competency of the *T. polium*. As the present study failed to find both rutin and apigenin as two of the active compounds of *T. polium* anticancer activities [72, 73], in order to find out the active compounds that play major role(s) in producing these effects, and possible molecular mechanisms, further studies are therefore necessary.

Conflict of Interests

The authors declare that there is no conflict of interests regarding the publication of this paper.

Acknowledgments

The authors would like to thank Universiti Putra Malaysia (UPM) for their funding of this research under RUGS-9367600. The authors would also like to acknowledge the staff of laboratories of nutrition, biochemistry, anatomy, stem cell, chemical pathology, immunology, and histopathology, the Microscopy Unit of the Institute of Bioscience, and Animal House at FMHS/FPSK.

References

[1] A. P. Venook, C. Papandreou, J. Furuse, and L. L. de Guevara, "The incidence and epidemiology of hepatocellular carcinoma: a global and regional perspective," *The Oncologist*, vol. 15, supplement 4, pp. 5–13, 2010.

[2] J. Ferlay, H.-R. Shin, F. Bray, D. Forman, C. Mathers, and D. M. Parkin, "Estimates of worldwide burden of cancer in 2008: GLOBOCAN 2008," *International Journal of Cancer*, vol. 127, no. 12, pp. 2893–2917, 2010.

[3] H. El-Serag and K. Rudolph, "Hepatocellular carcinoma: epidemiology and molecular carcinogenesis," *Gastroenterology*, vol. 132, no. 7, pp. 2557–2576, 2007.

[4] M. J. Strouch, Y. Ding, M. R. Salabat et al., "A high omega-3 fatty acid diet mitigates murine pancreatic precancer development," *Journal of Surgical Research*, vol. 165, no. 1, pp. 75–81, 2011.

[5] M. M. Marín Caro, A. Laviano, and C. Pichard, "Nutritional intervention and quality of life in adult oncology patients," *Clinical Nutrition*, vol. 26, no. 3, pp. 289–301, 2007.

[6] N. Fletcher, *Mediterranean Wildflowers (Pocket Nature)*, Dorling Kindersley, 2007.

[7] A. Zargar, *Botanical Drugs of Iran*, Tehran University Publications, Tehran, Iran, 1985, edited by A. Zargar.

[8] M. A. Esmaeili and R. Yazdanparast, "Hypoglycaemic effect of *Teucrium polium*: studies with rat pancreatic islets," *Journal of Ethnopharmacology*, vol. 95, no. 1, pp. 27–30, 2004.

[9] H. R. Rasekh, M. J. Khoshnood-Mansourkhani, and M. Kamalinejad, "Hypolipidemic effects of *Teucrium polium* in rats," *Fitoterapia*, vol. 72, no. 8, pp. 937–939, 2001.

[10] T. Baluchnejadmojarad, M. Roghani, and F. Roghani-Dehkordi, "Antinociceptive effect of *Teucrium polium* leaf extract in the diabetic rat formalin test," *Journal of Ethnopharmacology*, vol. 97, no. 2, pp. 207–210, 2005.

[11] M. Tariq, A. M. Ageel, M. A. al-Yahya, J. S. Mossa, and M. S. al-Said, "Anti-inflammatory activity of *Teucrium polium*," *International Journal of Tissue Reactions*, vol. 11, no. 4, pp. 185–188, 1989.

[12] S. Mansouri, "Inhibition of staphylococcus aureus mediated by extracts from Iranian plants," *Pharmaceutical Biology*, vol. 37, no. 5, pp. 375–377, 2008.

[13] S. Facciola, *Cornucopia: A Source Book of Edible Plants*, Kampong Publications, 1st edition, 1990.

[14] N. Nosrati, S. Aghazadeh, and R. Yazdanparast, "Effects of *Teucrium polium* on insulin resistance in nonalcoholic steatohepatitis," *Journal of Acupuncture and Meridian Studies*, vol. 3, no. 2, pp. 104–110, 2010.

[15] S. Rajabalian, "Methanolic extract of *Teucrium polium* L. potentiates the cytotoxic and apoptotic effects of anticancer drugs of vincristine, vinblastine and doxorubicin against a panel of cancerous cell lines," *Experimental Oncology*, vol. 30, no. 2, pp. 133–138, 2008.

[16] P. Ljubuncic, S. Dakwar, I. Portnaya, U. Cogan, H. Azaizeh, and A. Bomzon, "Aqueous extracts of *Teucrium polium* possess remarkable antioxidant activity in vitro," *Evidence-Based Complementary and Alternative Medicine*, vol. 3, no. 3, pp. 329–338, 2006.

[17] E. Bedir, D. Tasdemir, I. Çalis, and O. Zerbe, "Neo-clerodane diterpenoids from *Teucrium polium*," *Phytochemistry*, vol. 51, no. 7, pp. 921–925, 1999.

[18] IOM, "Dietary reference intakes for water, potassium, sodium, chloride, and sulfate," in *Dietary Reference Intakes*, Food and Nutrition Board, Ed., The National Academies, Washington, DC, USA, 2005, http://www.nap.edu/openbook.php?isbn=0309091691.

[19] K. S. Laaksonen, T. O. Nevalainen, K. Haasio, I. H. E. Kasanen, P. A. Nieminen, and H.-M. Voipio, "Food and water intake, growth, and adiposity of Sprague-Dawley rats with diet board for 24 months," *Lab Animal*, vol. 47, no. 4, pp. 245–256, 2013.

[20] U.S. EPA, "Recommendations for and Documentation of Biological Values for Use in Risk Assessment," 1988, http://www.tera.org/Tools/ratmousevalues.pdf.

[21] M. McDowell, C. D. Fryar, and C. L. Ogden, "Anthropometric reference data for children and adults: United States, 1988–1994," *Vital and Health Statistics. Series 11*, no. 249, pp. 1–68, 1988.

[22] A. Hackshaw, *A Concise Guide to Clinical Trials*, BMJ Books, 2009.

[23] D. Solt and E. Farber, "New principle for the analysis of chemical carcinogenesis," *Nature*, vol. 263, no. 5579, pp. 701–703, 1976.

[24] AIN, "Report of the American institute of nurtition ad hoc committee on standards for nutritional studies," *Journal of Nutrition*, vol. 107, no. 7, pp. 1340–1348, 1977.

[25] A. A. Adedapo, F. O. Jimoh, S. Koduru, P. J. Masika, and A. J. Afolayan, "Assessment of the medicinal potentials of the methanol extracts of the leaves and stems of Buddleja saligna," *BMC Complementary and Alternative Medicine*, vol. 9, article 21, 2009.

[26] S. M. Nabavi, M. A. Ebrahimzadeh, S. F. Nabavi et al., "Determination of antioxidant activity, phenol and flavonoid content of *Parrotia persica Mey*," *Pharmacologyonline*, vol. 2, pp. 560–567, 2008.

[27] W. Brand-Williams, M. E. Cuvelier, and C. Berset, "Use of a free radical method to evaluate antioxidant activity," *LWT—Food Science and Technology*, vol. 28, no. 1, pp. 25–30, 1995.

[28] A. Stevens, J. S. Lowe, B. Young, and P. R. Wheater, *Wheater's Basic Histopathology: A Colour Atlas and Text*, Churchill Livingstone, London, UK, 2002.

[29] K. P. Batts and J. Ludwig, "Chronic hepatitis. An update on terminology and reporting," *The American Journal of Surgical Pathology*, vol. 19, no. 12, pp. 1409–1417, 1995.

[30] J. Deng, N. Jin, X. Yin, G.-Y. Yang, Z. Zhang, and R. A. Omary, "Quantitative multiparametric PROPELLER MRI of diethylnitrosamine-induced hepatocarcinogenesis in wister rat model," *Journal of Magnetic Resonance Imaging*, vol. 31, no. 5, pp. 1242–1251, 2010.

[31] T. Shizuma, K. Ishiwata, M. Nagano, H. Mori, and N. Fukuyama, "Protective effects of fermented rice vinegar sediment (*Kurozu moromimatsu*) in a diethylnitrosamine-induced hepatocellular carcinoma animal model," *Journal of Clinical Biochemistry and Nutrition*, vol. 49, no. 1, pp. 31–35, 2011.

[32] NCI, Understanding Cancer Series: Cancer-National Cancer Institute, National Institutes of Health, 2013, http://www.cancer.gov/cancertopics/understandingcancer/cancer/AllPages.

[33] A. A. Terentiev and N. T. Moldogazieva, "Structural and functional mapping of alpha-fetoprotein," *Biochemistry*, vol. 71, no. 2, pp. 120–132, 2006.

[34] G. Motalleb, P. Hanachi, O. Fauziah, and R. Asmah, "Effect of Berberis vulgaris fruit extract on alpha-fetoprotein gene expression and chemical carcinogen metabolizing enzymes activities in hepatocarcinogenesis rats," *Iranian Journal of Cancer Prevention*, vol. 1, no. 1, pp. 33–44, 2008.

[35] E. Ruoslahti and M. Seppälä, "Studies of carcino-fetal proteins. 3. Development of a radioimmunoassay for -fetoprotein. Demonstration of -fetoprotein in serum of healthy human adults," *International Journal of Cancer*, vol. 8, no. 3, pp. 374–383, 1971.

[36] P. Hanachi, F. Othman, and G. Motalleb, "Effect of Berberis vulgaris aqueous extract on the apoptosis, sodium and potassium in hepatocarcinogenic rats," *Iranian Journal of Basic Medical Sciences*, vol. 11, no. 2, pp. 49–54, 2008.

[37] A. A. Fouad, A. S. Al-Mulhim, and I. Jresat, "Therapeutic effect of coenzyme Q10 against experimentally-induced hepatocellular carcinoma in rats," *Environmental Toxicology and Pharmacology*, vol. 35, no. 1, pp. 100–108, 2013.

[38] M. I. Azevedo, A. F. Pereira, R. B. Nogueira et al., "The antioxidant effects of the flavonoids rutin and quercetin inhibit oxaliplatin-induced chronic painful peripheral neuropathy," *Molecular Pain*, vol. 9, no. 1, article 53, 2013.

[39] C.-H. Chen, F.-C. Hu, G.-T. Huang et al., "Applicability of staging systems for patients with hepatocellular carcinoma is dependent on treatment method—analysis of 2010 Taiwanese patients," *European Journal of Cancer*, vol. 45, no. 9, pp. 1630–1639, 2009.

[40] M. J. Tong, D. Chavalitdhamrong, D. S. K. Lu et al., "Survival in Asian Americans after treatments for hepatocellular carcinoma: a seven-year experience at UCLA," *Journal of Clinical Gastroenterology*, vol. 44, no. 3, pp. e63–e70, 2010.

[41] M. C. Yu, K. M. Chan, C. F. Lee et al., "Alkaline phosphatase: does it have a role in predicting hepatocellular carcinoma recurrence?" *Journal of Gastrointestinal Surgery*, vol. 15, no. 8, pp. 1440–1449, 2011.

[42] J. M. Kim, C. H. D. Kwon, J.-W. Joh et al., "The effect of alkaline phosphatase and intrahepatic metastases in large hepatocellular carcinoma," *World Journal of Surgical Oncology*, vol. 11, no. 1, p. 40, 2013.

[43] H. Forouzandeh, M. M. E. Azemi, I. Rashidi, M. Goudarzi, and H. Kalantari, "Study of the protective effect of *Teucrium polium* L. extract on acetaminophen-induced hepatotoxicity in mice," *Iranian Journal of Pharmaceutical Research*, vol. 12, no. 1, pp. 123–129, 2013.

[44] A. Ardestani, R. Yazdanparast, and S. Jamshidi, "Therapeutic effects of *Teucrium polium* extract on oxidative stress in pancreas of streptozotocin-induced diabetic rats," *Journal of Medicinal Food*, vol. 11, no. 3, pp. 525–532, 2008.

[45] R. Amini, N. Nosrati, R. Yazdanparast, and M. Molaei, "*Teucrium polium* in prevention of steatohepatitis in rats," *Liver International*, vol. 29, no. 8, pp. 1216–1221, 2009.

[46] R.-Z. Yang, S. Park, W. J. Reagan et al., "Alanine aminotransferase isoenzymes: molecular cloning and quantitative analysis of tissue expression in rats and serum elevation in liver toxicity," *Hepatology*, vol. 49, no. 2, pp. 598–607, 2009.

[47] R. M. Green and S. Flamm, "AGA technical review on the evaluation of liver chemistry tests," *Gastroenterology*, vol. 123, no. 4, pp. 1367–1384, 2002.

[48] S. Gowda, P. B. Desai, V. Hull, A. A. K. Math, S. N. Vernekar, and S. S. Kulkarni, "A review on laboratory liver function tests," *The Pan African medical journal*, vol. 3, p. 17, 2009.

[49] H. Nyblom, E. Björnsson, M. Simrén, F. Aldenborg, S. Almer, and R. Olsson, "The AST/ALT ratio as an indicator of cirrhosis in patients with PBC," *Liver International*, vol. 26, no. 7, pp. 840–845, 2006.

[50] G. Schlossmacher, A. Stevens, and A. White, "Glucocorticoid receptor-mediated apoptosis: mechanisms of resistance in cancer cells," *Journal of Endocrinology*, vol. 211, no. 1, pp. 17–25, 2011.

[51] M. Goppelt-Struebe, D. Wolter, and K. Resch, "Glucocorticoids inhibit prostaglandin synthesis not only at the level of phospholipase A2 but also at the level of cyclo-oxygenase/PGE isomerase," *British Journal of Pharmacology*, vol. 98, no. 4, pp. 1287–1295, 1989.

[52] T. L. Larkins, M. Nowell, S. Singh, and G. L. Sanford, "Inhibition of cyclooxygenase-2 decreases breast cancer cell motility, invasion and matrix metalloproteinase expression," *BMC Cancer*, vol. 6, article 181, 2006.

[53] F. Hoellen, K. Kelling, C. Dittmer, K. Diedrich, M. Friedrich, and M. Thill, "Impact of cyclooxygenase-2 in breast cancer," *Anticancer Research*, vol. 31, no. 12, pp. 4359–4367, 2011.

[54] S. W. Fenwick, G. J. Toogood, J. P. A. Lodge, and M. A. Hull, "The effect of the selective cyclooxygenase-2 inhibitor rofecoxib on human colorectal cancer liver metastases," *Gastroenterology*, vol. 125, no. 3, pp. 716–729, 2003, http://www.ncbi.nlm.nih.gov/pubmed/1294971.

[55] H. Inoue, K. Umesono, T. Nishimori, Y. Hirata, and T. Tanabe, "Glucocorticoid-mediated suppression of the promoter activity of the cyclooxygenase-2 gene is modulated by expression of its receptor in vascular endothelial cells," *Biochemical and Biophysical Research Communications*, vol. 254, no. 2, pp. 292–298, 1999.

[56] J. A. Youssef and M. Z. Badr, "Hepatocarcinogenic potential of the glucocorticoid antagonist RU486 in B6C3F1 mice: effect on apoptosis, expression of oncogenes and the tumor suppressor gene *p53*," *Molecular Cancer*, vol. 2, no. 1, p. 3, 2003.

[57] S. L. Planey, M. T. Abrams, N. M. Robertson, and G. Litwack, "Role of apical caspases and glucocorticoid-regulated genes in glucocorticoid-induced apoptosis of pre-B leukemic cells," *Cancer Research*, vol. 63, no. 1, pp. 172–178, 2003.

[58] I. S. Fentiman, "Gamma-glutamyl transferase: risk and prognosis of cancer," *British Journal of Cancer*, vol. 106, no. 9, pp. 1467–1468, 2012.

[59] G. Hu, J. Tuomilehto, E. Pukkala et al., "Joint effects of coffee consumption and serum gamma-glutamyltransferase on the risk of liver cancer," *Hepatology*, vol. 48, no. 1, pp. 129–136, 2008.

[60] H. Sakuta and T. Suzuki, "Alcohol consumption and plasma homocysteine," *Alcohol*, vol. 37, no. 2, pp. 73–77, 2005.

[61] L. L. Wu and J. T. Wu, "Hyperhomocysteinemia is a risk factor for cancer and a new potential tumor marker," *Clinica Chimica Acta*, vol. 332, no. 1-2, pp. 21–28, 2002.

[62] S. C. R. de Carvalho, M. T. C. Muniz, M. D. V. Siqueira et al., "Plasmatic higher levels of homocysteine in non-alcoholic fatty liver disease (NAFLD)," *Nutrition Journal*, vol. 12, article 37, 2013.

[63] X. Yu, J. Lv, Y. Zhu, L. Duan, and L. Ma, "Homocysteine inhibits hepatocyte proliferation via endoplasmic reticulum stress," in *PLoS ONE*, R. Ray, Ed., vol. 8, no. 1, Public Library of Science, San Francisco, Calif, USA, 2013.

[64] J. Kucharczak, M. J. Simmons, Y. Fan, and C. Gélinas, "To be, or not to be: NF-kappaB is the answer—role of Rel/NF-kappaB in the regulation of apoptosis," *Oncogene*, vol. 22, no. 56, pp. 8961–8982, 2003.

[65] S. Mocellin and D. Nitti, "TNF and cancer: the two sides of the coin," *Frontiers in Bioscience*, vol. 13, pp. 2774–2783, 2008.

[66] X. Tian, P. Ma, C. Sui et al., "Comprehensive assessment of the association between tumor necrosis factor alpha G238A polymorphism and liver cancer risk," *Tumor Biology*, vol. 35, no. 1, pp. 103–109, 2014.

[67] G. Sethi, B. Sung, and B. B. Aggarwal, "TNF: a master switch for inflammation to cancer," *Frontiers in Bioscience*, vol. 13, pp. 5094–5107, 2008.

[68] T. Sukata, S. Uwagawa, K. Ozaki et al., "Alpha(2)-Macroglobulin: a novel cytochemical marker characterizing preneoplastic and neoplastic rat liver lesions negative for hitherto established cytochemical markers," *The American Journal of Pathology*, vol. 165, no. 5, pp. 1479–1488, 2004.

[69] M. Kotaka, G. G. Chen, B. P. S. Lai et al., "Analysis of differentially expressed genes in hepatocellular carcinoma with hepatitis C virus by suppression subtractive hybridization," *Oncology Research*, vol. 13, no. 3, pp. 161–167, 2002.

[70] S. M. Smorenburg, P. Griffini, A. M. B. C. Tiggelman, A. F. M. Moorman, W. Boers, and C. J. F. Van Noorden, "α2-macroglobulin is mainly produced by cancer cells and not by hepatocytes in rats with colon carcinoma metastases in liver," *Hepatology*, vol. 23, no. 3, pp. 560–570, 1996.

[71] M. S. Cooke, M. D. Evans, M. Dizdaroglu, and J. Lunec, "Oxidative DNA damage: mechanisms, mutation, and disease," *The FASEB Journal*, vol. 17, no. 10, pp. 1195–1214, 2003.

[72] E. J. Choi and G.-H. Kim, "5-Fluorouracil combined with apigenin enhances anticancer activity through induction of apoptosis in human breast cancer MDA-MB-453 cells," *Oncology Reports*, vol. 22, no. 6, pp. 1533–1537, 2009.

[73] S. Shukla and S. Gupta, "Apigenin: a promising molecule for cancer prevention," *Pharmaceutical Research*, vol. 27, no. 6, pp. 962–978, 2010.

Hindawi Publishing Corporation
Evidence-Based Complementary and Alternative Medicine
Volume 2014, Article ID 278917, 9 pages
http://dx.doi.org/10.1155/2014/278917

Review Article

The Possibility of Traditional Chinese Medicine as Maintenance Therapy for Advanced Nonsmall Cell Lung Cancer

Weiru Xu, Guowang Yang, Yongmei Xu, Qing Zhang, Qi Fu, Jie Yu, Mingwei Yu, Wenshuo Zhao, Zhong Yang, Fengshan Hu, Dong Han, and Xiaomin Wang

Oncology Department, Beijing Hospital of Traditional Chinese Medicine Affiliated to Capital Medical University, 23 Meishuguanhou Street, Dongcheng District, Beijing 100010, China

Correspondence should be addressed to Xiaomin Wang; ntxm100@sina.com

Received 14 April 2014; Revised 11 July 2014; Accepted 16 July 2014; Published 4 August 2014

Academic Editor: Senthamil R. Selvan

Lung cancer has become the leading cause of cancer deaths, with nonsmall cell lung cancer (NSCLC) accounting for around 80% of lung cancer cases. Chemotherapy is the main conventional therapy for advanced NSCLC. However, the disease control achieved with classical chemotherapy in advanced NSCLC is usually restricted to only a few months. Thus, sustaining the therapeutic effect of first-line chemotherapy is an important problem that requires study. Maintenance therapy is given for patients with advanced NSCLC if three is no tumor progression after four to six cycles of first-line platinum-based chemotherapy. However, selection of appropriate maintenance therapy depends on several factors, while traditional Chinese medicine (TCM) as maintenance therapy is recommended for all kinds of patients. It has been demonstrated that TCM can prolong the survival time, improve the quality of life (QOL), and reduce the side effects for advanced NSCLC. Although the trials we searched about TCM serving as maintenance therapy is only 9 studies, the results indicate TCM can prolong the progression free survival (PFS) and improve the QOL. So it is possible for TCM to be as maintenance therapy for advanced NSCLC. More rigorous trials are required to further verify its efficacy.

1. Introduction

Lung cancer has become the leading cause of cancer deaths in both men and women [1, 2]. Nonsmall cell lung cancer (NSCLC) accounts for around 80% of lung cancer cases [3]. At diagnosis, approximately 70% of patients present advanced stage of malignancy, for which curative therapy will not be available. Chemotherapy, radiotherapy, and targeted therapy are the conventional treatment for advanced NSCLC, among which chemotherapy is the main one. Platinum based doublets chemotherapy is the standard of care for advanced NSCLC. However, the disease control achieved with classical doublets chemotherapy in advanced NSCLC is usually restricted to only a few months [4–6]. About 20–80% of NSCLC patients cannot receive second-line chemotherapy for multiple reasons, including poor compliance [7]. Maintenance therapy can suppress disease progression and provide the opportunity to receive additional treatment. Thus, sustaining the therapeutic effect of first-line chemotherapy is an important problem that requires study. In recent years, maintenance therapy has become a new treatment strategy that aims to sustain a reduced tumor size and relieve tumor-related symptoms, in contrast to conventional chemotherapy that aims to maximize tumor cell death [7].

Maintenance therapy is an option in the National Comprehensive Cancer Network (NCCN) Guidelines only for responding and stable disease patients. Many clinical studies of multiple regimens and modalities about maintenance therapy are currently underway, which has been shown to improve the progression free survival (PFS) [8, 9]. However, some concerns remain regarding the overall survival (OS) and quality of life (QOL) [10]. The application of these chemotherapeutic drugs and molecular targeted drugs in maintenance therapy increase the financial burden of cancer treatment, which is another concern of this therapy.

Traditional Chinese medicine (TCM) has increasingly become popular in the west including in cancer patients [11]. It is estimated the United States National Cancer Institute

(NCI) spends around $120 million each year on complementary and alternative medicine (including TCM) related research projects [12]. It has been demonstrated that TCM can alleviate the clinical symptoms, improve the QOL, and reduce the side effects [13]. It helps NSCLC patients to "*survive with tumor*." So TCM is very suitable for maintenance therapy. In fact, TCM is widely used for NSCLC patients as consolidation therapy which actually includes TCM maintenance therapy. The difference is that maintenance therapy is between first-line and second-line therapy. TCM is endowed with new meaning as the introduction of the concept of maintenance therapy. If the disease is not progressed after first-line therapy, the tumor will be suppressed temporarily. The progression of the tumor is inevitable as time goes by. It is possible to stabilize the tumor, prolong the time to progression, and improve the QOL given with TCM maintenance therapy. Moreover, maintenance therapy is only recommended for patients with performance status (PS) 1-2, while TCM maintenance therapy is recommended for all kinds of patients no matter PS 1-2 or PS 3-4. So it is possible for TCM to be as maintenance therapy for advanced NSCLC.

2. The Present Situation of Maintenance Therapy

Maintenance therapy refers to systemic therapy that is given for patients with advanced NSCLC if the response is complete response (CR), partial response (PR), or stable disease (SD) after four to six cycles of first-line platinum-based chemotherapy [14]. The theoretical foundation of this therapy originates from the Goldie-Coldman theory [15], resistant and slowly growing cancer cells remain after first-line chemotherapy which has killed the sensitive and rapidly proliferating cells. Use of different non-cross-resistant chemotherapy regimens is effective in eradicating the remaining resistant cancer cells. Maintenance therapy can be classified into two types: continuation maintenance therapy and switch maintenance therapy. Continuation maintenance therapy refers to the use of at least one of the agents that was given in the first-line regimen. Switch maintenance therapy refers to the initiation of a different agent that was not included as part of the first-line regimen. Selection of appropriate maintenance therapy depends on several factors such as histologic type, performance status, and genetic alternations. NCCN version 2.2013 recommends continuation maintenance therapy using bevacizumab (category 1), cetuximab (category 1), pemetrexed (category 1), bevacizumab plus pemetrexed, and gemcitabine and switch maintenance therapy using pemetrexed, erlotinib, and docetaxel (category 2B).

Maintenance therapy is applied for the continuous treatment while patients can tolerate its side effects with favourable QOL. However, continuing cytotoxic agents will result in cumulative toxicity. Maintenance therapy with several cycles of cytotoxic drugs may damage the immune function, lower the QOL, and increase the risk of drug resistance for continuous therapy. Since researchers are more concerned with the acute toxicity accumulation, most clinical trials except large-scale studies did not evaluate QOL [7].

Based on the recent trials and Food and Drug Administration (FDA) approval, the NCCN Panel recommends single-agent pemetrexed as continuation maintenance therapy in patients with nonsquamous NSCLC who are EGFR mutation negative or ALK fusion negative. A recent phase III randomized trial found that continuation maintenance therapy with pemetrexed slightly increased PFS when compared with placebo [16]. Preliminary results suggest that continuation maintenance therapy with pemetrexed also improves overall survival (OS), but drug-related grades 3 to 4 anemia, fatigue, and neutropenia were significantly higher in pemetrexed-treated patients leading to the decrease of QOL [17]. Consequently, more clinical trials are expected to observe the OS and QOL.

The tolerable molecular targeted drugs are very expensive. Today, in the conditions of Chinese medical security system and the high incidence rate of lung cancer, maintenance therapy with targeted drugs is impossible to implement for most Chinese patients with no apparent disease progression after first-line chemotherapy. In addition, targeted therapy is only for those patients with specific genetic alternation [18], which in part limits its clinical application. Thus, maintenance therapy has some limitations to be applied in clinic due to population selection and high expenditure.

Maintenance therapy with chemotherapy or targeted therapy prolongs the PFS of NSCLC patients, but chemotherapy will accumulate the toxicity and increase the risk of drug resistance. The price of targeted therapy is very expensive and only NSCLC patients with specific gene phenotype will benefit. Some clinicians still doubt the efficacy of maintenance therapy, because most studies have not been shown to evaluate the QOL [7]. Owning to its treatment according to different syndromes, TCM is not limited to treat patients with histologic type, PS. or genetic alternations. These shortages of maintenance with chemotherapy or molecular targeted therapy make opportunities for TCM to treat as maintenance therapy.

3. The Theoretical Foundation of TCM in the Treatment of NSCLC

Lung cancer belongs to the disease of Feiji, Feiyong, and Xiji in ancient literature of TCM. The main pathogenesis of lung cancer is the deficiency of vital qi and the invasion of toxic pathogen, secondly for phlegm and blood stasis. Climatic pathogens or cancer toxin will invade into the human lung in case of the deficient vital qi and imbalance of yin and yang. The disharmony of lung function results in the obstruction of lung qi, impairment of dispersing and descending, stasis of blood flow, disturbance of body fluids in distribution. The accumulation of body fluids contributes to phlegm coagulation, causing qi stagnation and blood stasis in collaterals. Then the combination of the stagnation of qi, blood, phlegm and toxin gradually results in a mass in lung. Lung cancer is a kind of disease deficient in the whole body, and excessive in the local body. Deficiency in lung is

common with qi deficiency, yin deficiency, and deficiency of qi and blood, while excess in lung is common with phlegm coagulation, qi stagnation, blood stasis, and toxin retention.

TCM holds that the oncogenesis, development and outcome of cancer are the process of the struggle, growth, and decline between vital qi and pathogenic qi in the human body. There are sayings in ancient Chinese medical literature *Yellow Emperor's Inner Classic* "*the region where pathogenic factors invade must be deficient in qi*," "*when there is sufficient vital qi inside, pathogenic factors have no way to invade the body*." The oncogenesis is based on the theory of "*internal deficiency.*" As mentioned by Professor Rencun Yu the oncogenesis and extrinsic factor are the condition, the decisive factor is the intrinsic factor of *Internal Deficiency* [19]. The vital qi can sustain the normal physiological functions and defense the pathogenic factors. If the vital qi is deficient, the pathogenic qi will invade. When the stability of human internal environment and the balance between internal and external part are destroyed, the cancerigenic factor will take effect and contribute to oncogenesis, invasion, progression, and metastasis. So the oncogenesis was described in *Yi Zong Bi Du* (*Essential Readings for Medical Professionals*) as "*deficient vital qi leading to the lingering of pathogenic qi is the cause of cancer.*" Furthermore, the consumption caused by cancer itself and continuous treatment (operation, chemotherapy, and radiotherapy) will further injure the qi and blood. The cytotoxic chemotherapy fights against the pathogen post first-line chemotherapy for advanced NSCLC leading to the balance of vital qi and pathogenic qi in a short period of time. Whether the tumor can be controlled or not will be decided by the balance of the human internal environment. When the balance is broken, the tumor will relapse or progress. Thus, the maintenance therapy after first-line chemotherapy for advanced NSCLC obeys the rule of strengthening body resistance and eliminating pathogenic factors. Strengthening body resistance to restore its normal function in main combined with TCM of detoxication and anticancer is the principle to balance between the tumor and the internal environment. When the vital qi restores, it may inhibit the cancer cells, improve the QOL, and prolong the survival time.

In recent years, the theory of tumor microenvironment gains more and more attention of scholars which investigates the effects of tumor microenvironment on cancer relapse and metastasis. The Paget's "*Seed and Soil*" theory proposed in 1889 emphasizes the importance of the interaction between the tumor cell and its environment in order for metastasis and relapse to occur. The hypothesis states that cancer cells can seed to other tissue and change its surrounding cell quality by blood vessels and lymph. The metastasis site is not randomized, but some specific organs with the environment are suitable for the growth of cancer cells. The study shows that the primary tumor has been preparing the "soil" before metastasis so as to build its living environment. There is dynamic balance between the normal cells and its surrounding environment which regulates the cell activity, generation, differentiation, apoptosis, secretion, and expression of cell surface factors. While the oncogenesis of tumor is to break this balance, the tumor will establish the external environment to proliferate infinitely. This process runs through the whole procedure of tumor progression that is the root of oncogenesis and metastasis. This tumor microenvironment is similar to the TCM theory *balance of yin and yang* in human body. The theory of TCM holds that the pathogenesis of all diseases is caused by the imbalance of yin and yang in the body. It is recorded in *Su Wen* (*Plain Questions of the Yellow Emperor's Inner Classic*) that "*If yin and yang are in a relative equilibrium, life activities will be normally maintained; if yin and yang are separated, exhaustion of vital essence will happen*." The balance of yin and yang correlates with the harmony of the joint functions of each system, the Zang organs in particular. If the human body is balanced, people remain healthy. Otherwise, diseases or even death will occur. Just as the origins of all the diseases, the cause of cancer is also induced by the imbalance of yin and yang, which is manifested as the qi stagnation, phlegm coagulation, blood stasis, and retention of toxic heat. If the imbalance of yin and yang continues, "*yin may separate from yang*," and vital essence will be exhausted, leading to an ultimate stage of cancer. The imbalance of yin and yang is throughout the whole cause of cancer. The process of oncogenesis, progression, relapse and metastasis is the uninterrupt break of the whole or local yin and yang. So treatment principle is to restore the balance of yin-yang. As was proposed by two famous Chinese oncologists Rencun Yu and Jiaxiang Liu, the cancer treatment should follow the principle of regulating yin and yang to stabilize the internal environment and reestablish the internal balance. Then tumor can be controlled, the vital qi can be protected, the symptoms relieved, the QOL improved, and the survival time prolonged [20, 21]. The *wholism theory*, syndrome differentiation, and treatment in TCM correlate with the theory of tumor microenvironment from the macroscopic or microscopic angles. Recently, more and more scholars start to study the relationship between the TCM theory and tumor microenvironment. The internal environment is in the condition of the balance of yin and yang after first-line chemotherapy with tumor response or stable disease. This condition will be disturbed at any time nevertheless. TCM has an advantage of regulating yin and yang, balancing vital qi and pathogenic qi. Moreover, the therapeutic effects of TCM in the treatment of cancer are definite. So TCM as maintenance therapy for advanced NSCLC is to sustain this balance as long as possible.

4. Clinical Trials on TCM Treatment for Advanced NSCLC

TCM shows an advantage in the treatment of advanced NSCLC. It can combine with chemotherapy and radiotherapy that alleviates the side effects, enhances short-term therapeutic effects, stabilizes the disease, reduces the incidence rate of relapse and metastasis, and improves the long-term efficacy [22–25]. As to those patients who cannot accept operation, chemotherapy, or radiotherapy, TCM can ameliorate symptoms, reduce the pain, improve the QOL, and prolong the survival time with tumor [26]. So TCM shows

the irreplaceable role in the comprehensive treatment of advanced NSCLC.

In the early 1990s, studies about TCM in the treatment of NSCLC are not much. Chen et al. [27] studied a meta-analysis about TCM in the treatment of NSCLC compared with chemotherapy. It included 14 relevant papers with accumulated 1909 cases from 1990 to 1997. TCM for treating NSCLC in these papers included Chinese patent medicine (see [28–30], etc.), and decoction. The results showed that OR (odds ratios) of TCM group for stable rate (CR + PR + SD) was 2.1 (95% confidence intervals: 0.7–3.08), and OR of chemotherapy group for response rate (CR + PR) was 1.48 (95% confidence intervals: 1.03–2.24). The median survival time (MST) of 7 papers was included. The MST of TCM group was 335.4 days, while that of chemotherapy group was 231.8 days. This study indicates that TCM can prolong the MST, and chemotherapy group shows higher response rate but short MST. However, these studies did not limit the stage of NSCLC which resulted in clinical heterogeneity. More well-designed clinical trials are needed.

Yang et al. [31] reported the therapeutic effects of TCM in the treatment of advanced NSCLC in 2005. 136 cases were randomized into TCM group, integrated group (TCM + chemotherapy), and chemotherapy group. The response rate, syndrome differentiation, QOL, and MST were observed. The patients in both TCM group and integrated group were applied with decoction in combination with *Lanxiangxi Injection* (injection extracted from *Wenchow Turmeric Root Tuber*) and *Elemene Injection* (injection extracted from *Ma-yuen Jobstears Seed*). The results showed that the response rate (CR + PR) for TCM group was 2.1%, for chemotherapy group was 27.2% and for integrated group was 44.4%. The stable rate (CR + PR + SD) in integrated group was higher than other two groups ($P < 0.05$). The clinical symptoms and QOL in integrated group were better than chemotherapy group ($P < 0.05$, $P < 0.01$). The integrated group showed less side effects and toxicity compared to chemotherapy group. The MST in TCM group and integrated group were 11.5 months and 12.3 months, respectively, longer than that in chemotherapy group (9.2 months) ($P < 0.05$). The 1-year survival rates in TCM group and integrated group were 36.1% and 48.9%, respectively, higher than that (27.3%) in chemotherapy group ($P < 0.05$). This study supports that TCM can stabilize the tumor, improve the QOL, prolong the MST and attenuate the toxicity induced by chemotherapy.

A prospective, multicenter, randomized controlled trial was carried out in 6 hospitals [32]. 294 cases of III-IV NSCLC were allocated to TCM group, integrated group (TCM + chemotherapy), and chemotherapy group. *Shenyi Capsule* and *Hechan Pian* combined with decoction were applied to the patients in TCM group and integrated group. The MST of TCM group and integrated group were 292 days and 355 days. respectively, longer than that of chemotherapy group (236 days). The median time to progression (TTP) of TCM group and integrated group were 187 days and 239 days, respectively, longer than that of chemotherapy group (180 days). There was statistical indifference between groups because the sample was not large. But it shows the trend that TCM prolongs MST in III-IV NSCLC.

Zhu and Wu [33] studied a meta-analysis to evaluate the efficacy and safety of specialized TCM prescription integrated with chemotherapy in the treatment of III-IV NSCLC in 2013. Total of 17 randomized controlled trials (RCT) including 1163 cases were included in this meta-analysis. As compared with chemotherapy group, the specialized TCM prescription integrated with chemotherapy group achieved significant benefits in improving clinical response rate and QOL and reducing adverse effects. The ORs for clinical response rate, the improvement of QOL and the rates of adverse effects were 1.44 (95% confidence intervals: 1.12–1.85), 3.36 (95% confidence intervals: 2.45–4.59), and 0.23 (95% confidence intervals: 0.18–0.28), respectively. The results of this meta-analysis implies that the specialized TCM prescription integrated with chemotherapy in the treatment of stages III-IV NSCLC is more effective than chemotherapy alone. But the sample of these trials included is not large. The large sample, multicenter, randomized controlled trials are expected to further verify the efficacy of TCM for advanced NSCLC.

The achievements of TCM in the treatment of cancer have aroused the attention of Chinese government. Supported by our government, many hospitals have begun to develop clinical trials about TCM in the prevention and treatment of cancer. A multicenter, large-sample, randomized, double-blinded controlled trial (National Tenth Five-year Science Project) was led by Guang'an men Hospital, China Academy of Chinese Medical Sciences [22]. 587 nonoperable IIIA-IV NSCLC patients were enrolled. Integrated group (chemotherapy + *Shenyi Capsule* with the effects of tonifying qi and blood) was compared with western medicine group (chemotherapy + placebo). The observation time was two years. Statistical differences were shown in the clinical symptoms, Karnofsky performance status (KPS), chemotherapy induced side effects between integrated group and western medicine group (better in integrated group). The MST of integrated group was 12.03 months which was longer than that of western medicine group (8.46 months). There was statistical difference of MST between integrated group and western medicine group ($P = 0.0118$). This trial implies that integrated therapy can obviously improve the clinical symptoms, alleviate chemotherapy induced side effects and prolong the MST. This study also observes the effects of TCM in the treatment of non-operable IIIA-IV NSCLC patients. *Huachansu Injection*, *Elemene Injection*, *Lanxiangxi Injection* were either alternately applied or alone in TCM group. The MST of TCM group was 10.92 months. The QOL was improved. However, randomization approach was not applied. The latest cohort study supported by National Eleventh Five-year Science Project investigated comprehensive TCM regimen in the treatment of NSCLC [34]. The preliminary results showed that the MST of advanced NSCLC in integrated group was 16.6 months, and that in western medicine group was 13.13 months. These two trials provide high-level, evidence-based medical data for TCM in the treatment of advanced NSCLC. Therefore, it has been demonstrated that TCM alone or combined with conventional therapy in the treatment of advanced NSCLC can prolong the MST, improve the QOL, and reduce side effects.

International society shows a great interest while TCM achieved a series of achievements in the treatment of NSCLC. National Institute of Health collaborates with Guang'an men Hospital, China Academy of Chinese Medical Sciences to study the project Comprehensive TCM Regimen in the Treatment of Advanced NSCLC [26]. Longhua Hospital affiliated to Shanghai University of TCM collaborates with Memorial Sloan-Ketttering Cancer Center for the trial Jinfukang in the Treatment of NSCLC [35]. These international collaborations will provide more convinced evidence for TCM in the treatment of NSCLC.

5. Clinical Trials on TCM as Maintenance Therapy for Advanced NSCLC

TCM has a long history in China and is widely applied for cancer treatment. Actually, in clinic advanced NSCLC patients are given with decoction, Chinese patent medicine, injection of Chinese herbal extract, and so forth. If the PS of advanced NSCLC patient is 1-2, conventional therapy combined with TCM will be applied to the patient. TCM will be continuously given to the patients to consolidate the efficacy. If the PS of the patient is 3-4, TCM will be applied to the patient alone. TCM helps patients to relieve symptoms, improve the QOL, reduce the side effects induced by chemotherapy, radiotherapy, or targeted therapy, and prolong the TTP. TCM therapy runs through the whole process of the conventional therapy and is continuously applied after conventional therapy. This kind of consolidation therapy actually includes maintenance therapy. The difference is that maintenance therapy is the intensive treatment between first-line and second-line therapy. So TCM has already acted as the maintenance therapy in China. It has been demonstrated that TCM can in part help patients survive with tumor. So it is very suitable for TCM to be applied as maintenance therapy for advanced NSCLC. As mentioned before maintenance therapy with chemotherapy is only recommended for patients with PS 1-2, while TCM maintenance therapy is recommended for all kinds of patients no matter PS 1-2 or PS 3-4. So it is possible for TCM in the maintenance therapy of advanced NSCLC.

We searched the following sources up to March 2014 using PubMed, CNKI (China National Knowledge Infrastructure), Wanfang Database. Keywords searched were "maintenance therapy" "wei chi zhi liao", "nonsmall cell lung cancer" "fei xiao xi bao fei ai" or "NSCLC." No language restriction was applied. After screening titles and/or abstracts, 9 articles were included involving TCM as maintenance therapy in the treatment of advanced NSCLC from the electronic and manual searches. These trials were all conducted in China and published in Chinese. The characteristics of the 9 trials were summarized in Table 1. Most of these trials are small sample, randomized controlled studies. The results indicate that TCM as maintenance therapy can improve the QOL. Part of the studies show that TCM can prolong the PFS compared with the control group (follow-up group). Among them, one study shows that TTP in TCM group is equivalent to that of chemotherapy group, but shows better QOL. Furthermore, there is another study with 162 patients involved from 1992–2007 [36]. It is a nonrandomized controlled study aiming to evaluate the efficacy of TCM as consolidation treatment after conventional therapy. 162 IIIA-IV NSCLC patients after conventional therapy were assigned into TCM group (decoction was applied after conventional therapy) and control group (follow-up after conventional therapy). The results showed that the 2-year and 3-year survival rate of TCM group were much higher than those of the control group ($P < 0.05$). The MST of TCM group was 18 months, while that of control group was 12 months. So it supports that TCM as consolidation therapy can prolong the MST and improve the 2-year, 3-year survival rate. Although the IIIA-IV NSCLC patients after conventional therapy were included into this trial, which did not meet the criteria of maintenance therapy (advanced NSCLC after first-line chemotherapy with no tumor progression), it suggested that advanced NSCLC patients can benefit from TCM consolidation therapy to some degree.

Although the prescriptions (TCM applied) in these trials we mentioned above are different, it demonstrates the feasibility of TCM as maintenance therapy and suggests the profound knowledge of syndrome differentiation. Since previous data shows that TCM serving as maintenance therapy can improve the QOL and PFS. We hope to provide more opportunity for advanced NSCLC patients treated with TCM maintenance therapy to accept second-line therapy after the progression of first-line therapy. More clinical trials are required to further verify its efficacy.

6. Prospect on Maintenance Therapy with TCM for Advanced NSCLC

TCM has a long history in the treatment of advanced cancer patients and applied extensively in China. In clinic, TCM is commonly used for advanced NSCLC patients after chemotherapy, which has achieved certain therapeutic effects. This is a kind of maintenance therapy actually. Previous clinical trials have demonstrated that TCM has its own advantage in treating advanced NSCLC compared to western medicine. As we know, the curative therapy for advanced NSCLC is not available. TCM emphasize the *Wholism* and *Survival with Tumor*. TCM regulates the balance of the human body by adjusting the yin and yang, qi and blood, deficiency and excess, which dispels exogenous pathogen by avoiding hurting vital qi. TCM regards the human body more important than the tumor. Although the efficacy of TCM directly in killing and suppressing the tumor cells is not very obvious, it has its own characteristics in some aspects. It can improve the QOL and alleviate the side effects of chemotherapy and radiotherapy. Besides, both the clinical and experimental studies show that TCM especially the tonifying herbal medicine can improve the immune function by elevating the quantity of T-lymphocyte subtypes and natural killer cells, which improves the ability of the human body to fight against tumor cells [37–41]. In 2006, World Health Organization defines cancer as a kind of treatable, controllable chronic disease rather than the incurable disease [42]. This is similar to the idea of TCM *Survival with Tumor.*

Table 1: The characteristics of the trials for TCM as maintenance therapy in the treatment of advanced NSCLC.

Authors	TNM stage of NSCLC	Design of study	Patients (n)		Intervention		Measurements	PFS, OS, MST, and TTP (m)	Results/conclusion
			Treatment group	Control group	Treatment group	Control group			
Liu et al., 2009 [44]	Nonoperatable IIIA-IV	RCT	31	31	*Feitai Capsule*	—	FACT-L, KPS, clinical symptoms	—	*Feitai Capsule* can improve the QOL.
Chai et al., 2011 [45]	IIIB-IV	RCT	32	32	*Xiaoji Yin*	—	MST, PFS	PFS: 5.1 versus 2.5 ($P = 0.00$) MST: 6.43 versus 3.26 ($P = 0.00$)	*Xiaoji Yin* can prolong the MST and PFS.
Jiang et al., 2011 [46]	IIIB-IV	RCT	25	25	Comprehensive TCM therapy	Gemcitabine/Pemetrexed/Docetaxel	TTP, QOL(EORTC QLQ-LC43)	TTP: 2.9 versus 2.13 ($P = 0.063$)	The TCM comprehensive regimen had equivalent efficacy on TTP but better QOL when compared with single-agent chemotherapy.
Xi et al., 2011 [47]	III-IV	RCT	44	34	*Hechan Pian*	—	PFS, clinical symptoms	median PFS: 5.67 versus 4.12 ($P = 0.048$)	*Hechan Pian* can prolong the median PFS and improve the clinical symptoms.
Zeng et al., 2013 [48]	IV	RCT	34	35	*Shenyi Capsule*	—	Medin PFS, KPS, immune function (T-lymphocyte subtypes)	median PFS: 6.5 versus 6.2 ($P > 0.05$)	*Shenyi Capsule* can improve the QOL and immune function which helps more patients to accept second-line chemotherapy.
Yang 2013 [49]	III-IV	RCT	40	40	*Fuzheng Xiaoji Yin*	—	PFS	PFS: 7.5 versus 4.8 ($P < 0.01$)	*Fuzheng Xiaoji Yin* can prolong the PFS.
Liang and Zhang 2013 [50]	IIIB-IV	RCT	38	36	*Rongyan Capsule*	—	MST, PFS	PFS: 4.8 versus 2.37 ($P = 0.00$) MST: 6.23 versus 2.7 ($P = 0.00$)	*Rongyan Capsule* can prolong the MST and PFS.
Wang et al., 2013 [51]	IV	RCT	39	37	TCM therapy based on syndrome differentiation	—	PFS, QOL(EORTC-QLQ-C30), clinical symptoms	PFS: 7.2 versus 4.4 ($P < 0.01$)	TCM therapy based on syndrome differentiation can improve the QOL, clinical symptoms and prolong the PFS.
Wu et al., 2014 [52]	IIIB-IV	Nonrandomized controlled trial	20	20	*Shenyi Capsule*	—	DCR, PFS, OS	PFS: 4.35 versus 2.67 ($P < 0.01$) OS: 10 versus 7.8 ($P < 0.01$)	*Shenyi Capsule* can prolong the PFS and OS and improve the DCR.

RCT: randomized controlled trial; FACT-L: functional assessment of cancer therapy-lung; MST: median survival time; PFS: progression free survival; TTP: time to progression; QOL: quality of life; EORTC: European Organization for Research and Treatment of Cancer; KPS: Karnofsky performance status; TCM: traditional Chinese medicine; DCR: disease control rate; OS: overall survival.

Syndrome is the basic unit and a key concept in TCM theory. It is different from disease or symptom. TCM syndrome is the abstraction of a major disharmonious pathogenesis. *Syndrome Differentiation and Treatment* is the core of TCM, which requires treating patients with methods of inspection, listening and smelling, questioning, and pulse taking according to different person, area, and time. Based on this principle, TCM treats with different plans for different stages of cancer patients. Tonifying therapy is mainly for alleviating the side effects induced by chemotherapy and radiotherapy, improving the symptoms and promoting the body recovery. While after the chemotherapy and radiotherapy, dispelling the exogenous pathogen is mainly used for controlling the cancer so as to prevent cancer relapse and metastasis. *Syndrome Differentiation and Treatment* will show its advantage in maintenance therapy. No matter the PS 1-2 or PS 3-4, the gene phenotype, pathology, TCM can serve as maintenance therapy according to different syndromes. During maintenance therapy keeping a favourable living state is the premis, while TCM can improve the QOL and regulates the patient body in a balanced state. So the aim of TCM is similar to maintenance therapy. We believe that TCM as maintenance therapy is feasible.

7. Summary

Maintenance therapy with chemotherapy or targeted agents can prolong the PFS of advanced NSCLC patients to some degree, but chemotherapy may increase the toxicity and the risk of drug resistance, and targeted therapy is very expensive and only suited for certain patients with specific genetic alternation [43]. So some patients lose the opportunities to accept maintenance therapy. TCM is widely used in China for cancer patients. Although the effects of TCM in eradicating cancer cells are not obvious, it helps cancer patients to fight against cancer and restore the body into a balanced state by regulating the balance of yin and yang. Besides, TCM can be applied for NSCLC patients not limited in population selection. Recent studies demonstrate that TCM as maintenance therapy can improve the QOL of advanced NSCLC patients. There is some encouraging evidence of TCM for prolonging the PFS. However, there are only small sample clinical trials about TCM as maintenance therapy for advanced NSCLC. More large-scale trials of TCM as maintenance therapy for advanced NSCLC are expected.

Conflict of Interests

The authors declare that they have no conflict of interests.

Acknowledgments

This work was supported by Major Project of Beijing Science and Technology Program (no. D131100002213001), Special Fund of Ministry of Education for Doctoral Tutor (no. 20131107110014), National Natural Science Foundation of China (no. 81373815), and Beijing Natural Science Foundation (no. 7122083).

References

[1] P. Guo, Z. L. Huang, P. Yu, and K. Li, "Trends in cancer mortality in China: an update," *Annals of Oncology*, vol. 23, no. 10, pp. 2755–2762, 2012.

[2] R. Siegel, D. Naishadham, and A. Jemal, "Cancer statistics, 2013," *CA Cancer Journal for Clinicians*, vol. 63, no. 1, pp. 11–30, 2013.

[3] K. Zarogoulidis, P. Zarogoulidis, K. Darwiche et al., "Treatment of non-small cell lung cancer (NSCLC)," *Journal of Thoracic Disease*, vol. 5, supplement 4, pp. S389–S396, 2013.

[4] J. H. Schiller, D. Harrington, C. P. Belani et al., "Comparison of four chemotherapy regimens for advanced non-small-cell lung cancer," *The New England Journal of Medicine*, vol. 346, no. 2, pp. 92–98, 2002.

[5] G. V. Scagliotti, F. de Marinis, M. Rinaldi et al., "Phase III randomized trial comparing three platinum-based doublets in advanced non-small-cell lung cancer," *Journal of Clinical Oncology*, vol. 20, no. 21, pp. 4285–4291, 2002.

[6] F. Fossella, J. R. Pereira, J. von Pawel et al., "Randomized, multinational, phase III study of docetaxel plus platinum combinations versus vinorelbine plus cisplatin for advanced non-small-cell lung cancer: the TAX 326 Study Group," *Journal of Clinical Oncology*, vol. 21, no. 16, pp. 3016–3024, 2003.

[7] J. Lee and C. Chung, "Update on the evidence regarding maintenance therapy," *Tuberculosis and Respiratory Diseases*, vol. 76, no. 1, pp. 1–7, 2014.

[8] P. Fidias and S. Novello, "Strategies for prolonged therapy in patients with advanced non-small-cell lung cancer," *Journal of Clinical Oncology*, vol. 28, no. 34, pp. 5116–5123, 2010.

[9] T. E. Stinchcombe and M. A. Socinski, "Treatment paradigms for advanced stage non-small cell lung cancer in the era of multiple lines of therapy," *Journal of Thoracic Oncology*, vol. 4, no. 2, pp. 243–250, 2009.

[10] C. P. Belani, T. Brodowicz, T. E. Ciuleanu et al., "Quality of life in patients with advanced non-small-cell lung cancer given maintenance treatment with pemetrexed versus placebo (H3E-MC-JMEN): results from a randomised, double-blind, phase 3 study," *The Lancet Oncology*, vol. 13, no. 3, pp. 292–299, 2012.

[11] H. S. Boon, F. Olatunde, and S. M. Zick, "Trends in complementary/alternative medicine use by breast cancer survivors: Comparing survey data from 1998 and 2005," *BMC Women's Health*, vol. 7, article 4, 2007.

[12] L. Jia, "Cancer complementary and alternative medicine research at the US National Cancer Institute," *Chinese Journal of Integrative Medicine*, vol. 18, no. 5, pp. 325–332, 2012.

[13] L. H. Yoder, "Let's talk "cancer prevention"," *Medsurg Nursing*, vol. 14, no. 3, pp. 195–198, 2005.

[14] C. Gridelli, F. de Marinis, M. Di Maio et al., "Maintenance treatment of advanced non-small-cell lung cancer: results of an international expert panel meeting of the Italian association of thoracic oncology," *Lung Cancer*, vol. 76, no. 3, pp. 269–279, 2012.

[15] J. H. Goldie and A. J. Coldman, "A mathematic model for relating the drug sensitivity of tumors to their spontaneous mutation rate," *Cancer Treatment Reports*, vol. 63, no. 11-12, pp. 1727–1733, 1979.

[16] L. Paz-Ares, F. de Marinis, M. Dediu et al., "Maintenance therapy with pemetrexed plus best supportive care versus placebo plus best supportive care after induction therapy with pemetrexed plus cisplatin for advanced non-squamous non-small-cell lung cancer (PARAMOUNT): a double-blind, phase

3, randomised controlled trial," *The Lancet Oncology*, vol. 13, no. 3, pp. 247–255, 2012.

[17] L. G. Paz-Ares, F. de Marinis, M. Dediu et al., "PARAMOUNT: final overall survival results of the phase III study of maintenance pemetrexed versus placebo immediately after induction treatment with pemetrexed plus cisplatin for advanced nonsquamous non-small-cell lung cancer," *Journal of Clinical Oncology*, vol. 31, no. 23, pp. 2895–2902, 2013.

[18] M. Pérol, C. Chouaid, D. Pérol et al., "Randomized, phase III study of gemcitabine or erlotinib maintenance therapy versus observation,with predefined second-line treatment, after cisplatin-gemcitabine induction chemotherapy in advanced non-small-cell lung cancer," *Journal of Clinical Oncology*, vol. 30, no. 28, pp. 3516–3524, 2012.

[19] R. C. Yu, "The effects and prospect of traditional Chinese medicine in the prevention and treatment of cancer," *Chinese Journal of Integrated Traditional and Western Medicine*, vol. 27, no. 5, pp. 389–390, 2007.

[20] R. C. Yu and W. J. Tang, "Balance therapy in the application of integrative cancer therapy," *Oncology Progress*, vol. 2, no. 6, pp. 438–450, 2004.

[21] J. X. Liu, "Anti-cancer therapies of yin-yang balance and tonifying in the application of cancer treatment," *Jiang Su Zhong Yi Yao*, vol. 40, no. 9, pp. 1–2, 2008.

[22] H. S. Lin and Y. Zhang, "Evidence-based medical study of TCM on non small cell lung cancer," *World Science and Technology—Modernization of Traditional Chinese Medicine and Materia Medica*, vol. 10, no. 4, pp. 121–125, 2008.

[23] S. R. Ren, D. B. Liao, X. Q. Zhou, and J. Wang, "Shenqi Fuzheng Injection combined with radiotherapy on treating 34 senile advanced non small cell lung cancer patients," *Chinese Journal of Integrated Traditional and Western Medicine*, vol. 26, no. 10, p. 876, 2006.

[24] X. Z. Lan and Y. H. Jiang, "Radiotherapy combined with traditional Chinese medicine on treating 26 senile advanced non small cell lung cancer," *Zhong Yi Za Zhi*, vol. 43, no. 2, pp. 125–126, 2002.

[25] H. B. Cai, F. G. Dai, Q. F. Min, M. Shi, J. X. Liao, and R. C. Luo, "Clinical study of the effects of radiotherapy in combination with traditional Chinese medicine on non-small cell lung cancer," *Journal of First Military Medical University*, vol. 22, no. 12, pp. 1112–1114, 2001.

[26] H. S. Lin and Y. Zhang, "The review and the prospect of TCM oncology," *Global Traditional Chinese Medicine*, vol. 2, no. 5, pp. 321–326, 2009.

[27] Z. F. Chen, C. Z. Li, S. X. Liu, J. Hou, and J. M. Wang, "Meta analysis on primary non-small cell lung carcinoma treated by TCM in China," *Zhong Yi Za Zhi*, vol. 40, no. 5, 1995.

[28] B. K. Piao, W. X. Tang, Z. Q. Zhang, H. S. Lin, F. W. Duan, and G. Q. Yu, "Feiliuping Gao in the treatment of advanced primary lung cancer, an analysis of 339 cases," *Zhong Yi Za Zhi*, no. 4, pp. 21–23, 1991.

[29] P. W. Li, D. Z. Zhang, Y. X. Hao et al., "Pingfei Fang in the treatment of 109 non small cell lung cancer patients," *Zhong Yi Za Zhi*, vol. 36, no. 2, pp. 87–88, 1995.

[30] M. Q. Pan, Y. H. Li, J. A. Liu et al., "Feifu Fang in the treatment of 80 advanced primary bronchial squamous cancer patients controlled with chemotherapy," *Zhong Guo Yi Yao Xue Bao*, vol. 5, no. 3, pp. 19–23, 1990.

[31] G. W. Yang, X. M. Wang, D. Han et al., "Study on TCM comprehensive therapy in the treatment of advanced non-small cell lung cancer," *Zhong Guo Zhong Yi Yao Xin Xi Za Zhi*, vol. 12, no. 9, pp. 11–13, 2005.

[32] D. H. Zhou, L. Z. Lin, Y. Q. Zhou et al., "Effect of Chinese herbal medicine in prolonging median survival time in patients with non small cell lung cancer," *Guang Zhou Zhong Yi Yao Da Xue Xue Bao*, vol. 22, no. 4, pp. 255–258, 2005.

[33] M. Z. Zhu and W. Y. Wu, "Specialized TCM prescription integrated with chemotherapy in the treatment of stages III-IV non-small cell lung cancer: a meta analysis," *Tumor*, vol. 33, no. 6, pp. 534–545, 2013.

[34] Y. Zhang, W. Hou, and H. S. Lin, "The achievements and thinking of traditional Chinese medicine in the treatment of cancer," *Zhong Yi Za Zhi*, vol. 55, no. 6, pp. 523–525, 2014.

[35] B. R. Cassileth, N. Rizvi, G. Deng et al., "Safety and pharmacokinetic trial of docetaxel plus an Astragalus-based herbal formula for non-small cell lung cancer patients," *Cancer Chemotherapy and Pharmacology*, vol. 65, no. 1, pp. 67–71, 2009.

[36] J. H. Li, "A clinical comparative study on traditional Chinese Medicine serving as consolidation treatment in patients with advanced non-small cell lung cancer," *Chinese Journal of Lung Cancer*, vol. 10, no. 6, pp. 520–522, 2007.

[37] Z. Q. Liu, Q. T. Chen, Y. Li, Y. Song, and H. L. Sun, "Influences of Roucongrong on hematopoietic function and immune function in tumor-bearing mice after chemotherapy," *Journal of Beijing University of Traditional Chinese Medicine*, vol. 33, no. 11, pp. 758–761, 2010.

[38] Q. Zhang, X. M. Wang, G. W. Yang et al., "Guben Xiaoliu Capsule combined with Folfox4 regimen in the treatment of advanced colorectal cancer," *Beijing Journal of Traditional Chinese Medicine*, vol. 29, no. 4, pp. 255–258, 2010.

[39] H. P. Yao, T. Cui, Q. W. Zheng, and W. Y. Feng, "Antitumor and immunological regulation effects of Qibai capsule on mice bearing uterine cervical carcinoma," *Chinese Journal of Hospital Pharmacy*, vol. 33, no. 19, pp. 1567–1569, 2013.

[40] S. R. Zhuang, H. F. Chiu, S. L. Chen et al., "Effects of a Chinese medical herbs complex on cellular immunity and toxicity-related conditions of breast cancer patients," *British Journal of Nutrition*, vol. 107, no. 5, pp. 712–718, 2012.

[41] S. Zhuang, S. Chen, J. Tsai et al., "Effect of citronellol and the Chinese medical herb complex on cellular immunity of cancer patients receiving chemotherapy/radiotherapy," *Phytotherapy Research*, vol. 23, no. 6, pp. 785–790, 2009.

[42] J. Li, H. S. Lin, W. Hou, and B. J. Hua, "Idea and strategy of traditional Chinese medicine treatment for cancer," *China Cancer*, vol. 19, no. 11, pp. 735–738, 2010.

[43] K. Takeda, T. Hida, T. Sato et al., "Randomized phase III trial of platinum-doublet chemotherapy followed by gefitinib compared with continued platinum-doublet chemotherapy in Japanese patients with advanced non-small-cell lung cancer: results of a West Japan Thoracic Oncology Group Trial (WJTOG0203)," *Journal of Clinical Oncology*, vol. 28, no. 5, pp. 753–760, 2010.

[44] Z. Liu, Z. Yu, X. Ouyang et al., "Effects of Feitai Capsule on quality of life in patients with advanced non-small-cell lung cancer: a randomized controlled trial," *Journal of Chinese Integrative Medicine*, vol. 7, no. 7, pp. 611–615, 2009.

[45] X. S. Chai, C. X. He, W. Y. Wu, and L. N. Li, "Xiaoji Yin as maintenance therapy in the treatment of survival time of advanced non small cell lung cancer," *Shi Zhen Guo Yi Guo Yao*, vol. 22, no. 10, pp. 2547–2548, 2011.

[46] Y. Jiang, L. S. Liu, C. J. Li, J. H. Tian, L. P. Shen, and H. G. Li, "Effect of Chinese medicine comprehensive regimen as the

maintenance therapy on time to progression and quality of life of patients with advanced non-small-cell lung cancer," *Chinese Journal of Integrated Traditional and Western Medicine*, vol. 31, no. 10, pp. 1311–1316, 2011.

[47] C. X. Xi, G. Q. Yang, Z. G. Li, and W. X. Tao, "Clinical observations of maintenance therapy with Hechan Pian for patients in intermediate and advanced non small cell lung cancer," *Zhong Liu Fang Zhi Yan Jiu*, vol. 38, no. 10, pp. 1170–1172, 2011.

[48] D. X. Zeng, Y. Z. Bi, G. F. Sheng, Y. Z. Dong, and H. L. Song, "Effectiveness and safety of single-agent ginsenoside Rg3 maintenance therapy after response to first-line chemotherapy in patients with advanced non small cell lung cancer," *Oncology Progress*, vol. 11, no. 6, pp. 554–558, 2013.

[49] C. Q. Yang, "Clinical research on adjuvant chemotherapy and maintenance therapy of Fuzheng Xiaoji Yin treatment of non small cell lung cancer in middle and advanced stage," *Zhong Yi Xue Bao*, vol. 28, no. 187, pp. 1782–1784, 2013.

[50] J. R. Liang and L. H. Zhang, "Rongyan Capsule as maintenance therapy on the effects of survival time of advanced non small cell lung cancer," *Si Chuan Zhong Yi*, vol. 31, no. 1, pp. 100–101, 2013.

[51] L. Wang, Z. X. Sun, G. Q. Feng, and S. J. Ma, "Effect of maintenance treatment by traditional Chinese medicine syndrome differentiation on life quality and progress-free survival of patients with advanced non small cell lung cancer after chemotherapy," *Zhong Guo Shi Yan Fang Ji Xue Za Zhi*, vol. 19, no. 13, pp. 319–322, 2013.

[52] Y. F. Wu, S. Xu, J. Jia, and G. Wang, "Effect of maintenance treatment with Shenyi Capsule on survival period of advanced non small cell lung cancer patients after induction chemotherapy," *Guang Zhou Zhong Yi Yao Da Xue Xue Bao*, vol. 31, pp. 40–43, 2014.

Hindawi Publishing Corporation
Evidence-Based Complementary and Alternative Medicine
Volume 2014, Article ID 637528, 8 pages
http://dx.doi.org/10.1155/2014/637528

Research Article

Elemene Injection Induced Autophagy Protects Human Hepatoma Cancer Cells from Starvation and Undergoing Apoptosis

Yan Lin,[1,2] Keming Wang,[2] Chunping Hu,[3] Lin Lin,[3] Shukui Qin,[4] and Xueting Cai[3]

[1] *Institute of First Clinical Medicine, Nanjing University of Chinese Medicine, Nanjing, Jiangsu 210046, China*
[2] *Department of Oncology, The Second Affiliated Hospital of Nanjing Medical University, Nanjing, Jiangsu 210021, China*
[3] *Laboratory of Cellular and Molecular Biology, Jiangsu Province Institute of Traditional Chinese Medicine, 100 Shizi Street, Hongshan Road, Nanjing, Jiangsu 210028, China*
[4] *Oncology Center of Chinese, 81 Hospital of PLA, Nanjing, Jiangsu 210002, China*

Correspondence should be addressed to Shukui Qin; qinsk@csco.org.cn and Xueting Cai; caixueting@gmail.com

Received 20 May 2014; Accepted 23 May 2014; Published 24 July 2014

Academic Editor: Peng Cao

Elemene, a compound found in an herb used in traditional Chinese medicine, has shown promising anticancer effects against a broad spectrum of tumors. In an *in vivo* experiment, we found that apatinib, a tyrosine kinase inhibitor that selectively inhibits VEGFR2, combined with elemene injection (Ele) for the treatment of H22 solid tumor in mice resulted in worse effectiveness than apatinib alone. Moreover, Ele could protect HepG2 cells from death induced by serum-free starvation. Further data on the mechanism study revealed that Ele induced protective autophagy and prevented human hepatoma cancer cells from undergoing apoptosis. Proapoptosis effect of Ele was enhanced when proautophagy effect was inhibited by hydroxychloroquine. Above all, Ele has the effect of protecting cancer cells from death either in apatinib induced nutrient deficient environment or in serum-free induced starvation. A combination of elemene injection with autophagy inhibitor might thus be a useful therapeutic option for hepatocellular carcinoma.

1. Introduction

Primary liver cancer is the most common malignant tumor, which accounts for 45% of the global incidence of the morbidity and mortality rates are in the second tumor spectrum. Hepatocellular carcinoma (HCC), a primary liver cancer, is the most common type accounting for 90% of primary liver cancer. In our country the survival time of patients with advanced HCC is typically only 3–6 months. Elemene is extracted from traditional Chinese medicine *Curcuma zedoaria (Christm.) Rosc*. *In vivo* and *in vitro* experiments confirmed elemene injection (Ele) has good induction of apoptosis and antiangiogenic effects on a variety of tumor cells [1, 2]. In this study, we found elemene injection had both proapoptotic and proautophagic effect on human hepatoma cell line HepG2. Since autophagy can result in both survival and cell death, we then asked whether Ele-induced autophagy is protective or proapoptotic. The results revealed that Ele elemene injection induced autophagy protects human hepatoma cancer cells from starvation and undergoing apoptosis.

2. Materials and Methods

2.1. Materials. Elemene injection was obtained from Dalian Holley Kingkong Pharmaceutical (Dalian, China). Apatinib was provided by Jiangsu Hengrui Medicine Co., Ltd. Hydroxychloroquine (HCQ) was purchased from Jiangsu Province Hospital on Integration of Chinese and Western Medicine, China. MTT (3-(4,5-dimethylthiazol-2-yl)-2,5-diphenyltetrazolium bromide) was obtained from Sigma, USA. Lysis buffer was purchased from Beyotime, China. Antibodies (PARP, cleaved-caspase 3, cleaved-caspase 9, Bcl-2, and Bax) were obtained from Cell Signaling Technology, USA. Anti-LC3 antibody was purchased from Abcam

plc, USA. GAPDH antibody was purchased from Santa Cruz, USA. IRDye 800CW goat anti-rabbit IgG (H + L) and IRDye 680RD goat anti-mouse IgG (H + L) were obtained from LI-COR Biosciences, USA.

2.2. Cell Lines and Animals. Human hepatoma cell line HepG2 was purchased from the Cell Bank of Shanghai Institute of Biochemistry and Cell Biology, Shanghai Institutes for Biological Sciences, Chinese Academy of Sciences. Cells were cultured in DMEM medium supplemented with 10% fetal bovine serum (FBS), 100 U/mL penicillin, and 100 μg/mL streptomycin (all available from Invitrogen, Grand Island, NY, USA). All cultures were maintained in a humidified environment with 5% CO_2 at 37°C. Mouse hepatoma H22 cells were maintained in the peritoneal cavities of ICR mice provided by KeyGEN Biotech (Nanjing, China). ICR mice were purchased from Shanghai SLRC Laboratory Animal Co., Ltd. (Shanghai, China). Mice were housed under specific pathogen-free conditions and provided with a standard rodent laboratory diet from Shanghai SLRC Laboratory Animal Co., Ltd. All experimental protocols were approved by the Animal Care and Use Committee of Jiangsu Branch of China Academy of Chinese Medical Sciences and were in accordance with the Declaration of the National Institutes of Health Guide for Care and Use of Laboratory Animals (Publication no. 80-23, revised 1996).

2.3. Cytotoxicity Assay. The cytotoxicity of Ele on HepG2 cells was analyzed by MTT assay. HepG2 cells at mid-log phase were seeded in 96-well plate at a density of 1×10^4 cells per well in 100 μL medium. After 24 h incubation, cells were exposed to DMEM (used as control in all experiments), 0.05, 0.1, 0.15, or 0.2 mg/mL Ele for 24 and 48 h. After treatment, 10 μL of 5 mg/mL MTT was added and the cells were incubated for 4 h at 37°C. The supernatant was discarded and 100 μL of DMSO was added to each well. The mixture was shaken on a minishaker at room temperature for 10 min and the spectrophotometric absorbance was measured by Multiskan Spectrum Microplate Reader (Thermo, USA) at 570 nm and 630 nm (absorbance 570 nm, reference 630 nm). Triplicate experiments were performed in a parallel manner for each concentration point and the results were presented as mean ± SD. The net $OD_{570\,nm} - OD_{630\,nm}$ was taken as the index of cell viability. The net absorbance from the wells of cells cultured with DMEM was taken as the 0% inhibitory rate. The percent inhibitory rate (IR%) of the treated cells was calculated by the following formula:

$$\text{IR\%} = 1 - \frac{(OD_{570\,nm} - OD_{630\,nm})_{\text{treated}}}{(OD_{570\,nm} - OD_{630\,nm})_{\text{control}}} \times 100\%. \quad (1)$$

2.4. Apoptosis Assay. HepG2 cells were cultured, including positive and negative controls, for appropriate time to induce apoptosis. Apoptotic cells were determined with Guava Nexin Reagent (Millipore, USA) according to the manufacturer's protocol. Briefly, the cells were harvested and resuspended with 100 μL DMEM medium containing 1% FBS. The cells were then incubated for 20 min at room temperature in the dark with 100 μL of Guava Nexin Reagent containing Annexin V-PE and 7-AAD. Afterward, apoptosis was analyzed by flow cytometer (Guava 6HT, Merck-Millipore, USA). The data were analyzed using the software Guava 2.5.

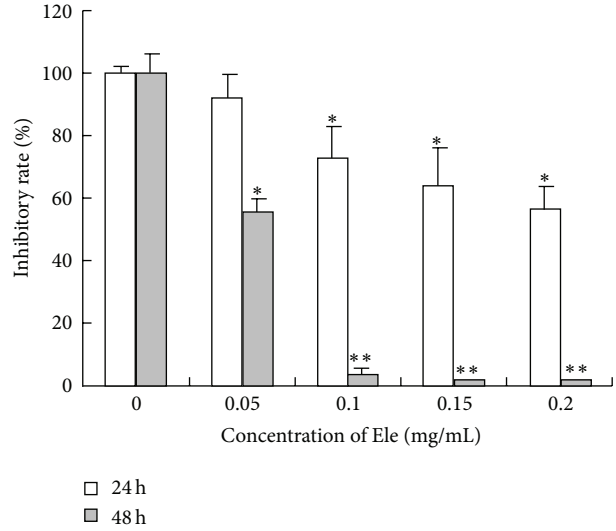

Figure 1: Cytotoxicity effect of Ele on HepG2 cells. The results shown were the mean of three parallel experiments (triplicate wells) for each concentration point (0.05, 0.1, 0.15, and 0.2 mg/mL) at 24 and 48 h. $^*P < 0.05$, $^{**}P < 0.01$ versus control.

2.5. Western Blotting Analysis. For preparation of cell extracts, cells were treated as described in the figure legends and lysed with lysis buffer (Beyotime, China) on ice. Lysate was centrifuged at 13,000 g for 5 min at 4°C. The concentration of protein in the supernatants was detected by Nanodrop 1000 Spectrophotometer (Thermo, NH, USA). Equal amount of protein was separated on 13% SDS-polyacrylamide gels (SDS-PAGE) and transferred onto the PVDF membranes (Millipore, MA, USA). After being blocked with 1% BSA in TBST (Tris Buffered Saline with Tween-20) for 2 h, membranes were incubated with primary antibodies overnight at 4°C. Blots were washed and incubated with secondary antibodies for 2 h at room temperature. Membranes were again washed three times with TBST. Detection was performed by LI-COR Odyssey Scanner (LI-COR Biosciences, USA).

2.6. Evaluation of Antitumor Activity of Ele Combined with Apatinib. H22 hepatoma cells were maintained in the peritoneal cavities of ICR mice. 20 ± 2 g ICR mice, half male and half female, were inoculated subcutaneously (s.c.) 0.2 mL H22 ascites tumor cell suspension (about 5×10^6/mL). Treatment was started the day after. The inoculated mice were randomized into six groups ($n = 9$): 200 mg/kg apatinib group, 75 mg/kg Ele group, 50 mg/kg Ele + 200 mg/kg apatinib group, 75 mg/kg Ele + 200 mg/kg apatinib group, 100 mg/kg Ele + 200 mg/kg apatinib group, 75 mg/kg Ele + 100 mg/kg apatinib group, 75 mg/kg Ele + 300 mg/kg apatinib group, and H22-bearing mice as negative control group (NS group). Ele was administered i.p. once daily while apatinib was used

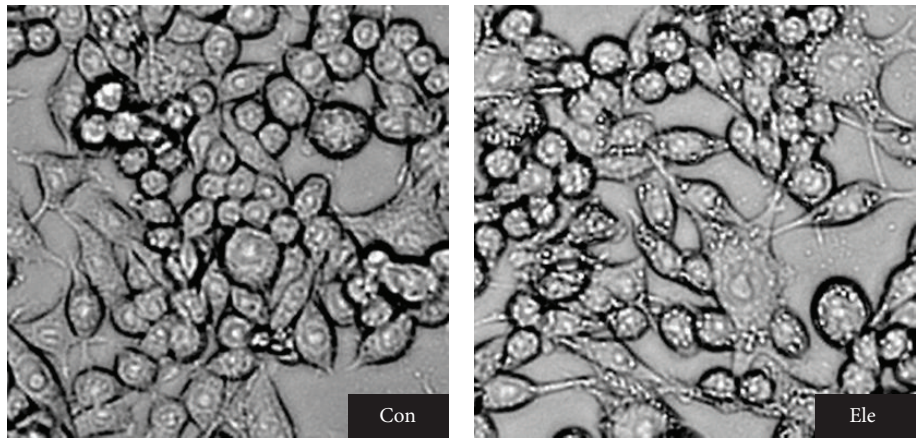

(a) (b)

Figure 2: Cell morphological assessment. Light micrograph of HepG2 cells after overnight incubation with Ele. Compared to the control cells, cells exposed to Ele presented typical autophagy morphology with marketable vacuoles (×200).

by intragastric injection administration once daily. Tumor size was measured using a caliper across its longest diameter (a) and the second longest diameter (b), and its volume was calculated using $TV = 0.5\,ab^2$. Inhibition ratio (IR) was calculated using $IR(\%) = \{(TV_{control} - TV_{treat})/TV_{control}\} \times 100$. All the mice were sacrificed after 8 days of treatment.

2.7. Statistical Analysis. All the data were expressed as mean ± standard deviation (SD). Statistical analysis was performed using the Student's t-test and $P < 0.05$ was indicated to be statistical significance.

3. Results

3.1. Ele Suppressed the Proliferation of Hepatoma Cancer Cells HepG2. MTT assay was applied to analyze the inhibition effect of Ele on cell growth. Figure 1 showed that Ele inhibited proliferation of HepG2 cells in a dose-dependent, time-independent manner. Interestingly, marketable vacuoles in the cytoplasm of Ele-treated cells were observed under an inverted light microscope (Figure 2). However, this phenomenon was not observed in negative control.

3.2. Ele Induced Both Cell Apoptosis and Autophagy on HepG2 Cells. Apoptosis was controlled by regulators, which either have an inhibitory effect on programmed cell death (antiapoptotic) or block the protective effect of inhibitors (proapoptotic) [3, 4]. After treatment with different concentrations of Ele for 24 h, a concomitant increase in the levels of cleaved-caspase 3, cleaved-caspase 9, and cleaved poly-ADP-ribose polymerase (PARP) was observed (Figure 3(a)), which indicted that Ele-induced cell apoptosis was a mitochondrial (intrinsic) pathway. HepG2 cells, which were exposed to Ele for different times, were lysed and prepared to detect the antiapoptotic proteins (Bcl-2) and proapoptotic protein (Bax). As shown in Figure 3(b), the expression of Bax was increased and the expression of Bcl-2 was decreased after 4 h and 8 h of treatment with 0.05 mg/mL Ele.

LC3 protein is a biochemical marker for autophagic cells [5]. To confirm that Ele also can induce autophagy on HepG2 cells, Western blotting was used to detect the impact of Ele on the cleavage of protein LC3. LC3 has two forms, LC3-I and LC3-II. The latter is located on the autophagosomes and always remains on the membrane. LC3-II is considered as the sign molecule of autophagy. As shown in Figure 3(b), exposure to Ele for different times, expression of LC3 I protein reduced while that of LC3 II increased at 4 h and 8 h time points, indicating that Ele could induce autophagy on HepG2 cells.

The Bcl-2/Bax protein ratio and LC3 I/LC3 II protein ratio were shown in Figure 3(c), during 0–8 hours, Bcl-2/Bax protein ratio gradually decreased with time course, indicating that the degree of cell apoptosis increased, and LC3 I/LC3 II protein ratio gradually decreased with time course, indicating that the degree of autophagy increased. But during the 16–24 hours, Bcl-2/Bax protein ratio and LC3 I/LC3 II protein ratio began to increase, indicating that cell apoptosis and autophagy began to reach a balance. Did autophagy protect the cell from dying via inhibiting cell apoptosis?

3.3. Ele Protected HepG2 Cells during Starvation. HepG2 cells were starved with serum-free medium for 12 h than treated with either control (DMEM) or 0.05 mg/mL Ele. Flowmetry assays showed that treatment with Ele significantly decreased cell apoptosis rate, compared with control group (9.6% versus 48.9%, $P < 0.05$) (Figure 4).

3.4. Ele Reduced the Effectiveness of Apatinib on H22 Solid Tumor in Mice. Using H22 solid tumor model, the result showed that Ele combined with Apa reduced the effectiveness of Apa in a dose-dependent manner (Figure 5). Apatinib, also known as YN968D1, is a tyrosine kinase inhibitor that selectively inhibits the vascular endothelial growth factor receptor-2 (VEGFR2, also known as KDR). It is an orally bioavailable, small molecule agent which is thought to inhibit angiogenesis in cancer cells; specifically apatinib inhibits

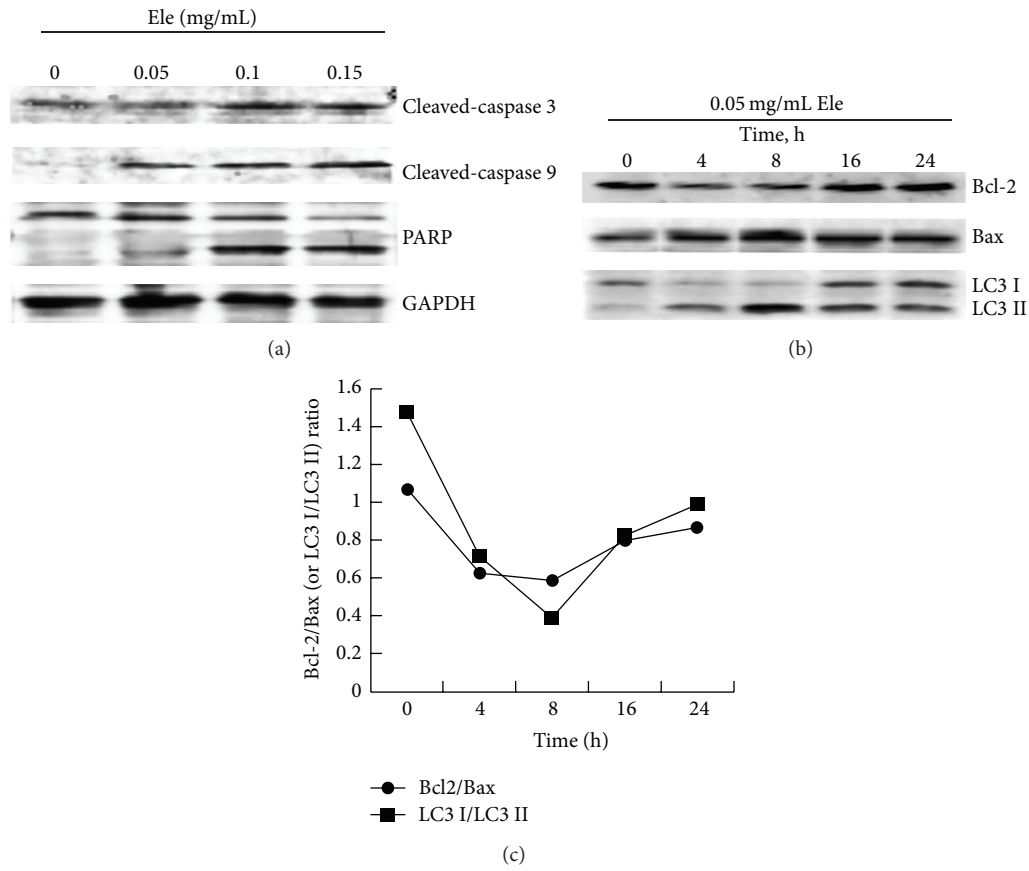

FIGURE 3: Ele-induced apoptosis and autophagy of HepG2 cells. HepG2 cells were untreated or treated with different concentration of Ele for 24 h or with 0.05 mg/mL Ele for different times. Apoptosis-related proteins (a) and autophagy-related proteins (b) were detected by Western blotting. The Bcl-2/Bax protein ratio and LC3 I/LC3 II protein ratio were shown in (c).

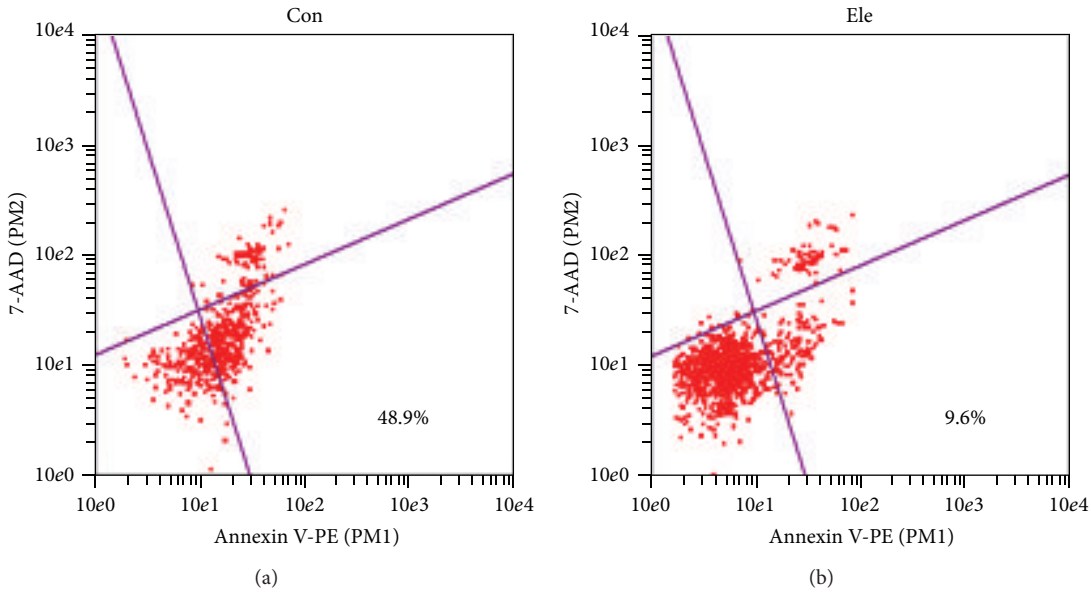

FIGURE 4: Ele protected HepG2 cells during starvation. HepG2 cells, starved for 12 h, were untreated or treated with 0.05 mg/mL Ele for 24 h. Flowmetry was used to detect the apoptosis cells.

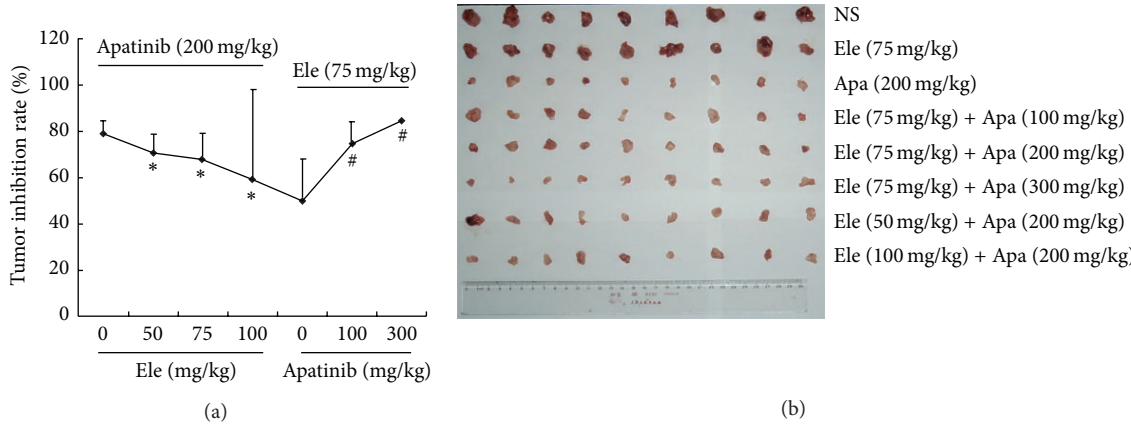

(a) (b)

Figure 5: Ele reduced the effectiveness of apatinib on H22 solid tumor in mice. The H22 bearing mice were randomized into six groups ($n = 9$): 200 mg/kg apatinib group, 75 mg/kg Ele group, 50 mg/kg Ele + 200 mg/kg apatinib group, 75 mg/kg Ele + 200 mg/kg apatinib group, 100 mg/kg Ele + 200 mg/kg apatinib group, 75 mg/kg Ele + 100 mg/kg apatinib group, 75 mg/kg Ele + 300 mg/kg apatinib group, and H22-bearing mice as negative control group (NS group). All the mice were sacrificed after 8 days of treatment. Inhibition ratio (IR) was calculated using $IR(\%) = \{(TV_{control} - TV_{treat})/TV_{control}\} \times 100$. $^{*}P < 0.05$ versus apatinib, $^{\#}P < 0.05$ versus Ele.

VEGF-mediated endothelial cell migration and proliferation, thus blocking new blood vessel formation in tumor tissue [6].

3.5. Ele-Induced Autophagy Protected HepG2 Cells from Undergoing Cell Apoptosis. Since autophagy can result in both survival and cell death, we then asked whether Ele-induced autophagy is protective or proapoptotic. HepG2 cells were treated with either 0.05 mg/mL Ele or 50 μM HCQ (a lysosomal alkalization agent could prevent autophagosome fusion with lysosomes, which is leading to increased accumulation of autophagosome, stopping autophagy at the late phase) or cotreated with Ele and HCQ for 24 h. Flowmetry assays showed that cotreatment with Ele and HCQ significantly decreased cell viability, compared with the cells treated with Ele alone (22.6 ± 1.9% versus 1.3 ± 0.7%, $P < 0.05$) (Figure 6).

4. Discussion

The treatment of advanced primary liver cancer is currently very poor due to the lack of effective treatment. An estimated 748,300 new liver cancer cases and 695,900 cancer deaths occurred worldwide in 2008, one of the first three cancer-related deaths [7]. Among primary liver cancers, hepatocellular carcinoma (HCC) represents the major histological subtype accounting for 70% to 85% of the total liver cancer burden worldwide [8]. At present, China still has the largest number of deaths and is the country of the highest prevalence, accounting for about 55% of the number of cancer cases worldwide and accounting for 45% of cancer deaths worldwide. Because liver cancer has insidious onset, rapid development, easy invasion, and easy transfer characteristics, patients have liver cancer which can be surgically removed is only 20%, while the majority of patients are found to have locally advanced or distant metastasis. HCC's prognosis is very poor; 5-year survival rate is less than 10% in Asian countries, 8% in Europe, and only about 5% in developing countries. Surgery and liver transplantation are currently the main treatment; 5-year recurrence rate after radical resection of hepatocellular carcinoma is still up to 60–70%; even in small HCC recurrence rate is also around 40–50% [9]. Due to limitations of liver transplantation in patients with hepatic sources, physical underlying diseases, and other factors, only a small number of people benefit. But even after a successful liver transplant there are some people who relapse and suffer from metastasis. Some patients will relapse even after a successful liver transplantation. Patients with middle and late stage primary liver cancer lost surgery and other local treatment opportunity, such as transcatheter arterial chemoembolization (TACE), microwave ablation (MWA), and percutaneous ethanol injection (PEI). Systemic chemotherapy for advanced hepatocellular carcinoma may have some effects and some patients' symptoms improved; however, many reported single-agent or combination chemotherapy effective rate is very low. Therefore, there is an urgent clinical need for an efficient and low toxicity treatment to improve survival in patients with advanced hepatocellular carcinoma. Elemene injection has better inhibitory role on tumor cells with low toxicity, mild side effects of liver, and kidney function, suitable for advanced hepatocellular carcinoma patients. In recent years, along with the fast development of traditional Chinese medicine, many modem Chinese herbal medicine were applied to clinical use. For example, ginsenosides Rg3 (Shenyi capsule) [10, 11], elemene injection [12–14], arsenic trioxide (As2O3) injection [15], Kanglaite injection, and Shenmai injection, which all have certain effect on inhibiting tumor cell proliferation and antitumor angiogenesis. Chinese materia medica preparation is characterized by certain antitumor effects; adverse reactions are mild, can enhance immunity, and improve the quality of life of patients, a wide range of applications, especially for advanced liver cancer which cannot be systemic chemotherapy or progression after chemotherapy, but the overall disadvantage of traditional Chinese medicines tumor is the fact that the cell killing

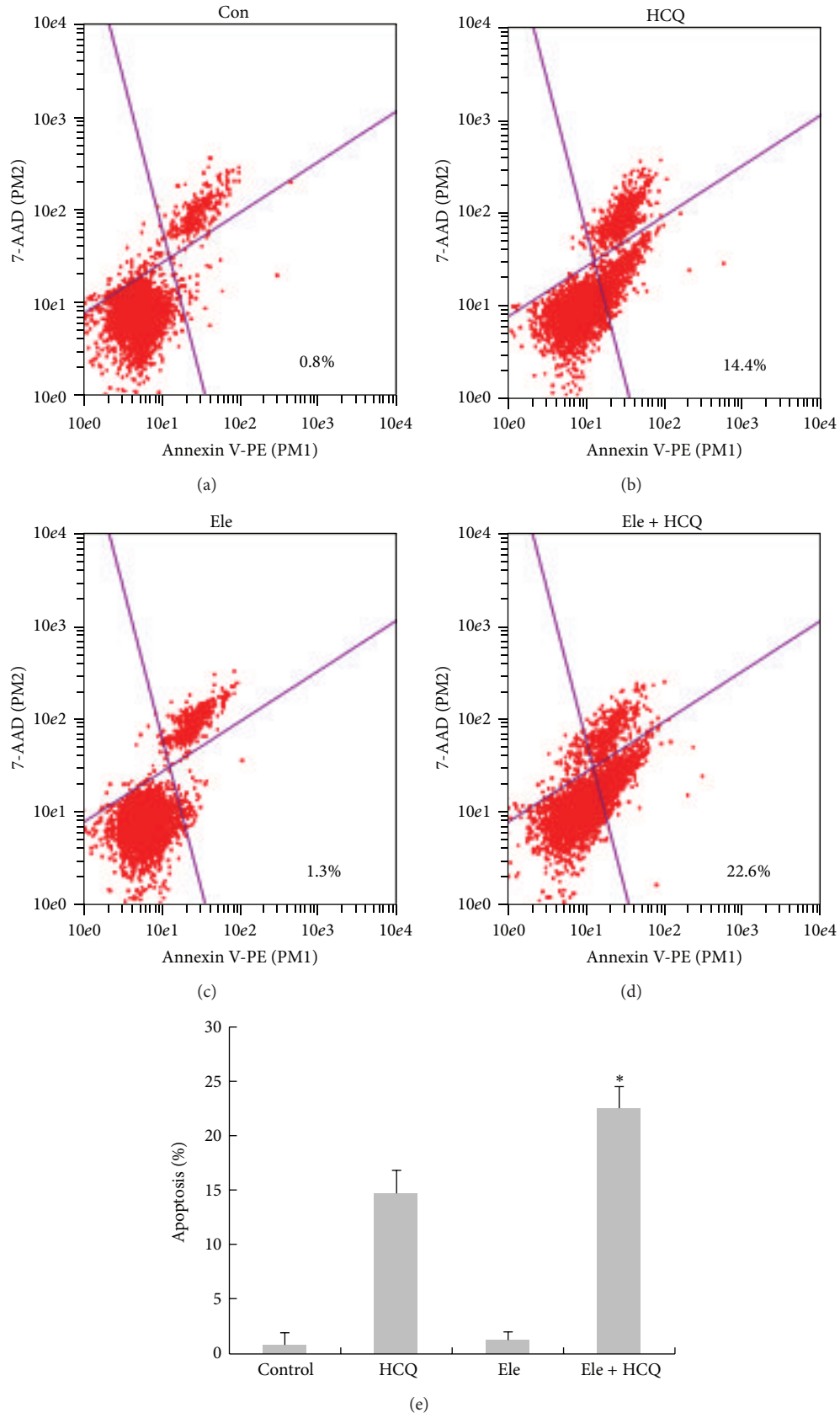

Figure 6: Ele-induced autophagy protected HepG2 cells from undergoing cell apoptosis. HepG2 cells, untreated or treated with either 0.05 mg/mL Ele or 50 μM HCQ or cotreated with Ele and HCQ for 24 h, were harvested and detected by Flowmetry. $^{*}P < 0.05$ versus HCQ group.

effect is weak. Elemene injection is considered strongest Chinese medicine in killing tumor cells in the present study. Recent experimental studies showed that elemene injection has significantly cytotoxicity on a variety of tumor cells [12–14], antitumor metastasis, invasion, and inhibition of tumor angiogenesis effect. In this study, elemene monotherapy inhibited tumors proliferation in H22 hepatoma bearing mice, consistent with the above-mentioned literature.

Autophagy (or autophagocytosis) is the basic catabolic mechanism that involves cell degradation of unnecessary or dysfunctional cellular components through the actions of lysosomes [16]. Oftentimes, cancer occurs when several different pathways that regulate cell differentiation are disturbed. Autophagy plays an important role in cancer in both protecting against cancer and potentially contributing to the growth of cancer [17]. Autophagy may protect against cancer by isolating damaged organelles, allowing cell differentiation, increasing protein catabolism, and even promoting cell death of cancerous cells [18]. However, autophagy can also contribute to cancer by promoting survival of tumor cells that have been starved. Herman-Antosiewicz et al. [19] indicated that induction of autophagy represents a defense mechanism against sulforaphane-induced apoptosis in human prostate cancer cells. In addition, chemotherapy and radiotherapy increased autophagic activity, and autophagy cleared the ionizing radiation or cytotoxic induced damaged mitochondria, blocking the mitochondrial apoptotic signal transduction cascade so that some cancer became drug resistant [20–22]. Some autophagy inhibitors help improve the antitumor therapeutic effect. 3-Methyladenine (3-MA) and chloroquine (CQ) are two common autophagy inhibitors. 3-MA inhibits phosphoinositide 3-kinase (P13K) and can inhibit MAP1-LC3 I transfer to MAPl-LC3 and thus interfere with or block autophagy. HCQ can increase the pH value inside the lysosome and inhibit the fusion of autophagy and lysosome.

In the present study apatinib inhibited tumor blood vessels leading to nutritional deficiencies; in that state, elemene injection induced autophagy and degradation of proteins in tumor cells for nutritional supplements, thereby reducing the efficacy of apatinib. When combined with HCQ, an autophagy inhibitor, further enhances cell apoptosis in Ele-treated HepG2 cells. Does elemene still have existing proautophagy effect in other tumor cells? Does elemene still have existing antagonistic effect when combined with other drugs, such as cytotoxic drugs, due to induction of autophagy? All these issues need to be clarified by further research.

Conflict of Interests

The authors declare that there is no conflict of interests regarding the publication of this paper.

Authors' Contribution

Yan Lin and Keming Wang contributed equally to this work; they are both the first authors of this paper.

Acknowledgments

This work was supported by the National Natural Science Foundation of China (nos. 81202967, 81274150, 81302968, and 81374018) and Jiangsu Province's Outstanding Leader Program of Traditional Chinese Medicine.

References

[1] J. M. Llovet, A. Burroughs, and J. Bruix, "Hepatocellular carcinoma," *The Lancet*, vol. 362, no. 9399, pp. 1907–1917, 2003.

[2] M. Hidalgo and S. G. Eckhardt, "Development of matrix metalloproteinase inhibitors in cancer therapy," *Journal of the National Cancer Institute*, vol. 93, pp. 178–193, 2001.

[3] D. L. Vaux, "A boom time for necrobiology," *Current Biology*, vol. 3, pp. 877–878, 1993.

[4] K. Wang, X. Yin, D. T. Chao, C. L. Milliman, and S. J. Korsmeyer, "BID: a novel BH3 domain-only death agonist," *Genes and Development*, vol. 10, no. 22, pp. 2859–2869, 1996.

[5] I. Tanida, "Autophagosome formation and molecular mechanism of autophagy," *Antioxidants and Redox Signaling*, vol. 14, no. 11, pp. 2201–2214, 2011.

[6] J. Li, X. Zhao, L. Chen et al., "Safety and pharmacokinetics of novel selective vascular endothelial growth factor receptor-2 inhibitor YN968D1 in patients with advanced malignancies," *BMC Cancer*, vol. 10, article 529, 2010.

[7] A. Jemal, F. Bray, M. M. Center, J. Ferlay, E. Ward, and D. Forman, "Global cancer statistics," *CA: A Cancer Journal for Clinicians*, vol. 61, no. 2, pp. 69–90, 2011.

[8] J. F. Perz, G. L. Armstrong, L. A. Farrington, Y. J. F. Hutin, and B. P. Bell, "The contributions of hepatitis B virus and hepatitis C virus infections to cirrhosis and primary liver cancer worldwide," *Journal of Hepatology*, vol. 45, no. 4, pp. 529–538, 2006.

[9] Z. Y. Tang, "Hepatocellular carcinoma surgery—review of the past and prospects for the 21st century," *Journal of Surgical Oncology*, vol. 91, pp. 95–96, 2005.

[10] E. H. Park, Y. J. Kim, N. Yamabe et al., "Stereospecific anticancer effects of ginsenoside Rg3 epimers isolated from heat-processed American ginseng on human gastric cancer cell," *Journal of Ginseng Research*, vol. 38, no. 1, pp. 22–27, 2014.

[11] S. I. Jang, Y. W. Lee, C. K. Cho, H. S. Yoo, and J. H. Jang, "Identification of target genes involved in the antiproliferative effect of enzyme-modified ginseng extract in HepG2 hepatocarcinoma cell," *Evidence-Based Complementary and Alternative Medicine*, vol. 2013, Article ID 502568, 8 pages, 2013.

[12] X. Chen, Y. Wang, H. Luo et al., "β-elemene acts as an antitumor factor and downregulates the expression of survivin, Bcl-xL and Mta-1," *Molecular Medicine Reports*, vol. 6, no. 5, pp. 989–995, 2012.

[13] X. Lu, Y. Wang, H. Luo et al., "β-elemene inhibits the proliferation of T24 bladder carcinoma cells through upregulation of the expression of Smad4," *Molecular Medicine Reports*, vol. 7, no. 2, pp. 513–518, 2013.

[14] H. Shi, L. Liu, J. Geng, Y. Zhou, and L. Chen, "beta-Elemene inhibits the metastasis of B16F10 melanoma cells by downregulation of the expression of uPA, uPAR, MMP-2, and MMP-9," *Melanoma Research*, vol. 24, pp. 99–107, 2014.

[15] H. Q. Hua, S. K. Qin, J. H. Wang, and H. Chen, "Study on effect of arsenic trioxide on adhesion and invasion of human hepatocarcinoma cells in vitro," *Chinese journal of integrated*

traditional and Western medicine, vol. 24, no. 10, pp. 922–925, 2004.

[16] N. Y. Lin, C. Beyer, A. Gießl et al., "Autophagy regulates TNFα-mediated joint destruction in experimental arthritis," *Annals of the Rheumatic Diseases*, vol. 72, no. 5, pp. 761–768, 2013.

[17] K. S. Choi, "Autophagy and cancer," *Experimental & Molecular Medicine*, vol. 44, pp. 109–120, 2012.

[18] R. Mathew, C. M. Karp, B. Beaudoin et al., "Autophagy suppresses tumorigenesis through elimination of p62," *Cell*, vol. 137, pp. 1062–1075, 2009.

[19] A. Herman-Antosiewicz, D. E. Johnson, and S. V. Singh, "Sulforaphane causes autophagy to inhibit release of cytochrome c and apoptosis in human prostate cancer cells," *Cancer Research*, vol. 66, no. 11, pp. 5828–5835, 2006.

[20] C. Ji, L. Zhang, Y. Cheng et al., "Induction of autophagy contributes to crizotinib resistance in ALK-positive lung cancer," *Cancer Biology & Therapy*, vol. 15, no. 5, pp. 570–577, 2014.

[21] J. Wang and G. S. Wu, "Role of autophagy in cisplatin resistance in ovarian cancer cells," *The Journal of Biological Chemistry*, vol. 289, no. 24, pp. 17163–17173, 2014.

[22] M. K. Sannigrahi, V. Singh, R. Sharma, N. K. Panda, and M. Khullar, "Role of autophagy in head and neck cancer and therapeutic resistance," *Oral Diseases*, 2014.